Theses and Dissertations--Computer Science

Computer Science

2019

A DIVERSE BAND-AWARE DYNAMIC SPECTRUM ACCESS ARCHITECTURE FOR CONNECTIVITY IN RURAL COMMUNITIES

Vijay K. Shah
University of Kentucky, vijay.shah@uky.edu
Digital Object Identifier: https://doi.org/10.13023/etd.2019.226

Right click to open a feedback form in a new tab to let us know how this document benefits you.

STUDENT AGREEMENT:

I represent that my thesis or dissertation and abstract are my original work. Proper attribution has been given to all outside sources. I understand that I am solely responsible for obtaining any needed copyright permissions. I have obtained needed written permission statement(s) from the owner(s) of each third-party copyrighted matter to be included in my work, allowing electronic distribution (if such use is not permitted by the fair use doctrine) which will be submitted to UKnowledge as Additional File.

I hereby grant to The University of Kentucky and its agents the irrevocable, non-exclusive, and royalty-free license to archive and make accessible my work in whole or in part in all forms of media, now or hereafter known. I agree that the document mentioned above may be made available immediately for worldwide access unless an embargo applies.

I retain all other ownership rights to the copyright of my work. I also retain the right to use in future works (such as articles or books) all or part of my work. I understand that I am free to register the copyright to my work.

REVIEW, APPROVAL AND ACCEPTANCE

The document mentioned above has been reviewed and accepted by the student's advisor, on behalf of the advisory committee, and by the Director of Graduate Studies (DGS), on behalf of the program; we verify that this is the final, approved version of the student's thesis including all changes required by the advisory committee. The undersigned agree to abide by the statements above.

<div align="right">

Vijay K. Shah, Student

Dr. Simone Silvestri, Major Professor

Dr. Mirek Truszczynski, Director of Graduate Studies

</div>

A DIVERSE BAND-AWARE DYNAMIC SPECTRUM ACCESS
ARCHITECTURE FOR CONNECTIVITY IN RURAL COMMUNITIES

DISSERTATION

A dissertation submitted in partial
fulfillment of the requirements for
the degree of Doctor of Philosophy
in the College of Engineering at the
University of Kentucky

By
Vijay K. Shah
Lexington, Kentucky

Co-Directors: Dr. Simone Silvestri,
Assistant Professor of Computer Science, University of Kentucky, Lexington
and Dr. Sajal K. Das,
Professor of Computer Science, Missouri S&T, Rolla 2019

ABSTRACT OF DISSERTATION

A DIVERSE BAND-AWARE DYNAMIC SPECTRUM ACCESS
ARCHITECTURE FOR CONNECTIVITY IN RURAL COMMUNITIES

Ubiquitous connectivity plays an important role in improving the quality of life in terms of economic development, health and well being, social justice and equity, as well as in providing new educational opportunities. However, rural communities which account for 46% of the world's population lacks access to proper connectivity to avail such societal benefits, creating a huge "digital divide" between the urban and rural areas. A primary reason is that the Information and Communication Technologies (ICT) providers have less incentives to invest in rural areas due to lack of promising revenue returns. Existing research and industrial attempts in providing connectivity to rural communities suffer from severe drawbacks, such as expensive wireless spectrum licenses and infrastructures, under- and over-provisioning of spectrum resources while handling heterogeneous traffic, lack of novel wireless technologies tailored to the unique challenges and requirements of rural communities (e.g., agricultural fields).

Leveraging the recent advances in Dynamic Spectrum Access (DSA) technologies like wide band spectrum analyzers and spectrum access systems, and multi-radio access technologies (multi-RAT), this dissertation proposes a novel Diverse Band-aware DSA (d-DSA) network architecture, that addresses the drawbacks of existing standard and DSA wireless solutions, and extends ubiquitous connectivity to rural communities; a step forward in the direction of the societal and economic improvements in rural communities, and hence, narrowing the "digital divide" between the rural and urban societies. According to this paradigm, a certain wireless device is equipped with software defined radios (SDRs) that are capable of accessing *multiple* (un)licensed spectrum bands, such as, TV, LTE, GSM, CBRS, ISM, and possibly futuristic mmWaves. In order to fully exploit the potential of the d-DSA paradigm, while meeting heterogeneous traffic demands that may be generated in rural communities, we design efficient routing strategies and optimization techniques, which are based on a variety of tools such as graph modeling, integer linear programming, dynamic programming, and heuristic design. Our results on realistic traces in a large variety of rural scenarios show that the proposed techniques are able to meet the heterogeneous traffic requirements of rural applications, while ensuring energy efficiency and robustness of the architecture for providing connectivity to rural communities.

Author's signature: Vijay K. Shah

Date: May 30, 2019

A DIVERSE BAND-AWARE DYNAMIC SPECTRUM ACCESS
ARCHITECTURE FOR CONNECTIVITY IN RURAL COMMUNITIES

By
Vijay K. Shah

Co-Director of Dissertation: Dr. Simone Silvestri

Co-director of Dissertation: Dr. Sajal K. Das

Director of Graduate Studies: Dr. Mirek Truszczynski

Date: May 30, 2019

To my family...
parents, brothers, wife
for their unconditional love and support.

ACKNOWLEDGMENTS

Lastly, I would like to acknowledge my loving family – my parents, brothers, and wife, whose unconditional love and support has always directed me towards a successful and meaningful life. This dissertation would not have been possible without their constant love, encouragement, and support. Thank you for being there for me always.

TABLE OF CONTENTS

LIST OF TABLES

Chapter 1 Introduction

Ubiquitous connectivity plays an important role in improving the quality of life in terms of economic development, health and well-being, social justice and equity, and educational opportunities, to name a few [1, 2, 3]. However rural communities, which accounts for almost 46% of the world population [4], lacks (or have limited) access to adequate connectivity to avail such societal and economic benefits. A primary reason is that the Information and Communication Technologies (ICT) providers have less incentives to invest in rural communities due to lack of promising revenue returns, despite the government subsidies [5]. This creates huge "digital divide" between the urban and rural communities, which results in severe societal disparities across regions [6, 7, 8]. Since providing ubiquitous *connectivity* to rural and remote communities offers key challenges to enable economic development and improved societal well being, they have attracted significant interests in recent years from academia [9, 10, 11] and industry [3, 12, 13].

Recent studies in providing rural connectivity (e.g., DakNet [10], JaldiMAC [9], [14], [15, 16]) and commercial projects (e.g., Alphabet's project Loon [12] and Facebook Internet.org [13]) aim to deliver limited Internet connectivity to rural areas. These solutions utilize either (a) short-range standard technologies (e.g., WiFi, Bluetooth, ZigBee and 6LowPAN) operating in the unlicensed spectrum (e.g., 2.4, 5 GHz), or (b) long-range cellular solutions (e.g., WiMax, 3/4G, LTE/LTE-A, GSM) operating in the licensed spectrum (e.g., 700-900, 1700-2100 MHz) or a combination of thereof. Short-range technologies are not adequate for providing rural connectivity covering wide geographical areas, due to their limited transmission coverage. Although cellular technologies provide larger transmission coverage and offer promising solutions in rural context, limited business cases prohibit significant industry investments in rural connectivity, despite government subsidies [5]. Recently, LoRa [17] and Sigfox [18] are proposed as potential wireless technologies for rural connectivity due to their low power consumption and long-range connectivity. However, very limited data rates prohibit their widespread adoption in rural context. More importantly, all these standard wireless technologies, including LoRa and Sigfox, are restricted only to an individual homogeneous band, be it ISM or LTE band. Such homogeneity of legacy spectrum policy does not provide the flexibility to efficiently handle the heterogeneous network traffic that may be generated in the rural areas. In other words, this triggers the disadvantage of spectrum resources being under or over-provisioned [19] that may negatively impact the network performance.

To overcome the limitations of existing wireless technologies and better utilize the under-utilized licensed spectrum resources, *Dynamic Spectrum Access* (DSA) [20, 21] has emerged as an enabling technology. DSA allows an unlicensed secondary device to dynamically access a free channel in certain spectrum bands (called *whitespaces*) on the condition of non-interference with the primary license holders (or *primary users*). DSA networking is allowed (or in memoranda) by the United States Federal

Communications Commission (FCC) in the TV band [22, 23, 24], Group Special Mobile (GSM) band [5], Long-Term Evolution (LTE) band [25], and Citizens Broadband Radio Service (CBRS) or Radar Band [26]. Similar policies and regulations are being adopted in other countries, such as Canada [27], Singapore [28], South Africa [29], UK [30], Malaysia [31], Kenya [32], Namibia [33, 34], and Argentina [35]. Only recently, DSA technologies have been investigated for providing connectivity to rural communities. Most approaches are based on TV whitespaces (TVWS) [24, 23, 36, 37, 3], GSM whitespaces [5] and LTE whitespaces [38]. Although existing DSA architectures allow secondary devices to opportunistically access an unoccupied channel, they are restricted to *an individual primary band* only.

In this dissertation, we show that utilizing an individual primary band only for providing rural connectivity, is neither efficient nor effective when dealing with heterogeneous traffic demands that may be generated in the rural communities, and suffer greatly from spectrum resources being under or over-provisioned. To overcome such limitations, we leverage the recent advancements in DSA technologies, such as wide band spectrum analyzers [39] and the notion of spectrum access systems [40], and multi-radio access technologies (multi-RAT) [41, 42] to design a novel network architecture, which is based on an innovative *Diverse Band-aware DSA* (d-DSA) paradigm. According to this paradigm, nodes in this architecture, either static or mobile, are equipped with software defined radios (SDRs) that are capable of accessing *multiple spectrum bands*, e.g., TV, CBRS, LTE, GSM, unlicensed Industrial, Scientific and Medical (ISM) band, and possibly futuristic millimeter waves. The innovative d-DSA network architecture is promising in rural context, for it addresses the drawbacks of existing standard (non-DSA) and classical DSA wireless solutions, and extends ubiquitous connectivity to rural communities; a step forward in the direction of fostering societal and economic improvements in rural communities, and hence narrowing the "digital divide" between the urban and rural communities.

In order to fully exploit the potential of the d-DSA paradigm, while meeting the heterogeneous traffic demands that may be generated in the rural communities, we design novel routing strategies and optimization techniques, which are based on a variety of tools such as graph modeling, integer linear programming, dynamic programming, and heuristic design. Our results on realistic traces in a large variety of rural scenarios show that the proposed techniques are able to meet the heterogeneous quality of service requirements of rural applications, while ensuring energy efficiency and reliability of the architecture for providing connectivity to rural communities.

In summary, we believe that the innovative d-DSA network architecture is not only an apt solution for providing ubiquitous connectivity to rural communities, but would prove to be a very effective model in designing other computer and communication networks, like, Internet of Things networks and post-disaster communications. In fact, our initial study on utilizing d-DSA network architectures for enabling low-cost, high quality, and *green* communication systems, in order to collect (and distribute) heterogeneous decision and monitoring information in futuristic Smart and Connected Communities (or Smart cities), has shown a great promise [43, 44]. To this end, we believe our study will open new research directions in various wireless networking fields, including, rural connectivity and d-DSA networks.

1.1 Contributions of This Dissertation

In this dissertation, we propose to design a novel d-DSA network architecture for extending ubiquitous connectivity to rural communities. Following this, we design novel routing strategies and optimization techniques for (both static and dynamic) d-DSA network architectures, that would enable optimal routing of various data traffic (e.g., texts, logs, audios, streaming videos etc.). The main contributions of this dissertation are summarized below:

A Literature Survey of Standard (non-DSA) and DSA Architectures

This contribution is presented in Chapter 2 where we provide a comprehensive overview of the related literature on the standard (non DSA) and DSA approaches for providing connectivity to rural communities. Following this, we highlight the key limitations of both standard and DSA wireless solutions, and motivate the need of the proposed d-DSA architecture in order to provide ubiquitous connectivity in rural setting.

Diverse band-aware Dynamic Spectrum Access (d-DSA) Architecture

We describe this contribution in Chapter 3, and propose a novel *diverse band-aware Dynamic Spectrum Access* (d-DSA) network architecture, which is suited for rural connectivity. This chapter discusses the key components of the proposed d-DSA architecture, adopted mechanism for spectrum discovery and selection of unoccupied (or non-interfered) channel within a certain primary band, and other underlying assumptions.

Characterization of Communication over Diverse Spectrum Bands

We discuss this contribution in Chapter 4. Here, we characterize the distinct electromagnetic (EM) properties (such as, operating frequency, channel bandwidth, transmit power etc.) of different primary bands, that may be available in the proposed d-DSA architecture. We then show that these EM properties significantly impact important transmission properties, including energy efficiency, delay, and coverage. These characterizations will be at the basis of designing efficient routing strategies presented in subsequent Chapters 5, 6, and 7.

Routing with Static (Infrastructure) d-DSA Network Architectures

We describe this contribution in Chapter 5 where we design efficient routing schemes for an infrastructure d-DSA network architecture, in which the component communication d-DSA devices are fixed. Specifically, our proposed routing protocols attempt to intelligently match the quality of service requirements of a message to a suitable band type, by exploiting the distinct EM characteristics of various spectrum bands. Since data traffic generated in rural communities are typically valuable only when delivered with a certain hard (or soft) deadline, we formulate a linear optimization problem for determining the most energy-efficient route that ensures a delivery time

within the hard deadline. After proving that such a problem is NP-Hard, we propose an exact pseudo-polynomial time dynamic programming algorithm to solve it, followed by a polynomial time greedy heuristic. Additionally, we formulate a non-linear optimization problem to find the optimal path when the message delivery time is defined as a *soft* deadline, and extend our greedy heuristic to handle soft deadlines. Compared to the standard (or single band) DSA architectures, our extensive simulation study shows that our routing protocol on top of the envisioned d-DSA architecture significantly improves the achievable energy efficiency while meeting various hard and soft deadlines. The preliminary version of this contribution (Chapter 5) appeared in ACM BuildSys 2017, and the extended version in IEEE Transactions on Sensor Networks (TOSN) 2018.

Routing with Dynamic yet Sufficiently Predictable d-DSA Architectures

This contribution is presented in Chapter 6. Here, we consider a d-DSA network architecture with sufficiently predictable mobility, as in the case of public transportation network, where the mobility patterns of buses are generally known with acceptable accuracy. The underlying idea is to deploy d-DSA radio devices on the public transportation vehicles, such as public buses and municipal trucks. This architecture is particularly suitable for providing connectivity to scenarios, where the fixed infrastructure is not able to provide the full coverage, a typical scenario in rural setting. Specifically, we propose a novel routing protocol, termed *diverse DSA aware Routing* (dDSAaR) protocol, that jointly exploits various spectrum bands and the time-varying yet sufficiently predictable mobility of public transportation vehicles. The dDSAaR protocol is based on a novel representation of d-DSA network topology, termed *Space-Time-Band* (STB) graph, that comprehensively captures the communication opportunities across the space, time, and multiple bands. We compare the proposed d-DSA architecture, utilizing dDSAaR, to the conventional non-DSA/DSA architectures, utilizing a standard (single band) routing protocol (e.g., Epidemic). We use real bus mobility traces collected at the University of Massachusetts, Amherst campus. Results show that the envisioned d-DSA architecture achieves better message delivery, negligible message overhead, and better energy expenditure, at the expense of a slight increase in delay. Nevertheless, the delay improves with higher predictable mobility. This contribution has been reported in IEEE INFOCOM 2019.

Routing with Dynamic d-DSA Architecture with Unpredictable Mobility

We describe this contribution in Chapter 7, where we further consider the case of d-DSA network, in which the mobile nodes may have unpredictable mobility (e.g., private cars). This results in a d-DSA aware delay tolerant network (DTN) [45, 46], (in short, referred to as d-DSA DTN), in which each node can utilize multiple communication opportunities over diverse spectrum bands, if available. To this end, we first highlight the shortcomings of routing schemes originally designed for standard (single-band) DTNs, while dealing with such d-DSA DTNs. Following this, we formulate an integer linear programming (ILP) optimization problem that aims to de-

termine a suitable path route for each message traffic in such a network, such that the end-to-end network delay is minimized. Since this would require complete knowledge of topology dynamics and future message traffic demands, it becomes an impractical solution for such d-DSA DTNs, which are both *dynamic* and *unpredictable*. Hence, we propose an efficient lightweight *d-DSA aware Geographical Routing* (dDSA-GR) protocol, which is based on georouting principle, and determines a path route, i.e., optimal *spectrum band* at each node, and *next hop relay node*, that minimizes end-to-end delay for each message in such d-DSA DTNs. Finally, we compare the proposed dDSA-GR protocol against the standard (single-band) GR protocol, and other two benchmark DTN routing protocols, namely Epidemic Routing (ER) [45] and Spray and Wait (SnW) [47], and also their extended d-DSA aware versions. Results on realistic traces based on the map of Lexington city, KY, USA show that the proposed dDSA-GR protocol achieves much better network delay, message delivery, energy efficiency, and negligible message overhead, compared to standard GR, ER, and SnW routing protocols, and their extended d-DSA versions. The preliminary version of this contribution appeared in IEEE ISC2 2018, and the detailed work will be submitted to IEEE Transactions of Network Service and Management (TNSM) 2019.

1.2   Organization of This Dissertation

The rest of the dissertation is organized as follows. Chapter 2 reviews the related works on the traditional (non DSA) and DSA approaches for providing connectivity in rural communities. In Chapter 3, we describe the key components of the proposed d-DSA network architecture and the underlying assumptions. Next, we characterize the unique electro-magnetic characteristics of various spectrum bands that may be available in the proposed d-DSA network architecture in Chapter 4. In Chapter 5, we design efficient routing strategies for infrastructure d-DSA network architectures. We develop intelligent routing scheme for time-varying yet sufficiently predictable d-DSA architecture in Chapter 6. In Chapter 7, we consider the case of d-DSA network architectures where the devices have unpredictable mobility. Here, we primarily highlight the limitations of existing DTN routing protocols while dealing with time-varying yet unpredictable d-DSA network architectures. Furthermore, we propose a novel d-DSA aware Geographical Routing (dDSA-GR) protocol, which is based on georouting principle, and effectively exploits the multiple communication opportunities (due to diverse spectrum bands) that may be available in the envisioned d-DSA network architecture. Finally, we conclude the dissertation by providing concluding remarks and future directions in Chapter 8.

Chapter 2 A Literature Survey of Standard (non-DSA) and DSA Network Architectures

In this chapter, we provide a comprehensive overview of the related literature for both standard (non-DSA) in Section 2.1 and DSA (or Spectrum sharing approaches) in Section 2.2 for providing efficient connectivity to rural and remote communities. Following this, we highlight the key limitations of both standard and DSA wireless solutions, and motivate the need of the proposed d-DSA network architecture in order to provide ubiquitous connectivity in rural setting.

2.1   Standard Network Architectures

Several standard (non-DSA) wireless communication architectures, e.g., DakNet [10] and KioskNet [48], have been proposed to provide connectivity to rural communities. For example, DakNet [10] utilizes public transportation vehicles (equipped with computers having Wi-Fi radios) to transfer emails and information requests to Internet using the access points installed at the bus station in the nearest city and delivers their responses when the transport returns to the village (See Fig. 2.1).
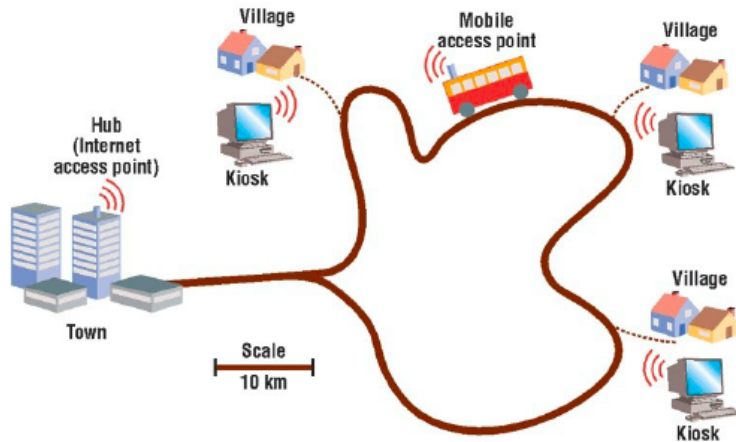
Figure 2.1: DakNet Architecture [10]

On contrary, JaldiMAC [9] uses long distance outdoor WiFi mesh to provide connectivity to provide broadband Internet in sparsely populated areas that suffer from large set-up delays. Heimerl et al. [14] propose the deployment of low power GSM based Village Base Station (VBTS) for rural telephony. In LifeNet [15] and Twimight [49], the authors propose the connectivity utilizing hand-held wireless devices for transient conditions. In [50, 16], the authors propose a four-tier hybrid

architecture consisting of hand-held devices in the lowest tier, WiFi enabled drop-boxes in the second tier, data mules equipped with WiFi antennas in the third tier, and long range WiFi towers in the fourth tier, thus providing connectivity in challenging scenarios such as post-disaster scenarios. Hazra et al. [51] proposes to utilize cellular towers and vehicles equipped with WiFi routers, for providing connectivity to resource-constrained post-disaster environments. Several network architectures based on mesh technologies, e.g., Serval Project [52] (BatPhone-provides mesh mobile telephony platform), and Hybrid Wireless Mesh Network (HWMN) [53] are proposed to provide connectivity in rural communities and emergency situations. Application of UAVs [54] can overcome hurdles where physical connectivity is restricted.

Alphabet project Loon [12] introduces the network of balloons traveling on the edge of space, designed to extend Internet connectivity to people in rural and remote areas. See Fig. 2.2 for illustration. It uses base stations on Earth, below the balloon's trajectories, and creates a mesh network between the balloons to transfer messages to these base stations with Internet connectivity to transmit replies and requests. Users can connect to the balloons via LTE devices through a local carrier's infrastructure.

Figure 2.2: Project Loon [12]

Facebook Internet.org [13] utilizes local cellular infrastructure, along with satellite communications and UAVs, to deliver limited Internet connectivity to rural areas (See Fig. 2.3. Users need an Internet.org account or be affiliated with Facebook local mobile partner and they will have access to a limited set of applications e.g., Facebook, local news, employment, health, and weather websites.

However, all of these research and industrial efforts utilize standard wireless technologies such as WiFi, WiMax, GSM base station, VSAT (very small aperture terminal), WLAN, wireless mesh, or a combination thereof, in order to provide limited Internet connectivity to rural communities. Such wireless solutions utilize either short-range technologies, such as WiFi, Bluetooth, ZigBee and 6LowPAN or cellular technologies such as, 3G/4G, LTE/LTE-A and GSM. The short-range technologies, due to their limited transmission coverage, are not adequate for rural connectivity where long distances quite common. Although cellular technologies provide higher transmission coverage and are promising wireless solutions in rural context, tradi-

Figure 2.3: Facebook Internet.org [13]

tional telecommunication companies are not inclined to make huge investments in rural infrastructure, due to expensive wireless spectrum licenses, even considering government subsidies [5]. This is because it is marginally profitable at best, particularly given the lucrative opportunity and profit margin in deploying 3G/4G infrastructure in the urban areas. Recently, LoRa [17] and Sigfox [18], due to low power consumption and long-range connectivity, are being considered as potential wireless technology for rural connectivity. The devices use unlicensed sub-gigahertz radio spectrum like 915 MHz in the Industrial, Scientific, and Medical (ISM) spectrum band, and offer very poor bandwidth connections, in the order of few kilohertzs.

Notice that all the standard wireless technologies, including LoRa and Sigfox, are restricted to *an individual spectrum band only*– usually ISM (mostly), LTE or GSM bands. Such homogeneity of spectrum access policy does not provide the flexibility to efficiently handle the heterogeneous network traffic (e.g., logs, texts, images, audios, high streaming videos, etc.) with varying message sizes and quality of service (QoS) demands that may be generated in the rural communities. In other words, this triggers the disadvantage of spectrum resources being under- or over-provisioned [19], and thereby negatively impacting the network effectiveness and performance.

2.2 DSA Network Architectures

Most research on DSA has focused on developing techniques and protocols for four key functionalities of the DSA technology, namely efficient spectrum sensing [55, 56], spectrum decision [57, 58, 59, 60, 61], spectrum sharing [62, 63], and spectrum mobility [64]. Refer to [20, 64] for the detailed study on the four key functionalities of DSA technology.

Only recently, DSA technologies have been investigated to provide connectivity in rural areas. Most approaches are based on TV band whitespaces (TVWS) [23, 36, 3] and GSM band whitespaces [5]. In [24], the authors proposed the design and implementation of WhiteFi, the first WiFi like wireless network constructed on top of TVWS. In [37], the opportunistic use of very/ultra high frequency (VHF/UHF) TV

8

bands is proposed through cognitive radio technology and DSA paradigm, such as IEEE 802.22 technology, for rural connectivity. Here the authors address two important issues that can affect the success of IEEE 802.22 technology in rural deployments. First, they propose suitable service model that combined TV broadcasting and data services to facilitate service adoption. Second, they propose an adaptive time division duplexing (TDD) approach to eliminate the requirement for long TDD turn-around time of existing IEEE 802.22 technology. In [23] TVWS is used in conjunction with 5G infrastructure for Internet access in rural areas. A TVWS based backhaul architecture for rural India is proposed in [36]. Microsoft has also initiated deployments of TVWS based Internet connectivity in various countries, such as Jamaica, Namibia, the Philippines, United Kindom, and USA [3]. In [5], the authors propose a hybrid sensing and database-driven spectrum sharing scheme, called *Nomadic GSM*, that utilizes GSM whitespaces for providing affordable rural connectivity. Nomadic GSM enables safe coexistence of primary and secondary users without requiring coordination or cooperation from existing license holders. Finally, the authors in [38] proposes to utilize LTE whitespaces for deploying a LTE-A network in order to facilitate the provisioning of high data rate streaming services.
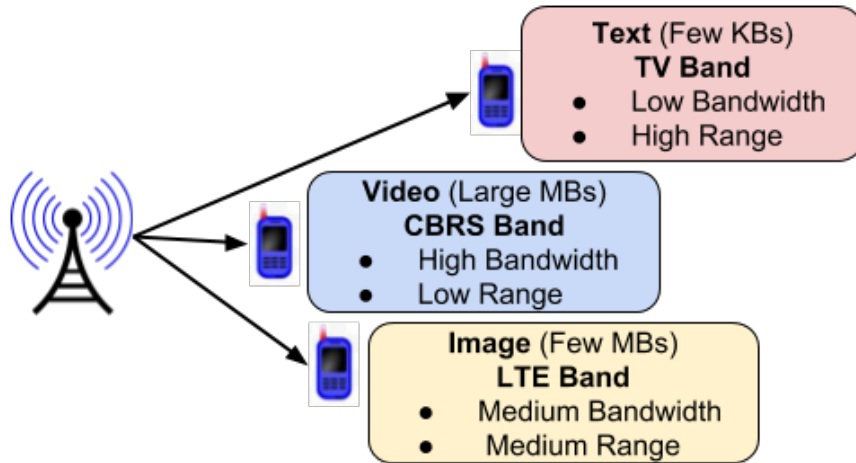
Figure 2.4: An example motivating the d-DSA paradigm: different bands are preferable depending on the traffic characteristics.

Although existing DSA architectures allow secondary devices to opportunistically access an unoccupied channel, they are restricted to *an individual primary band* only - be it TV or GSM band. In this dissertation, we demonstrate that it is neither efficient nor effective under heterogeneous traffic demands, and greatly suffer from under- or over-provisioning of spectrum. For instance consider an example as illustrated in Fig. 2.4. Assuming the objective is providing low end-to-end delay, to transmit a certain text (usually, few Kilobytes) at large distances (several kms), a TV band is possibly optimal, because it offers high transmission coverage (tens of kms), and adequate bandwidth (6 MHz). Whereas, for transmitting a large-sized video at very short distances (few hundred meters), it may be more efficient to communicate it over the CBRS band, which offers very high channel bandwidth (40 MHz), and low

(yet sufficiently large) transmission coverage. Similarly, owing to decent coverage and channel bandwidth, an LTE band is more promising to transmit a medium-sized image at relatively small distances (few kms).

Motivated by the recent advances in DSA technologies, such as wide band spectrum analyzers [39] and the notion of spectrum access systems [40], and multi-radio access technologies (multi-RAT) [41, 42], this dissertation envisions a novel communication paradigm for rural connectivity, referred to as *Diverse Band-aware DSA* (in short, d-DSA) paradigm. The innovative d-DSA paradigm extends the classical DSA approach by enabling a certain wireless device (secondary user) to dynamically utilize an empty channel in *any* diverse set of spectrum bands, ranging from TV, LTE, GSM, CBRS, unlicensed ISM to futuristic mmWaves, on the condition of non-interference with the primary licensees (users). Our dissertation addresses the unique challenges of the d-DSA communication paradigm in rural setting, such as, the characterization of the communications over diverse spectrum bands, and efficient multi-hop routing tailored to the heterogeneous traffic with varying QoS requirements, introduced by the d-DSA communication paradigm.

Chapter 3 Proposed d-DSA Network Architecture

In this chapter, we describe the proposed *Diverse band-aware Dynamic Spectrum Access* (d-DSA) network architecture for providing ubiquitous connectivity to rural communities. In particular, we discuss in Section 3.1 the key components of the proposed d-DSA architecture, the adopted mechanism for spectrum discovery and selection of unoccupied (or non-interfered) channel within a certain primary band, and other underlying assumptions. Subsequently in Section 3.2, we describe the three distinct types of d-DSA network topologies, depending upon the varying mobility patterns of component d-DSA radio devices.

3.1   Key Components

Sensor block

A sensor block is a rural geographical region such as a village, an agricultural field, or a rural hospital that needs to communicate with a certain access point (or *connectivity hub*) with Internet access. A sensor block, constituting mobile devices, smart meters, and sensors, may generate heterogeneous messages over time such as texts, logs, emails, images, and videos. Such messages may have different sizes, ranging from few Kilobytes (e.g., texts, emails, audios) to several Megabytes (e.g., images, high streaming videos). We assume that each sensor block is equipped with a *dropbox*. Using a multi-hop standard wireless network (say, using WiFi or Bluetooth) within the sensor block, messages are exchanged between smart devices/sensors and the dropbox. It is not required for smart devices and sensors to be equipped with d-DSA radios. Conversely, the dropbox acts as a bridge between these standard devices and the d-DSA network, as described in the following.

Dropbox

A dropbox, similar to the rural kiosk in the DakNet architecture [10], is a laptop or a smart device installed within a sensor block. The dropbox has: (i) *a memory storage* to store messages received from various sensors and smart devices, (ii) *a standard wireless technology* (e.g., WiFi) to communicate with standard (non-DSA) smart devices and sensors in its sensor block, (iii) *d-DSA radio* so as to communicate with other d-DSA radio devices such as data mules, or other dropboxes (if in communication range over a certain band).

Physical Infrastructure node and Data mule

A physical infrastructure node refers to an electric pole, lamp post, or road-side assistance unit (RSU) [65, 66], equipped with d-DSA radio devices, that are capable of accessing multiple spectrum bands, such as TV, LTE, CBRS, GSM, and unlicensed
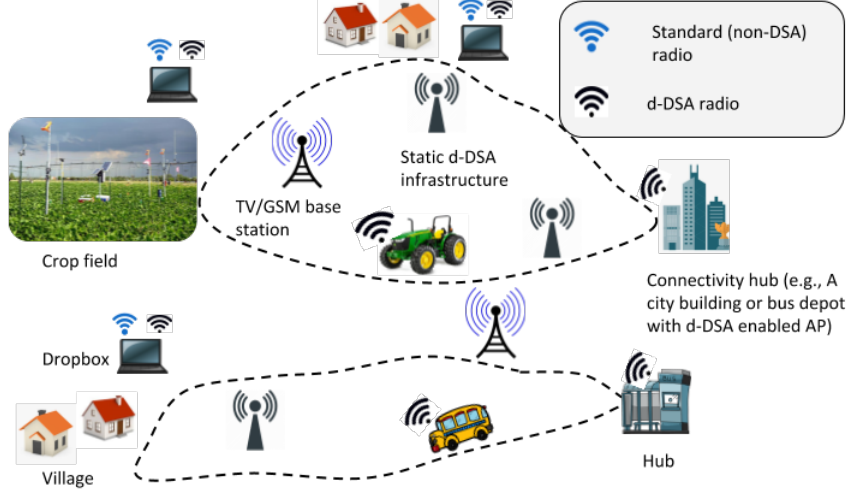
Figure 3.1: Proposed d-DSA Architecture

ISM bands. Though we consider these infrastructure nodes to be equipped with d-DSA capabilities, we do not require all nodes to have access to all bands, or have the same communication potentials.

A data mule is a public transport vehicle, such as, a public bus, taxi etc., that travels on a pre-assigned route and visits one or more sensor blocks in a periodic fashion. For example, a public bus starts its trip from a bus station, visits one or more sensor blocks (e.g., villages), and returns to the station. Similarly, a municipal vehicle starts from the municipality depot, visits one or more sensor blocks, like villages or hospitals, and returns to the depot. Each data mule is equipped with d-DSA radio device, and therefore can communicate with dropboxes, data mules, infrastructure nodes, or connectivity hubs over a certain spectrum band (if in communication range).

Such static infrastructures nodes and mobile data mules, equipped with d-DSA radio devices, inherently act as the *relay nodes* for message traffic exchange between the dropboxes and the *connectivity hubs*.

Connectivity hub

A connectivity hub is a communication node, equipped with wireless access point (AP) connected to the Internet, where the generated messages need to be delivered. A hub is also equipped with a d-DSA radio, and is therefore, capable of communicating with other d-DSA radio devices (data mule, dropbox, infrastructure node) over any spectrum band, if in communication range. A d-DSA node may be heterogeneous in terms of transmit power, accessible spectrum bands, and multiple input multiple output (MIMO) capability, such as single vs. multiple antenna(s). Unless otherwise stated, we consider single transmitter and single receiver antennas in rest of the dissertation.

Primary users

In the proposed d-DSA architecture, there may exist *primary users* (e.g., TV or GSM base stations) that have exclusive access to certain licensed bands. Provided that a primary user accesses a certain channel in a given band, a d-DSA radio device in its geographical proximity *is forbidden* to utilize that channel (and interfere with the primary user). This is the utmost requirement for any d-DSA radio device by the FCC policy and is usually referred as the *Incumbent Primary user protection* [20, 67]. Hence, the discovery and selection of unoccupied (or non-interfered) channel in a certain band is a crucial requirement for a d-DSA radio device in the proposed architecture.

Channel discovery and selection mechanism

The specifics of discovery and selection of unoccupied (non-interfered) channel within a given band has been extensively studied in the DSA literature [20, 68, 69]. Broadly, it can be either (i) sense and use in the DSA radio device itself, (ii) through an off-device environmental sensing capability [26], or (iii) a central geo-location whitespace database or a spectrum access system (SAS) database [70]. Unless otherwise stated in this dissertation, we consider a *sense and use mechanism* for whitespace channel discovery and selection in a certain spectrum band. This approach is particularly apt for rural contexts, since it does not require access to the centralized geo-spatial whitespace databases [70] nor need dedicated environmental sensing framework. However, our d-DSA architecture will also work seamlessly with the geo-location whitespace database (as considered in case of sufficiently predictable d-DSA architectures) or off-device environmental sensing capability, if available. It is noteworthy to mention that the majority of channels in a certain band would be available in the rural context mainly due to lack of primary users in the region. For instance, at any given time, atleast 80% TV channels are available in rural India [36]. Our proposed routing strategies exploit this observation as discussed later in next chapters.

3.2   d-DSA Network Topology

As discussed in the previous Section 3.1, the proposed d-DSA architecture may constitute static infrastructure nodes or mobile data mules, or a combination of both. Depending upon it, the envisioned d-DSA architecture may result into three distinct types of d-DSA network topologies, which are described as follows:

Static (Infrastructure) d-DSA Network

In this case, the d-DSA architecture only constitutes those d-DSA radio devices as component nodes, whose locations are always fixed, such as, infrastructure nodes, dropboxes and hubs. Each d-DSA node shares its geographical location and spectrum availability with other nodes in the architecture via a dedicated *common control channel* or other synchronization techniques as discussed in the recent DSA standards [26, 22]. Hence, in such a fixed d-DSA network, each node possesses the *global*

knowledge about *approximate geographical location* and *spectrum availability* at every other node. We design efficient routing strategies for such static d-DSA networks in Chapter 5.

Time-varying yet sufficiently predictable d-DSA Network

In this case, the envisioned d-DSA architecture may constitute mobile component nodes, such as, public transportation vehicles (e.g., public buses) whose mobility patterns are sufficiently predictable and can be known apriori with acceptable accuracy; in addition to the static d-DSA nodes. Such a network is particularly suitable for providing connectivity to scenarios, where the fixed infrastructure is not able to provide the full coverage, however have access to the public transportation system, a typical scenario in rural setting. In such a sufficiently predictable d-DSA network scenario, it may be possible to construct the global knowledge of the network with acceptable accuracy over space and time. To ensure this, we consider that one prespecified connectivity hub, referred to as the *network manager* has the access (via Internet) to the geo-location or Spectrum Access System (SAS) whitespace database, which maintains the occupancy profile (free or busy) of all channels within each band, given a geographical location and time [70]. Moreover the network manager collects the vehicles' mobility information over time. Following this, we propose a novel routing protocol, that utilizes the mobility information of vehicles and spectrum availability at each d-DSA node (collected by the network manager), and constructs a unified graph model, termed *Space-Time-Band* (STB) graph, that comprehensively captures the communication opportunities over spatial, temporal, and diverse spectrum bands. Following this, the protocol computes the suitable communication routes for each message, which includes the set of suitable relay nodes and optimal band type at each node, such that the selected route enhances the desired performance metric, e.g., end-to-end delay. We discuss these aspects in detail in Chapter 6.

Time-varying d-DSA Network with Unpredictable Mobility

This is the worst-case and most generalized scenario, where the proposed d-DSA architecture may constitute several types of mobile nodes, such as, private vehicles, whose mobility patterns may not be known nor sufficiently predicted apriori. Such an approach of including private vehicles as the integral component nodes of the d-DSA network architecture are critical for realizing the true power of ubiquitous connectivity in rural setting. In such a scenario, a node would not be able to obtain the global knowledge of the geographical location and spectrum availability at other nodes in the network. However, it may gather local knowledge about the neighboring nodes. We discuss these aspects in detail and design suitable routing strategies for such unpredictable d-DSA networks in Chapter 7.

Chapter 4 Characterization of Communication Over Diverse Spectrum Bands

This chapter characterizes the distinct electro-magnetic (EM) properties of different spectrum bands, that may be available in the proposed d-DSA network architecture. Specifically, we focus on properties like end-to-end energy efficiency, transmission delay, and coverage, that can be exploited in designing efficient routing strategies for both the envisioned (static or mobile) d-DSA network architectures.
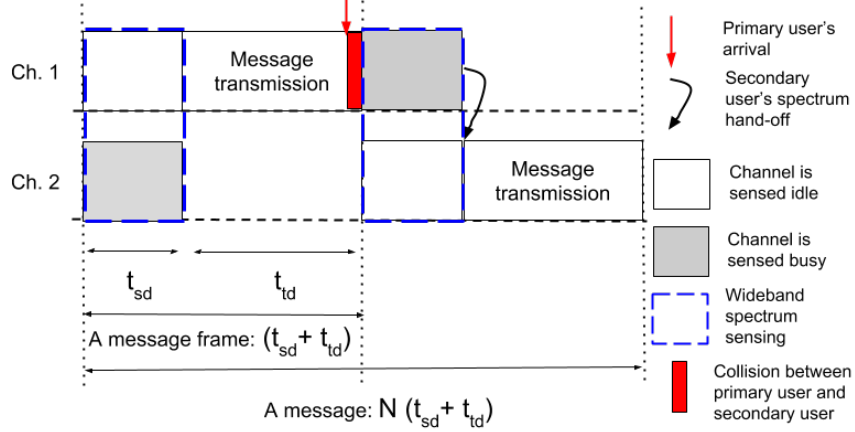
Figure 4.1: A node message transmission - periodic sensing, message transmission, and spectrum handoff.

4.1 Energy Consumption and Transmission Delay Characterization

To characterize the communication opportunities in terms of energy consumption and transmission delay, we consider several EM factors, such as operating frequency, channel bandwidth, and interference. In the following, i and j refer to nodes while s indicates a specific band in the set S of spectrum bands. According to the sense and use mechanism assumed in the proposed d-DSA architecture (See Chapter 3), the message transmission is slotted via periodic sensing [71]. A periodic sensing frame consists of a sensing slot duration t_{sd} and a transmission slot duration t_{td}. Figure 4.1 shows the activities in transmitting a message. In the sensing slot, the node performs wide-band spectrum sensing to obtain the availability status of all channels, whereas the node sends the message packets over the chosen free channel in the transmission slot. This transmission may be interrupted due to primary user (PU) transmission (red arrow), in which case the secondary user (SU) waits until the beginning of a new sensing slot in order to repeat the process. Under this consideration, we discuss the impact of various EM factors to the end-to-end energy consumption and network delay for a certain message later in this chapter.

Now, given a path $p(u, v)$ for a certain message m (with size L) from a source node u to destination node v, the total energy consumed is given by:

$$w_{uv}(L) = \sum_{e_{ij}^{(s)} \in p(u,v)} w_{ij}^s(L) \tag{4.1}$$

where $w_{ij}^{(s)}(L)$ is the energy cost over link $e_{ij}^{(s)}$, and $e_{ij}^{(s)}$ is an intermediate link in path $p(u, v)$.

Energy Calculation Over a Certain Link $w_{ij}^{(s)}(L)$

Similar to the energy consumption model presented in [71], the energy cost $w_{ij}^{(s)}(L)$ over a link $e_{ij}^{(s)}$ to transmit a message of size L, can be expressed as Eq. (4.2):

$$w_{ij}^{(s)}(L) = N t_{sd} \tilde{P} + N \mathcal{P} w_{sw} + T_{td} P_i^{(s)} \tag{4.2}$$

where N is the number of time slots required for one message transmission, and can be calculated as the fraction of message size (L) to the effective bit rate $(\mathbb{R}_{ij}^{(s)})$ offered by a channel in a certain band s, i.e., $\lceil \frac{L}{\mathbb{R}_{ij}^{(s)}} \rceil$. In addition, t_{sd} is the sensing slot duration; $\tilde{P}$ is the spectrum sensing power (in Watts); $\mathcal{P}$ is the probability of switching to an idle channel, termed as *spectrum hand-off*; w_{sw} is the energy cost (in Joules) of one channel switching; $P_i^{(s)}$ is the transmit power at node i over band s. Finally, T_{td} is the average time required to transmit the entire message, and can be computed as $T_{td} = N \mathcal{P} t_{td}$, where t_{td} denotes the transmission slot duration (see Fig. 4.1). For each message frame, the d-DSA node has to sense for t_{sd}, and N frames are required for one message transmission. Hence the energy consumed in sensing is $N t_{sd} \tilde{P}$. Given that the node switches to another channel with probability $\mathcal{P}$, it consumes $N \mathcal{P} w_{sw}$ amount of energy in channel switching. The last part of Eq. (4.2) indicates the total energy consumed in transmitting message of size L over a channel in spectrum band s. Usually, t_{sd} and t_{td} are pre-determined values for any given band type, and w_{sw} is negligible. Thus, $N = \lceil \frac{L}{\mathbb{R}_{ij}^{(s)}} \rceil$ and $P_i^{(s)}$ are the two main contributing factors for the energy cost of any link.

Transmission Delay Calculation Over a Certain Link $w_{ij}^{(s)}(L)$

Given t_{sd}, t_{td}, N and $\mathcal{P}$, the total transmission delay (or *message transmission time*) over a certain link $w_{ij}^{(s)}(L)$, denoted by $t_{ij}^{(s)}(L)$, for a message m can be calculated as follows:

$$t_{ij}^{(s)}(L) = N(t_{sd} + \mathcal{P} t_{td}) = \left\lceil \frac{L}{\mathbb{R}_{ij}^{(s)}} \right\rceil (t_{sd} + \mathcal{P} t_{td}) \tag{4.3}$$

The notations are similar to the ones used in the previous subsection 4.1. Here again, t_{sd} and t_{td} are predetermined values for a certain spectrum band, thus, N is the sole main contributing factor for the transmission delay cost of any link.

4.2 Impact of EM properties

Based on the above energy consumption and transmission delay characterization, we discuss the impact of different EM characteristics offered by various bands on the overall energy efficiency and network delay of the d-DSA network architecture.

Impact of Operating Frequency

It is known that the received signal strength at a receiver must meet some reception threshold, τ, to be able to decode a signal accurately. The generalized Frii's transmission equation [72] provides the relationship between the received power at receiver j and the transmit power from transmitter i over any channel with a representative frequency[1] $f^{(s)}$ in band s,

$$P_j^{(s)} = P_i^{(s)} G_i G_j \Big(\frac{\mathbb{C}}{4\pi f^{(s)} d} \Big)^{\alpha} \geq \tau \qquad (4.4)$$

where, G_i and G_j are the transmitter and receiver antenna gains, α is path loss exponent, $\mathbb{C}$ is the speed of light, d is the distance between i and j, $P_i^{(s)}$ is the transmit power of i, and $P_j^{(s)}$ is the received power at j. Now let $\phi = G_i G_j (\frac{\mathbb{C}}{4\pi})^{\alpha}$ be a constant.

Thus the above equation becomes $P_j^{(s)} = \phi \frac{P_i^{(s)}}{(f^{(s)} d)^{\alpha}}$. It is evident that for higher frequencies, the transmit power $P_i^{(s)}$ ought to be increased to maintain the same $P_j^{(s)} \geq \tau$, even though the distance d is unchanged. The resultant increased transmit power causes more energy consumption (refer to Eqs. 4.1 and 4.2). Alternatively, if the transmit power is not increased, then τ is only met at a lower distance. Hence, more intermediate hops would be required to traverse the same distance d, leading to the additional transmission and reception operations at each intermediate hop which causes higher energy expenditure and higher transmission delay.

Moreover, the lower frequencies have larger wavelengths yielding better obstacle and wall penetration capabilities. This implies the lower frequencies are less error prone, thus reducing (re)transmission overheads and enabling better non line-of-sight connectivity. Among the bands that allow DSA, the TV and LTE bands have lower frequency allocations than traditionally used unlicensed band of 2.4 GHz. In other words, these bands should be seemingly more energy efficient.

However, lower frequencies come at a trade-off in the sense that they usually have much lesser bandwidth of 6 MHz as opposed to the LTE (upto 20 MHz) and CBRS (upto 40 MHz). For larger message sizes, the message transmission time (refer to Eq. 4.3) will be higher as the number of time slots (N) increases. Supporting high data rate applications are also challenging for lower frequencies offering smaller bandwidths. On the other hand, frequencies offering higher bandwidths will reduce the transmission time for a given message size, and thereby also saving energy. An important research question, therefore, is whether the reduction in the transmission

---

[1]For example, $f_s = 2.4$ GHz for the frequencies in the range 2.412 - 2.462 GHz used by legacy WiFi devices in ISM band

time for higher frequencies offsets the gain in energy efficiency due to the reduced hop count.

Impact of Channel Bandwidth

The relationship between the bandwidth and the dissipated power could be understood through Rayleigh-Parseval Equation [73]:

$$P_{dis}^{(s)} = \int_{f_1^{(s)}}^{f_2^{(s)}} \mathbb{S}_i(f^{(s)}) df \tag{4.5}$$

where $\mathbb{S}_i$ is the power spectral density, $\Delta f^{(s)} = f_2^{(s)} - f_1^{(s)}$ is the bandwidth of any channel in the band type s, and $P_{dis}^{(s)}$ is the total power dissipated over band s. From Eq. 4.5, it is clear that a channel offering higher bandwidth causes larger power dissipation. Given a fixed transmission time for any message, the higher bandwidth channels will consume more energy than the lower ones. The typical bandwidths for various spectrum is listed in Table 7.4.

Conversely, from Shannon-Hartley theorem [74], the effective bit rate ($\mathbb{R}_{ij}^{(s)}$) between a transmitter i and receiver j over any channel in band s with representative frequency $f^{(s)}$ is given by:

$$\mathbb{R}_{ij}^{(s)} = B^{(s)} log_2 \Big(1 + \chi_{ij}^{(s)}\Big) = B^{(s)} log_2 \Big(1 + \phi \frac{P_i^{(s)}}{(f^{(s)}d)^\alpha N^{(s)}}\Big) \tag{4.6}$$

where $B^{(s)}$ is the bandwidth of any channel in band type s and $\chi_{ij}^{(s)} = \frac{P_j^{(s)}}{N^{(s)}}$ is the ratio of the communication signal power to the interference and noise at the receiver (SINR). The rest of the notations are the same as above. From Eq. 4.6, given that the SINR is unchanged, a higher bandwidth channel would offer a higher effective bit rate, thereby decreasing the required message transmission time (or transmission delay).

Therefore, from the above relationships of bandwidth with (i) dissipated transmit power (Eq. 4.5) and (ii) effective bit rate (Eq. 4.6), the higher the channel bandwidth, the higher is the dissipated power but the lower is the message transmission time. Thus, the trade-off is whether to choose a high bandwidth channel that reduces the message transmission time and increases the dissipated power, or vice-versa.

Impact of Channel Interference

Channel interference occurs when two different transmitters use the same channel (or frequency), termed as *Co-channel interference* (CCI) or adjacent channels, termed as *Adjacent channel interference* (ACI). Adjacent channel interference is usually due to imperfect receiver filters, and can be handled by using sharp band filters, careful channel assignment (significant frequency separation). However, CCI is a serious concern and can be handled only by allowing a unique transmitter (among all the transmitter in the interference radius) to use a channel at a given time. Interference

Table 4.1: Spectrum Profile with Bandwidths

Spectrum	Bandwidth
54-216 MHz (VHF TV Band)	6MHz
470-698 MHz (UHF TV Band)	6MHz
698-806 MHz (700 MHz Band/FirstNet)	6 MHz
700-800 MHz/1700-2100 MHz (LTE Band)	5 - 20 MHz
902 - 928 MHz (ISM Band)	3-8 MHz
2.4 - 2.5 GHz (ISM Band)	2 - 50 MHz
3.5 - 3.7 GHz (CBRS Band)	10 - 40 MHz
5.7 - 5.8 GHz (ISM Band)	20 - 80 MHz

radius is the distance from a transmitter i until which the SINR at receiver j (signal power of transmitter i to the sum of interference and noise) is greater than a reception threshold (ξ_{th}). SINR can be calculated as follows:

Assume that the desired transmitter for a given receiver j is i, then, the SINR $\chi_{ij}^{(s)}$ over channel c_k^s in band s is

$$\chi_{ij}^{(s)} = \frac{P_i^{(s)}}{\left((f^{(s)}d_{ij})^\alpha \left(\sum_{l \neq i, l \in V} \left(\frac{P_l^s}{((f^{(s)}d_{lj})^\alpha}\right) + N_o\right)\right)} \tag{4.7}$$

where P_i^s is the signal power of desired transmitter i, P_l^s is the interference power of transmitter $l \in V \backslash i$ and N_o is the background noise. d_{ij} and d_{lj} are the euclidean distance from transmitter i and interfering transmitter $l \in V \backslash i$ to receiver j, respectively. Other notations are the same as above.

Increased cross device interference will increase the noise floor as more and more devices coexist in the unlicensed spectrum (2.4 GHz) and GSM/LTE (1700-2100 MHz) band. Therefore, from Eqs. (4.6) and= 4.7, it is evident that the SINR will decrease, and thus to maintain a certain required SINR, the transmit power needs to be increased (and energy consumption worsened). However, switching to a whitespace (non-interfered) channel in any other spectrum band using the innovative d-DSA paradigm would allow to achieve the same SINR with a low transmit power, thus saving consumed energy.

Chapter 5 Routing with Static d-DSA Network Architectures

In this chapter, we propose efficient *dynamic band selection* routing approach for the static (or infrastructure) d-DSA network architecture. The key idea of the proposed dynamic band selection routing approach is to intelligently exploit the diverse spectrum bands, and match a certain message requirement to a suitable band, so as to meet the desired quality of service requirements. Recall such a static d-DSA network architecture only constitutes fixed communication infrastructure nodes equipped with d-DSA radio devices, such as, RSUs and lamp posts etc. (See Chapter 3 for the details of the proposed d-DSA architecture.) Specifically in this chapter, we first model the static d-DSA network topology as a directed graph, where each node has the capability of accessing multiple bands in Section 5.1. Since data traffic generated in rural communities are typically valuable only when delivered with a certain hard (or soft) deadline, in Section 5.2 we formulate a linear optimization problem for determining the most energy-efficient route that ensures a delivery time within the hard deadline. After proving that such a problem is NP-Hard, we propose an exact pseudo-polynomial time dynamic programming algorithm to solve it, followed by a polynomial time greedy heuristic. Additionally, in Section 5.3, we formulate a non-linear optimization problem to find the optimal path when the message delivery time is defined as a *soft* deadline, and extend our greedy heuristic to handle soft deadlines. We briefly analyze the benefits of such d-DSA network architecture against resource cost (in terms of d-DSA radio devices) in Section 5.4. Compared to the standard (single-band) band access approaches, our extensive simulation study in Section 5.5 shows that our dynamic band selection approach significantly improves the achievable energy efficiency while meeting various hard and soft deadlines.

5.1   Network Model

As illustrated in Figure 7.1, we model the static (or infrastructure) d-DSA network topology as a directed graph $G = (V, S, E)$, where $V = Q \cup C \cup R$ is the set of all nodes including dropboxes, communication infrastructure nodes and connectivity hubs; S is the set of spectrum band types; and $E \subset (V \times V \times S)$ is the set of all directed links between two nodes over any common (free) channel in any band type. A link $e_{ij}^{(s)} \in E$ is a directed link from node i to node j over band $s \in S$. Hence, there may exist at most $|S|$ unique links between any node pair $i, j \in V$. A message traversing through G is denoted by $m :< u, v, L, T >$ where u is the source, v is the destination, L is the message size, and T is the hard delivery deadline. Now, for any given message m, each link is characterized by a tuple $< w_{ij}^{(s)}(L), \hat{t}_{ij}^{(s)}(L) >$, denoting the energy and latency costs, respectively. Note that, this model is used for hard deadlines while soft deadlines are discussed in Section 5.3.
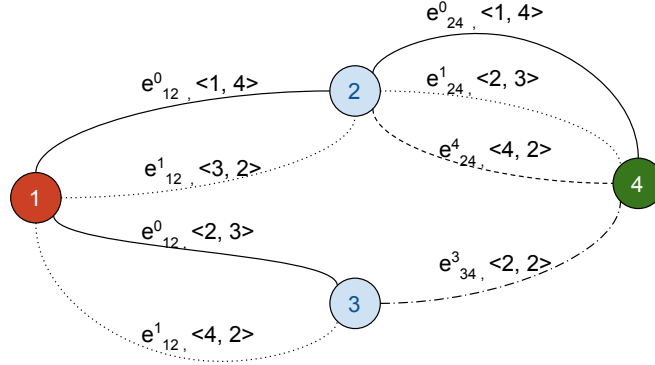
Figure 5.1: Network Model. e_{12}^0 and e_{12}^1 represent the links between node 1 and 2 over band type 0 and 1, respectively. Moreover, the tuples $< 1, 4 >$ and $< 3, 2 >$ signify the energy and latency costs across those links, i.e. e_{12}^0 and e_{12}^1, respectively.

The energy cost $w_{ij}^{(s)}(L)$ refers to the total energy consumed in spectrum sensing and discovery, spectrum hand-off (or switching to an idle channel), and actual message transmission over a free channel in band s. We discussed the calculation of $w_{ij}^{(s)}(L)$ in Section 4.1. On the other hand, the latency cost $\hat{t}_{ij}^{(s)}(L)$ denotes the total delay incurred due message transmission time (see Eq. 4.3), propagation time, and queuing delay (see Eq. 5.6).

5.2 Proposed Routing Approach under Hard Deadlines

In this section, we discuss the proposed *dynamic band selection* routing approach for static (or infrastructure) d-DSA network topology where messages have hard delivery deadline requirements. In such a topology (see Chapter 3), each node possesses global knowledge about the approximate geographical location and spectrum availability at every other node in the network. The key idea of the proposed routing approach under hard deadlines is to intelligently match each heterogeneous message $m :< u, v, L, T >$ to a suitable spectrum band at each intermediate node between the source node u and the destination node v; so as to construct an optimal hard deadline constrained energy-efficient (HcE) path $p(u, v)$. We first formulate the HcE path determination as a constrained linear optimization problem and show that it is NP-hard. Then, we present a pseudo-polynomial dynamic programming (DP) approach that selects both the optimal spectrum band and the intermediate nodes, and thus, constructs an optimal HcE path for any given message. Following it, we propose a faster (though not optimal) polynomial-time greedy heuristic for solving the HcE problem.

HcE Problem Formulation

As mentioned, the HcE path problem aims at determining the most energy-efficient path for any given message that also meets the hard delivery deadline. Although we solve the optimization problem for a certain message m, it will also work well for

concurrent messages. This is because a band is composed of several channels, that can be simultaneously accessed by concurrent messages (should they end up choosing the same band in the same geographical region), unless in the unlikely rare event where the number of such messages exceed the total number of available channels [1]. There may be a small channel access delay due to channel bargaining within the selected band, which is negligible in the range of micro seconds [75], and hence is ignored in the optimization formulation.

Given a directed graph $G = (V, S, E)$, a source-destination node-pair $u, v \in V$, a message $m :< u, v, L, T >$, each link $e_{ij}^{(s)} \in E$ characterized by energy cost $w_{ij}^{(s)}(L)$ and latency cost $\hat{t}_{ij}^{(s)}$, the HcE path problem can be formally defined as:

$$\underset{p(u,v) \in P'(u,v)}{} \sum_{e_{ij}^{(s)} \in p(u,v)} w_{ij}^{(s)}(L) \tag{5.1}$$

where $P'(u, v) \subset P(u, v)$ is the set of all paths from the source node u to the destination node v, which meets the following five constraints:

(i). SINR constraint. For successful decoding of any message m at receiver j, the achieved SINR $\chi_{ij}^{(s)}$ at receiver j must be greater than or equal to prespecified SINR threshold χ_{th}, typically a small value, say -75 dBm.

$$\chi_{ij}^{(s)} \geq \chi_{th} \tag{5.2}$$

(ii). Transmit power constraint. As per the federal communications commission (FCC) guidelines, the maximum transmit power, $P_i^{(s)}$ at any transmitter i must be less than or equal to a fixed value, the maximum effective isotropically radiated power (EIRP), $P_{max}^{(s)}$ over any chosen band $s \in S$.

$$P_i^{(s)} \leq P_{max}^{(s)} \tag{5.3}$$

(iii). Transmission coverage constraint. For successful data communication over any intermediate link $e_{ij}^{(s)} \in p$, the Euclidean distance d_{ij} must be less than or equal to the transmission coverage $\gamma^{(s)}$ achieved in the chosen band s, where $\gamma^{(s)} = \left[G_i G_j \left(\frac{c}{4\pi f^s} \right)^\alpha \frac{\tau}{P_j^s} \right]^{\frac{1}{\alpha}}$ (Refer to Frii's transmission equation Eq. 4.4 for details).

$$\gamma^{(s)} \geq d_{ij} \tag{5.4}$$

---

[1] We can safely infer that majority of channels in a certain band, due to absence of primary users, would be available in the rural context. For instance, at least 80% TV channels are available in rural India at any given time [36].

(iv). Unique spectrum constraint. Any transmitter-receiver node pair $i, j \in V$ must tune to a common available channel in a unique spectrum band $s \in S$. That is, though there are potentially $|S|$ possible links between nodes i and j, only one link over a certain band can be utilized at any point of time (due to hardware constraints).

$$\sum_{s \in S} e_{ij}^{(s)} \leq 1, \quad \forall e_{ij}^{(s)} \in p \tag{5.5}$$

(v). Hard delivery deadline constraint. Any message must be delivered within the hard deadline from its source node u to the destination v. Hence, as shown in Eq. 5.6, the latency cost $\hat{t}_{ij}^{(s)}(L)$ i.e., the sum of message transmission time $t_{ij}^{(s)}(L)$, propagation time $\frac{d_{ij}}{\mathbb{C}}$, and queuing time ($q_\epsilon$) over each intermediate link in the path $p(u, v)$, must be less than or equal to the hard deadline T. Thus,

$$\sum_{e_{ij}^{(s)} \in p(u,v)} \hat{t}_{ij}^{(s)}(L) = \sum_{e_{ij}^{(s)} \in p(u,v)} t_{ij}^{(s)}(L) + \frac{d_{ij}}{\mathbb{C}} + q_\epsilon \leq T \tag{5.6}$$

where $\mathbb{C}$ is the propagation speed of any spectrum (usually speed of the light). The propagation time ($\frac{d_{ij}}{\mathbb{C}}$) and queuing time [2] ($q_\epsilon$) are usually negligible compared to the message transmission time $t_{ij}^{(s)}(L)$. In the generalized term, the total of latency cost is equivalent to the total message transmission time, i.e., $\sum_{e_{ij}^{(s)} \in p(u,v)} \hat{t}_{ij}^{(s)}(L) = \sum_{e_{ij}^{(s)} \in p(u,v)} t_{ij}^{(s)}(L) \leq T$.

Theorem 5.2.1. *The HcE path determination problem is NP-Hard.*

Proof. We provide a reduction from the *Restricted Shortest Path* (RSP) problem [76, 77]. Let us consider a generic instance of the RSP problem. Consider a graph $G_{rsp}(V_{rsp}, E_{rsp})$ where V_{rsp} is the set of nodes and $E_{rsp} \subseteq (V_{rsp} \times V_{rsp})$ is the set of edges. Each edge $e_{ij} \in E_{rsp}$ is associated with a cost c_{ij} and an additional metric t_{ij}. Then, given a source node u, a destination node v, and constraint bound D, the goal of the RSP problem is to determine the least cost path $p_{rsp}(u, v)$ such that $\sum_{e_{ij} \in p_{rsp}(u,v)} t_{ij} \leq D$.

We reduce this RSP problem to an instance of the HcE problem as follows. Consider a d-DSA network topology graph $G(V, S, E)$ where a node in V is created for each node in V_{rsp}. Assume that S contains a single band and an edge is added to E for each edge in E_{rsp}. In addition, for each edge e_{ij} we set $w_{ij}^{(1)}(L) = c_{ij}$ and $\hat{t}_{ij}^{(1)}(L) = t_{ij}$. Finally, we set the hard deadline $D = T$.

Given such an instance, the HcE problem determines the least energy cost path $p(u, v)$ that also meets the hard deadline T. Such path also corresponds to an optimal solution of the RSP problem, since it is the shortest cost path satisfying the constraint D. Therefore, if we were able to solve HcE problem in polynomial time, the RSP

---

[2]This becomes extremely significant under constrained scenarios where the message generation rates are very high and channel availability in certain spectrum bands are limited. We would investigate such constrained scenarios as a part of our future work.

problem will also be solvable in polynomial time. Since RSP is NP-Complete, we conclude that the HcE problem is NP-Hard. □

Dynamic Programming Approach

In the following, we present an exact pseudo-polynomial dynamic programming (DP) algorithm for solving the HcE optimization problem. The DP algorithm intelligently matches a message m to an optimal (energy-efficient) band such that the total energy cost incurred in path $p(u, v)$ is minimized while meeting the hard deadline and other constraints. The proposed DP algorithm is a combination of the Floyd-Warshall algorithm for all pair shortest paths and the dynamic programming solution of the Knapsack problem [78].

Now, for a message m with L bits and a hard deadline T, the graph $G(V, S, E)$ can be represented by a 3D adjacency matrix $A : |V| \times |V| \times |S|$. An element of $A[i, j, s]$ is an ordered pair $< w_{ij}^{(s)}(L), \hat{t}_{ij}^{(s)}(L) >$ where the first and second parts denote the energy and latency costs, respectively, for a message m along the link e_{ij}^s from node i to node j over band $s \in S$.

Here

$$
w_{ij}^{(s)}(L) = \begin{cases} 0, & i = j \\ w_{ij}^{(s)}(L), & i \neq j, \text{ and first four constraints in Section 5.2 are met} \\ \infty & \text{otherwise} \end{cases}
$$

(5.7)

Similarly, $\hat{t}_{ij}^{(s)}(L)$ can be defined.

The proposed DP algorithm is based on the notion of *intermediate node*, defined as follows:

Definition 5.2.1 (Intermediate node)**.** Given a path $p =< 1, 2, ..., (|l| - 1), |l| >$, where nodes in the path are represented as integers, an intermediate node i is one such as $2 \leq i \leq |l| - 1$.

The DP algorithm is based on the following observation. Consider a subset of nodes $\{1, \ldots k\}$. For any node pair $i, j \in V$, let p be the path with the least energy cost, out of all paths between i and j whose intermediate nodes are in $\{1, \ldots k\}$. Then, there are two possible cases:

a) k is not an intermediate node of p: In this case, all the intermediate nodes of path p are in $\{1, \ldots, k-1\}$. Hence, the energy-efficient path from i to j with intermediate nodes $\{1, \ldots, k\}$ is also the energy-efficient path from i to j with intermediate nodes in $\{1, \ldots, k-1\}$.

b) k is an intermediate node of p: In this case, p can be broken into two sub-paths: p_1 from i to k and p_2 from k to j. Since p is the energy-efficient path, k can only appear once in p. Therefore, k can not be an intermediate node of p_1 or p_2. Moreover, *by the principle of optimality (that states that the sub-paths of a shortest path are also shortest paths)*, both p_1 and p_2 are the shortest i.e., energy-efficient paths between i and k, and k and j, respectively, with intermediate nodes in the set $\{1, \ldots k-1\}$. Figure 5.2 provides an illustration.
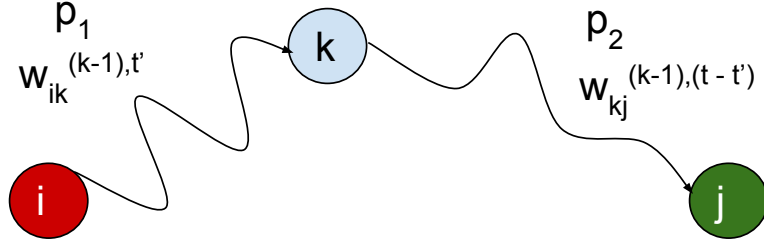
Figure 5.2: Path p is the energy-efficient path from node i to node j with deadline t, and k is the highest numbered intermediate node of path p. Sub-path p_1 from node i to j, has all the intermediate nodes in $\{1, 2, \ldots k-1\}$ and the hard deadline is t'. Similarly, sub-path p_2 from node k to j, has all intermediate nodes in $\{1, 2, \ldots k-1\}$ and hard deadline $(t - t')$.

Let us now define the subproblems used by the DP approach that uses the intermediate nodes used and satisfies the hard deadline. Let $w_{ij}^{(k,T)}$ be the energy cost of the energy-efficient path from node i to j that meets hard deadline T and uses only intermediate nodes in the set $\{1, 2, ..., k\}$. The solutions of subproblems can be formulated recursively as follows, leading to the solution of the overall problem.

1. For $T = 0$, there is no path, hence $w_{ij}^{(k,0)} = \infty$, for each $i, j \in V$.

2. For $k = 0$, there are no intermediate nodes in the path, hence for each $i, j \in V$,

$$w_{ij}^{(0,T)} = \begin{cases} _{s \in S} \ w_{ij}^{(s)}(L), \ if \ \exists \ s \in S \text{ such that } \hat{t}_{ij}^{(s)}(L) \leq T \\ \infty \qquad \text{otherwise} \end{cases} \tag{5.8}$$

3. For $k > 0$ and $T > 0$, we can select a path with the least energy cost either using k as the intermediate node or not. If k is used, let t_1 be the delay over the sub-path between i and k, and t_2 the delay for the sub-path between k and j. In order to ensure that the overall path meets the deadline T, we need to find the value of $t \in [1, \ldots, T]$ such that if given t_1, then $t_2 = t - t_1$. Formally,

$$w_{ij}^{(k,T)} =_{t=1...T} \left(w_{ij}^{(k-1),t}, {}_{,t_1=0...t} \left(w_{ik}^{(k-1),t_1} + w_{kj}^{(k-1),(t-t_1)} \right) \right) \tag{5.9}$$

When $k = |V|$ and $t = T$, we obtain the final solution, which is the total energy cost for the energy-efficient path for each pair of source-destination node-pair with hard deadline T. In other words, $W^{(|V|,T)} = (w_{ij}^{(|V|,T)})$ for all $i, j \in V$.

Algorithm 1: DP Algorithm

Input: Source u, Destination v, T, $A[i,j,s]$ $\forall i,j,s$
Output: Optimal HcE Path $p(u,v)$

1 *//Step 1: Initialization*
2 **for** $i \leftarrow 0$ **to** $|V|$ **do**
3   **for** $j \leftarrow 0$ **to** $|V|$ **do**
4   **for** $t \leftarrow 0$ **to** T **do**
5             $w_{ij}^{(0,t)} =_{s \in S, \hat{t}_{ij}^{(s)} \leq t} A[i,j,s].w_{ij}^{(s)}(L)$;
6   **if** $w_{ij}^{(0,t)} \neq \infty$ *and* $w_{ij}^{(0,t)} \neq 0$ **then**
7                 $P_{ij}^{(0,t)} = i$;
8   **else**
9                 $P_{ij}^{(0,t)} = -1$;

10 *//Step 2: HcE path via band selection*
11 **for** $k \leftarrow 0$ **to** $|V|$ **do**
12   **for** $t \leftarrow 0$ **to** T **do**
13   **for** $i \leftarrow 0$ **to** $|V|$ **do**
14   **for** $j \leftarrow 0$ **to** $|V|$ **do**
15   **for** $t_1 \leftarrow 0$ **to** t **do**
16   **if** $w_{ij}^{(k,t)} > w_{ik}^{(k-1),t_1} + w_{kj}^{(k-1),(t-t_1)}$ **then**
17                         $w_{ij}^{(k,t)} = w_{ik}^{(k-1),t_1} + w_{kj}^{(k-1),(t-t_1)}$;
18                         $P_{ij}^{(k,t)} = P_{kj}^{(k-1),(t-t_1)}$;

19 Recursively navigate path tracking matrix $P_{u,v}^{(|V|,T)}$ to obtain the optimal HcE path $p(u,v)$.

DP Algorithm Description. Algorithm 1 uses a series of 3D matrices $W^{(k,t)}$ for $k = 0, \ldots |V|$ and $t = 0, \ldots T$. The matrix $W^{(k,t)}$ contains the elements $w_{ij}^{(k,t)}$, that is the hard deadline ($1 \leq t \leq T$) constrained energy-efficient path between i and j using the intermediate nodes in $\{1, \ldots k\}$. Also, we keep track of the optimal HcE path in another matrix $P_{ij}^{(k,t)}$. The algorithm has the following two steps:

Step 1 (Initialization): The algorithm first initializes the matrix $W^{(0,T)}$ to $A[i,j,s]$. The HcE path tracking matrix, $P^{(0,T)}$ is also initialized in lines 1 - 12 (see Eq. 5.10).

$$w_{ij}^{(0,t)} = \begin{cases} 0 & \text{if } i = j \\ min\left(w_{ij}^{(0,t-1)},_{s \in S} w_{ij}^{(s)}(L) \right) & \text{if } i \neq j \text{ and } \hat{t}_{ij}^{(s)}(L) = t \\ \infty & otherwise \end{cases} \quad (5.10)$$

Step 2 (HcE path via band selection): After the initialization, the algorithm applies the recursive formula to calculate $W^{(k,t)}$ given $W^{(k-1,t_1)}$ and $W^{(k-1,t-t_1)}$, where $1 \leq$

26

$t_1 \leq t$, as shown in Algorithm 1. Also, the path tracking matrix P is updated recursively (Lines 11 - 19).

Finally, any source node u delivers the message $m(u, v, L, T)$ from a source u to the destination v via the computed optimal HcE path $p(u, v)$ obtained from the path tracking matrix P.

Time Complexity. From the description of Algorithm 1, the time complexity of Step 1 (lines 1 - 12) is $O(|V|^2 T)$, whereas the time complexity of Step 2 (lines 11 - 18) is $O(|V|^3 T^2 + |V|)$, where $|V|$ is the number of nodes and T is the hard deadline. Thus, the overall time complexity of the DP algorithm is $O(|V|^3 T^2)$, which is not polynomial in the input size, since it also depends on the *value* of T. Such time complexity is referred to as pseudo-polynomial.

HcE Greedy Heuristic

This section presents a polynomial time greedy heuristic for an approximate solution of the HcE path $p^*(u, v)$ for a given message in the network. The underlying idea is to calculate a weight h_{ij} for each edge $e_{ij} \in E$ that combines the energy cost $w_{ij}^{(s)}(L)$ with the latency cost $\hat{t}_{ij}^{(s)}(L)$. A parameter $\beta \in [0, 1]$ defines the weighted average between the two, such that $h_{ij} = \beta \times w_{ij}^{(s)}(L) + (1 - \beta) \times \hat{t}_{ij}^{(s)}(L)$. Intuitively, using Dijkstra algorithm [78] and setting $\beta = 0$, we can use such weights to calculate the minimum delay path, which may not necessarily be energy efficient. Similarly, if we set $\beta = 1$ we can calculate the most energy efficient path, which may not meet the deadline T. By increasing β from 0 to 1 in steps of $\Delta\beta$, we can find a path that trade-offs energy efficiency and delay.

The pseudo code of the proposed greedy heuristic is presented in Algorithm 2. Given a value of β the proposed heuristic computes the weighted metric h_{ij} for each node pair i, j which forms the matrix H_{ij}^β as follows (see line 5):

$$H_{ij}^\beta = \beta w_{ij}^{(s)}(L) + (1 - \beta)\hat{t}_{ij}^{(s)}(L) \tag{5.11}$$

The heuristic then calls Dijkstra's algorithm to compute the least weighted path P_{uv}^β from source u to the destination v (line 9) using the values of H_{ij}^β as edge weights. Then, it computes the total energy cost denoted by $E(P_{uv}^\beta)$, and the total latency cost denoted by $T(P_{uv}^\beta)$ in order to compute the least weighted path P_{uv}^β. The above steps (lines 1 - 9) are iterated for all values of β in the increased interval of $\Delta\beta$. Finally, the HcE path $p^*(u, v)$ is chosen as the path with minimum $E(P_{uv}^\beta)$, $\forall \beta$ such that $T(P_{uv}^\beta) \leq T$.

Time Complexity. The time complexity of Algorithm 2 is $O\left(\frac{1}{\Delta\beta}|V|^2 + \frac{1}{\Delta\beta}|V|log(|V|) + \frac{1}{\Delta\beta}\right)$ since the algorithm performs $O(\frac{1}{\Delta\beta})$ iterations and it takes $O(|V|^2)$ time to compute H_{ij}^β, $\forall i, j \in V$. Similarly, it takes $O(|V|log(|V|))$ time to run Dijkstra's algorithm and $O(1)$ time to compute the minimum $E(P_{uv}^\beta)$, $\forall \beta$. Hence, the time complexity of the greedy heuristic is $O(\frac{1}{\Delta\beta}|V|^2)$.

The following theorem proves the non trivial property that the heuristic always returns a solution, if one exists. In other words, the greedy choices of the algorithm,

---

Algorithm 2: Greedy Heuristic

    Input: Source u, Destination v, T, $\Delta\beta$, $A[i,j,s] \; \forall i,j,s$
    Output: HcE path $p^*(u,v)$

1 $\beta = 0.0$;
2   **while** $\beta \leq 1.0$ **do**
3   **for** $i \leftarrow 0$ **to** $|V|$ **do**
4   **for** $j \leftarrow 0$ **to** $|V|$ **do**
5 $H_{ij}^{\beta} =_{s \in S} \left(\beta A[i,j,s].w_{ij}^{(s)}(L) + (1-\beta)A[i,j,s].\hat{t}_{ij}^{(s)}(L) \right)$;

6   Least weighted path, $P_{uv}^{\beta} = $ DIJKSTRA-ALGO (H^{β}, u, v);
7 $\beta = \beta + \Delta\beta$;
8   Compute overall energy cost, $E(P_{uv}^{\beta})$, and latency cost, $T(P_{uv}^{\beta})$ over computed path P_{uv}^{β}

9   Return the path with $\left(\underset{\beta, T(P_{uv}^{\beta}) \leq T}{} E(P_{uv}^{\beta}) \right)$;

---

although potentially not optimal, do not prevent us from finding a path that meets the hard delivery deadline, T.

Theorem 5.2.2. *Provided that there exists at least a HcE path $p'(u,v)$ for a message m with size L and hard deadline T in the d-DSA network, the greedy heuristic will always find such a solution.*

Proof. Consider the weight parameter $\beta = 0$ at the first iteration of the heuristic. Then, the weight metric H_{ij}^{β} is given by $H_{ij}^{\beta} = \hat{t}_{ij}^{(s)}(L)$, $\forall i,j \in V$. This implies the latency cost of each link $e_{ij}^{(s)}$ for a message m is used as the weight. By executing Dijkstra's algorithm with these weights, the path between u and v with minimum latency can be obtained. If such a path meets the deadline T, then this becomes a more energy-efficient path. Otherwise, there exists no solution since all the paths found in the subsequent iterations will not also meet the deadline. This also implies that such path iss the shortest in terms of latency. $\qquad\qquad\square$

5.3   Proposed Routing under Soft Deadlines

In this section, we extend our proposed dynamic band selection routing approach for the static d-DSA network topology to the case in which messages have soft delivery deadlines. Soft deadlines have been largely investigated in the context of real-time systems and scheduling theory [79, 80, 81, 82, 83, 84]. In general, a soft deadline allows a certain message to be delivered after a desired delivery deadline, however by incurring a penalty defined by the *penalty function*. The penalty function is a non-negative function of the message delivery time as explained later in this section. Using the commonly adopted exponential penalty function, we formulate a non-linear programming (NLP) optimization problem, termed the *ScE* problem, to determine an optimal energy-efficient path under soft delivery deadlines. Since NLP problem is

hard to solve practically [85], we extend our proposed greedy heuristic for HcE to solving the ScE problem.

Penalty function

The penalty function increases as the delay in delivering a certain message increases. Thus, the penalty is a non-negative function of message delivery time. There exist several possible definitions of soft deadline requirements, such as: (i) no more than X consecutive deadlines can be missed, (ii) no more than X deadlines in an interval of time T can be missed, (iii) the deadline miss ratio (percentage or total missed deadlines over the total number of deadlines) must not exceed a certain threshold, and (iv) the penalty of delivering a message is zero before a desired deadline T_d; it increases according to a prespecified penalty function up to a maximum tardiness T_{max}, after which the penalty becomes infinity.

In this chapter, we adopt the last definition as also extensively used in real-time scheduling [81, 82, 83]. In this context, it is intuitive to observe that any linear and non-linear increasing function of time with a cutoff at T_{max} can be used for a suitable penalty function. We choose an exponential function $\phi(t)$, where t is the delivery time, as commonly adopted in soft deadline modeling [79]. It is defined as follows:

$$\phi(t) = \begin{cases} e^{\alpha(t-T_d)} & \text{if } T_d < t \leq T_{max} \\ \infty & \text{if } t > T_{max} \\ 0 & \text{otherwise} \end{cases} \tag{5.12}$$

Here, α is an arbitrary non-negative value that controls the penalty growth rate.

ScE Problem Formulation

As aforestated, we formulate the ScE path determination problem as a non-linear programming (NLP) optimization problem. The ScE path problem aims at determining, for any message, an optimal path that maximizes energy efficiency, and simultaneously minimizes the penalty.

Given a directed graph $G = (V, S, E)$, a source node $u \in V$, a destination $v \in V$, a message $m :< u, v, L, T_d, T_{max} >$, and each link $e_{ij}^{(s)} \in E$ characterized by the energy cost $w_{ij}^{(s)}(L)$ and the latency cost $\hat{t}_{ij}^{(s)}(L)$, the ScE problem minimizes the following objective function:

$$\min_{p(u,v) \in P'(u,v)} \Big(\sum_{e_{ij}^{(s)} \in p(u,v)} w_{i,j}^{(s)}(L) \Big) + \phi \Big(\sum_{e_{ij}^{(s)} \in p(u,v)} \hat{t}_{ij}^{(s)}(L) \Big) \tag{5.13}$$

Here $P'(u, v) \subset P(u, v)$ is the set of all paths from the source node u to the destination node v which meets the first four constraints related to the SINR, maximum power, transmission coverage, and unique spectrum described in Section 5.2.

ScE Greedy Heuristic

Following the HcE greedy heuristic, we propose an efficient greedy heuristic to determine the ScE path $p(u, v)$ for any message with soft deadline in the d-DSA network. As shown in Algorithm 2 (Section 19), the HcE greedy heuristic computes the least weighted path P_{uv}^{β} from source u to destination v using the values of the weight matrix H_{ij}^{β} as edge weights. Then, it computes the total energy cost $E(P_{uv}^{\beta})$, latency cost $T(P_{uv}^{\beta})$ for least weighted path P_{uv}^{β}. And, finally the HcE heuristic chooses the path $p^*(u, v)$ as the path with minimum $E(P_{uv}^{\beta})$, $\forall \beta$, such that $T(P_{uv}^{\beta}) \leq T$, the hard deadline. Differently, the ScE heuristic chooses the path $p^*(u, v)$ as the path that minimizes the objective function in Eq. (5.3) across all values of β, that is:

$$p^*(u, v) = \left\{ P_{uv}^{\beta} | \min_{\beta} E(P_{uv}^{\beta}) + \phi\big(T(P_{uv}^{\beta})\big) \right\} \qquad (5.14)$$

We omit the pseudo code of the algorithm, as it can be easily obtained by replacing line 9 of Algorithm 2 with the above equation. This heuristic will also find a solution as long as one exists according to Theorem 5.2.2. The time complexity of the ScE greedy heuristic is $O(\frac{1}{\Delta_{\beta}}|V|^2)$, which is similar to that of HcE heuristic.

5.4 Cost-Benefit Analysis

Many detractors of sustainability argue that energy-efficient (or green) computing incurs higher capital expenditure and operational cost which drains the economy/revenue and makes such designs infeasible in practice. We claim that our proposed approach to dynamic band selection for designing green communication systems, is mostly free from such disadvantages due to following reasons: (i) The use of d-DSA (or DSA) enabled access philosophy does not require a provider to own dedicated spectrum licenses, which is worth millions of dollars; and (ii) Multiple smart communities can be connected by a small set of d-DSA (or DSA) nodes, each costing on the average around $1700 - $1900 [86]. In contrast, our design obviates the need for new dedicated infrastructure such as macro cellular base station ($300,000$/station) or micro cellular base stations ($100,000$)[87] in rural areas, and the need for extensive wire line communications to increase the available bandwidth in urban areas. Also, our approach obviates the burdening of existing networks with additional communication infrastructures such as access points and switches. Some real examples of DSA based deployment has already taken place in relatively rural areas in the developing world, such as Papua [5], Rural South Africa [88], Mexico [89], and the Philippines [90].

To summarize, there is sufficient practical evidence to suggest that the equipment and operational costs of d-DSA (or DSA) network architecture are far less compared to the traditional approaches. The major hurdles are the policy issues which surround spectrum planning. Significant breakthroughs in spectrum policy [26, 22] have been made in recent years; moreover, DSA enabled devices mounted over drones, smart public transport [91], and private smart cars [92] are becoming a reality. Let us reiterate that our proposed architecture and solution approach work on top of existing infrastructures (e.g., public buses) to be mounted with an extended d-DSA radio

device (e.g., ER-N210 [86]) capable of dynamic band access. As a result, our approach notably improves energy efficiency of the network via suitable band selection for varying message requirements. Hence, our proposed approach promises to design green yet cost-effective communication systems for realizing rural communities.

The following theorem 5.4.1 proves that the network energy efficiency can be significantly improved by increasing the number of existing infrastructures, such as public buses or municipal vehicles, mounted with a d-DSA enabled device. However, it comes at a higher equipment cost due to the requirement of a larger number of d-DSA radio devices. As part of our future work, we propose to study the trade-off between the achieved network energy efficiency and equipment cost, for a given rural or urban area.

Theorem 5.4.1. *Given a d-DSA network topology $G(V, S, E)$ with a set of messages (say, M), the energy consumed in the HcE (or ScE) path $p(u, v)$ for any message $m \in M$ either improves or remains unaffected due to the introduction of a new d-DSA node v^* in the network.*

Proof. The introduction of a new node v^* in network G, let the modified network become $G^*(V^*, S, E^*)$ where the node set is $V^* = V \cup v^*$ and the edge set is given by $E^* = E \cup e_{iv^*}^{(s)} \quad \forall i \in V, \forall s \in S$, if $d_{iv^*}^{(s)} \leq \gamma_{iv^*}^{(s)}$. Now, the newly determined HcE (or ScE) path $p^*(u, v)$ in the modified G^* may (or may not) choose one or more intermediate edges from the set $E^* \setminus E$. If the path $p^*(u, v)$ chooses at least one intermediate edge from set $E' \setminus E$, then the energy consumed in $p^*(u, v)$ is less than that of path $p(u, v)$ in the original G. If not, the energy consumed in $p^*(u, v)$ in G^* is the same as that of $p(u, v)$ in G.

Therefore, the energy consumption on the HcE (or ScE) path $p(u, v)$ either improves or remains unaffected with the introduction of a new d-DSA node v^* in the network G. Since the network energy efficiency is the summation of energy savings on each such path for each message $m \in M$, the overall network energy efficiency is also bound to either improve or remain unchanged with increasing number of d-DSA nodes in the network. □

5.5   Experimental Results

In this section, we evaluate the performance of the proposed band selection routing approach that utilizes diverse spectrum band (multi-band) against conventional homogeneous band (single-band) access approaches for the static d-DSA network architecture under both hard and soft deadlines. The performance metrics include: (i) *Energy Efficiency* - the average amount of energy consumed to transfer all generated messages from the sensor blocks to their intended connectivity hubs; and (ii) *Message Delivery Ratio (MDR)* - the fraction of messages successfully delivered to the connectivity hub within the (hard or soft) delivery deadline to the total number of messages generated at the sensor blocks.

For the case where messages have hard deadlines over d-DSA architecture, we first analyze the performance of our proposed dynamic band selection routing ap-

proach using optimal dynamic programming (DP) as well as greedy algorithms for determining HcE paths, against homogeneous band access approaches.

For extensive analysis, we evaluate both the performance metrics considering (i) *varying message sizes*, (ii) *varying hard deadlines*, and (iii) *varying source-destination node pair distances*. The first two parameters represent the message (or QoS) heterogeneity, while the third one represents the geographical heterogeneity. For the scalability analysis, we also analyze how the number of d-DSA nodes in the network impacts the performance metrics of the proposed solution. Finally, we also provide a detailed analysis on the performance of the proposed dynamic band selection approach under soft deadlines.

Simulation Settings: We simulate a simple rural setting with 5 connectivity hubs, 15 dropboxes, 200 communication infrastructures nodes, and 30 sensor blocks, each with 50 - 100 sensing devices. We consider that each d-DSA node has the knowledge of location and spectrum availability at every other node in the network. Unless otherwise stated, we consider that each sensor block generates messages, each of size 250 MB with hard deadline $T = 3$ hours, and the farthest distance between a sensor block and the corresponding connectivity hub is $d = 45$ km.

We consider the usually allowable transmit power for all bands on a secondary basis, such as 1 W for ISM band, 4 W for TV and LTE bands, and 10 W for CBRS band. Recall that each band has a FCC mandated maximum allowable transmit power which can not be exceeded by any node operating on a d-DSA basis. Finally, the considered values of other controlling parameters are as follows: path loss factor $\alpha = 2.5$ (rural area), $SINR = -75$ dBm (3.16×10^{-8} mW), received power threshold (τ) = -20 dBm (0.01 mW), sensing power $\tilde{P} = 40$ mW, probability of switching to the idle channel $\mathcal{P}$ is 0.5, sensing slot duration $t_{sd} = 0.1$ s, transmission slot duration $t_{td} = 1$ s, and energy cost of one channel switching $w_{sw} = 1$ mJ.

Message Heterogeneity

This section evaluates the performance of dynamic band selection approach against homogeneous band access approaches, for varying message sizes and hard deadlines.

Varying Message Sizes: As shown in Figs. 7.7(d), and 7.4(d), the proposed diverse band selection approach outperforms the homogeneous band access approaches in terms of both energy efficiency and message delivery ratio (MDR). The proposed approach achieves an average of 19% energy savings compared to the best homogeneous band access approach (i.e., LTE Band), particularly for message size $L \leq 500$ MB. The reason is evident as the proposed band selection approach utilizes suitable band at each intermediate d-DSA node so as to attain the most energy-efficient path for any given message. For larger message sizes, $L > 500$ MB, the energy consumption by homogeneous band access approaches (except CBRS band) is missing as none of these bands (i.e., ISM, LTE and TV bands) are able to successfully deliver any message of size $L > 500$ MB to the connectivity hub within the hard deadline, i.e., MDR = 0. Note that the ISM band consumes significantly smaller energy, however, it suffers from severely poor MDR, and hence does not meet the QoS requirements.

The greedy heuristic for the proposed approach yields similar energy efficiency as that of the optimal DP algorithm.
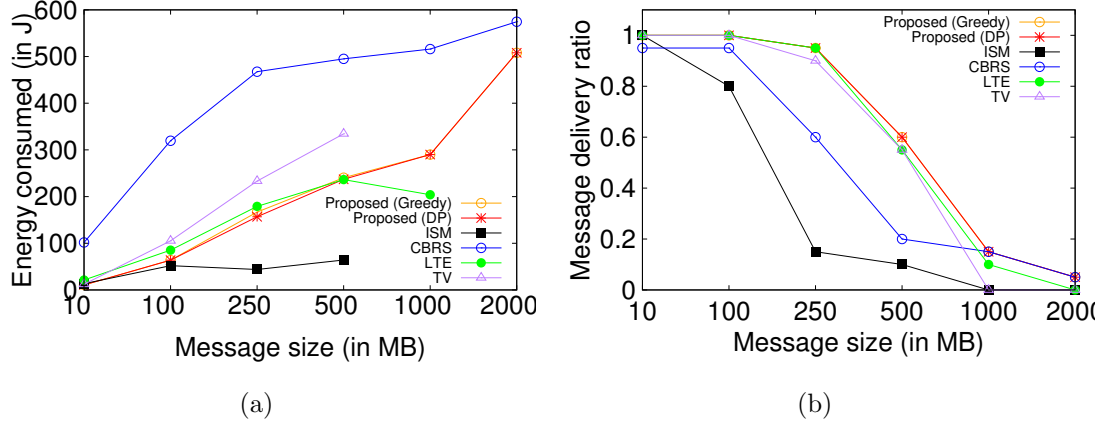
Figure 5.3: Varying message sizes: (a) Energy efficiency, and (b) Message Delivery Ratio

Our proposed approach yields similar or slightly better MDR (up to 5%) compared to the best homogeneous approach, i.e., LTE band for message size $L \leq 500$ MB, and CBRS band for larger message sizes. This is because unlike homogeneous approaches where the node is restricted to access only one predetermined band, the proposed approach intelligently chooses the most suitable energy-efficient band at each intermediate node while guaranteeing the hard deadline for every message and hence MDR or QoS. Recall that for any given message, both DP algorithm, (owing to being optimal) and greedy algorithm (from Theorem 5.2.2) are able to determine a HcE path (if it exists) for a given source-destination pair that meets the hard deadline, and hence always guarantee the highest MDR.
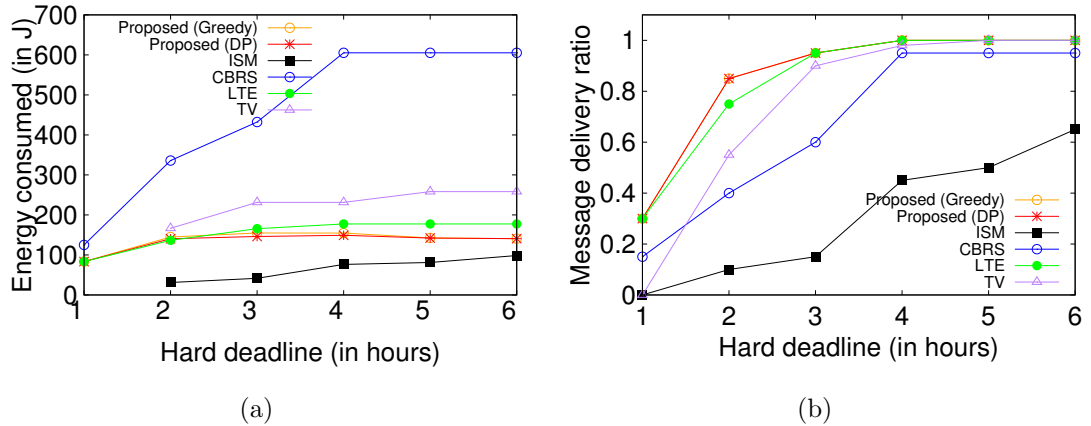
Figure 5.4: Varying hard deadlines: (a) Energy efficiency, and (b) MDR

Varying Hard Deadlines: Fig. 7.7(e) shows that the proposed diverse band selection approach yields better energy efficiency compared to that of the homogeneous band access approaches for increased hard deadlines. Our approach saves energy consumption by up to 22% on the average compared to the best homogeneous band (i.e., LTE band) provided that it also guarantees comparable MDR. Here again, the ISM band yields the best energy efficiency, thanks to the low transmit power; however, it suffers from poor MDR (refer to Fig. 7.4(e)). The CBRS band yields very poor energy efficiency because the transmit power is very high compared to its counterparts.

As shown in Fig. 7.4(e), the proposed multi-band selection approach achieves similar MDR compared to the homogeneous band access approaches. This is because our proposed approach for HcE path determination simultaneously accounts for hard delivery deadlines besides enhancing energy savings. Since the homogeneous band approaches do not have the flexibility of choosing any other band than the prespecified one, they perform relatively poorly. Note that both the greedy heuristic and the DP algorithm work almost equally well in improving energy efficiency and MDR irrespective of varying hard delivery deadlines.
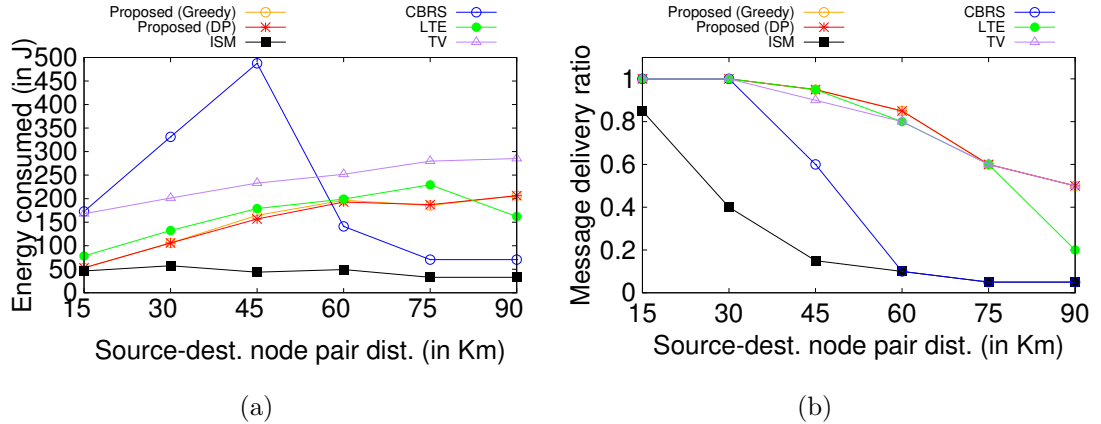
Figure 5.5: Geographical Heterogeneity: (a) Energy efficiency, and (b) MDR

Geographical Heterogeneity

As depicted in Figs. 5.5(a) and 5.5(b), the dynamic band selection approach outperforms the homogeneous band access approaches in terms of both energy efficiency and MDR for varying source-destination node-pair distances (this is geographical heterogeneity). The proposed approach enhances energy efficiency by up to 32% compared to the best homogeneous band access approach that also yields comparable MDR, particularly for distance $d \leq 60$ km. We observe that the CBRS band yields very poor energy efficiency until distance $d \leq 45$ km and then, improves significantly. This is because the CBRS band, owing to its limited transmission coverage, is not able to deliver messages successfully, and therefore do not dissipate energy in message transmission, for larger distances between source-destination node-pairs. The ISM band

34

again owing to its low transmit power, yields significantly better energy efficiency; however it suffers greatly in terms of MDR, thus defeating the purpose of effective and efficiency rural connectivity.

Our proposed approach achieves slightly better MDR (about 7% on an average) compared to the LTE Band, the best homogeneous band selection approach. The reasons are as explained above. The greedy heuristic works very well in determining optimal HcE path, and hence yields similar energy efficiency and MDR as that of the DP algorithm employed for band selection.

Cost-benefit Analysis

We evaluate the benefits of the dynamic band selection approach in terms of both energy efficiency and MDR (QoS) against varying number of d-DSA nodes in the proposed infrastructure d-DSA network architecture.
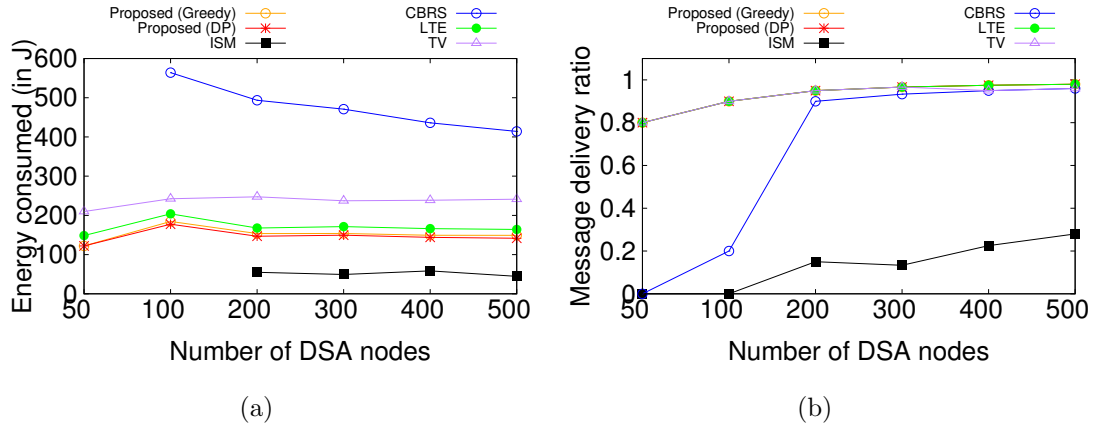
Figure 5.6: Varying number of d-DSA nodes: (a) Energy efficiency, and (b) MDR

As shown in Figs. 5.6(a) and 5.6(b), the proposed band selection approach largely outperforms all homogeneous band access approaches in terms of both energy efficiency and MDR, irrespective of the number of d-DSA nodes. Our approach enhances energy efficiency by up to 18% compared to the best homogeneous band (i.e., LTE Band). Furthermore, the energy consumption increases with increase in the number of d-DSA nodes until $|V| = 100$. After that, it gradually decreases until $|V| = 300$ nodes and remains almost unchanged afterwards. This is because initially $|V|$ itself is small and yields slightly lower MDR, thus the energy consumption in delivering messages is also less. In contrast, when $|V|$ is sufficiently large, say ≥ 200, the proposed approach is able to determine better energy-efficient paths, and so consumes less energy at each intermediate node while achieving very high MDR.

Energy consumed by ISM and CBRS bands are 0 J for $|V| \leq 200$ and 100, respectively. This is because none of the messages was delivered to their intended connectivity hub within hard deadlines; therefore they are not desirable for data communication in rural context (see Fig. 5.6(b)). Moreover, the greedy heuristic also

determines near-optimal HcE paths and achieves similar energy efficiency and MDR as that of the DP algorithm using the proposed approach.

Band Selection Analysis

This section investigates how our proposed band selection approach dynamically chooses suitable band types at the intermediate d-DSA nodes for each message, thereby enhancing energy efficiency of the network while meeting the QoS. As shown in Figs. 5.7(a) - 5.7(d), the proposed approach extensively utilizes the ISM and LTE bands, compared to the other two remaining bands. This is reasonable given that the simulated rural scenario is characterized by $|V| = 200$ and $d = 45$ km, forming a relatively dense d-DSA network topology. Now, given that the message size $L = 250$ MB and the hard deadline $T = 3$ hours, it becomes a suitable case for ISM and LTE bands to achieve energy-efficient data communications. This is because these bands are characterized with relatively low transmit power, good bandwidth and comparatively good coverage.
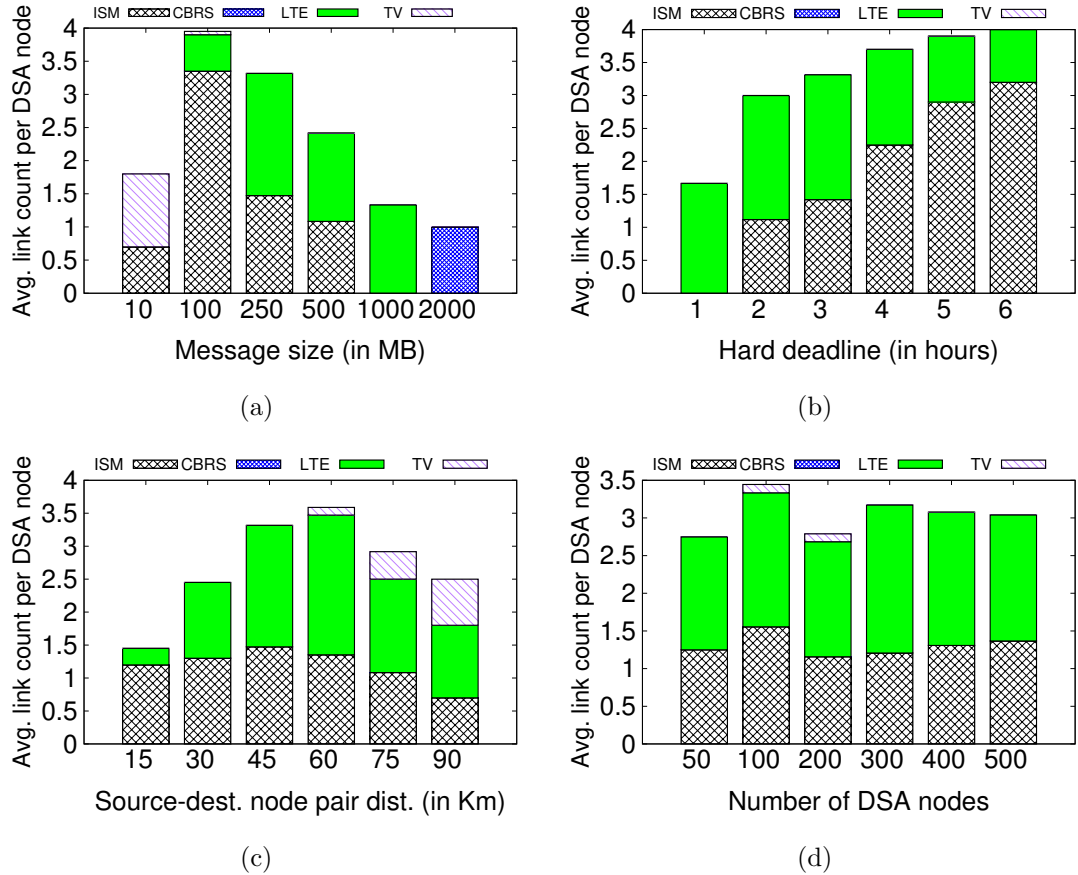
Figure 5.7: Band selection analysis: (a) Message sizes, (b) hard deadlines, (c) Source-destination node pair distances, and (d) Number of d-DSA nodes

However, as shown in Fig. 5.7(a), for message size $L < 250$ MB, our dynamic band selection approach also utilizes the TV band for energy-efficient message transmissions. This is because the TV band offers energy-efficient HcE paths for lower message sizes, thanks to its sufficiently adequate bandwidth (6 MHz) and very high transmission coverage (several kms). It is interesting to note that messages with size $L = 2000$ MB were delivered with hard deadline over the CBRS band only. The reasons is unlike other bands, the CBRS band offers high bandwidth and therefore requires very low transmission time and meets hard deadlines, for larger message sizes.

As shown in Fig. 5.7(b), the proposed approach utilizes the ISM band more with increasing hard deadline. This is evident because this band, owing to its low transmit power, can now be utilized along energy-efficient paths that meet hard deadlines, for larger number of messages.

Similarly, as shown in Fig. 5.7(c), for larger source-destination node-pair distances $d > 45$ km, the proposed approach again significantly utilizes the TV band for delivering messages in an energy-efficient manner. Intuitively, the TV bands offer high transmission coverage, and thus proves to be useful bands for energy-efficient communications for higher distances. Note that the CBRS bands are rarely utilized by the proposed approach due to the fact that it offers limited coverage and requires very high transmit power.

Finally, as shown in Fig. 5.7(d), the proposed approach utilizes the ISM band more for increasing number of d-DSA nodes. This implies, as the network gets denser, the ISM band can be utilized for energy-efficient communications at the intermediate nodes of HcE paths for larger number of messages.

Soft Deadlines Analysis

In this section, we study the performance of the proposed band selection approach for the infrastructure d-DSA network topology where messages have soft deadlines. For the experiments, we consider the same rural scenario discussed in the simulation settings. The values of all parameters including the message size, the number of d-DSA nodes, and source-destination distance are also kept unchanged. Finally, we set the desired deadline to $T_d = 2$ hours. The performances are discussed in terms of message delivery ratio (MDR) and energy efficiency against the maximum tardiness T_{max} and the penalty growth rate α defining the penalty function (see Eq. 5.12).

Figure 5.8(a) shows the values of the penalty function under several settings of α and T_{max}. As expected, the penalty value is 0 before the desired deadline T_d (2 hours in our experiments), irrespective of the growth rate, α. However, after T_d, the penalty value grows exponentially, and different values of α strongly influence the growth rate, making the penalty value more or less dominant in the objective function in Eq. (5.3). This aspect will be necessary to understand the following results.

Figure 5.8(b) demonstrates the energy consumption by increasing T_{max}, under different settings of α. By keeping the desired deadline T_d fixed and increasing T_{max}, there are more potential paths that can be followed. As a result, we can initially deliver more messages, and consequently increase the energy consumption until the

(a)

(b)

(c)

(d)
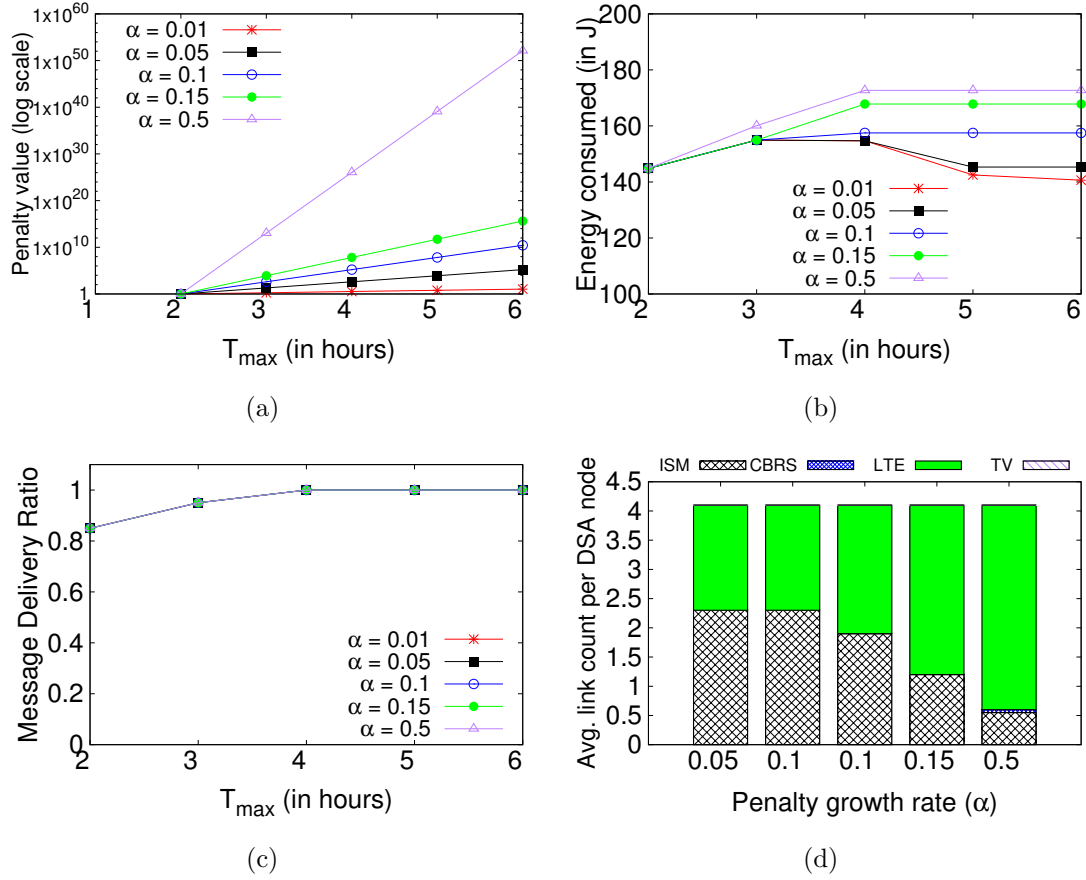
Figure 5.8: Soft deadlines: a. Energy Efficiency, b. Message Delivery Ratio (MDR), and c. Band selection

MDR saturates around 4 hours (see Fig. 5.8(c)). After that time, the value of α determines the trend of the energy consumption. Specifically, if α is low (0.01, 0.05), the impact of the penalty function is minimal, and the algorithm would target paths which may deliver the messages later but are more energy efficient. Conversely, if α is high (say ≥ 0.1), the penalty function makes these paths unattractive, orienting the algorithm towards less energy-efficient paths that would deliver the messages sooner. To further support this observation, Fig. 5.8(d) shows the breakdown of the average link counts per d-DSA nodes for varying values of penalty growth rate α. Clearly, as the penalty function becomes more dominant, the LTE bands are preferred over the ISM bands, since they lower transmission times at the cost of higher energy consumption, as discussed in Section 4.1.

Figure 5.8(c) depicts the MDR for varying T_{max} under different settings of α. Intuitively, MDR is bound to increase with the increase in T_{max}. However, the MDR remains unaffected by change in α. This is because, provided there exists at least one valid path for any message that meets soft deadline requirement, our proposed heuristic would always find a solution (similar to Theorem 5.2.2 for messages with

hard deadlines).

We do not show the plots for homogeneous band selection approach as they remain unaffected by the change in T_{max} or α. This is because, as shown in Eqs. 4.2 and 4.3, the message transmission time is directly proportional to the energy consumed for a fixed pre-determined band. Hence determining an energy-efficient path is equivalent to determining a path with the least transmission time. It is intuitive that energy efficiency and MDR achieved by our proposed approach would be significantly better than the homogeneous band access approaches, irrespective of varying T_{max} values and lower α values. Even for a higher value of α, the energy efficiency achieved by our proposed approach is either better or comparable to the best homogeneous (LTE) band as shown in Fig. 5.8(d). Finally, we observe that the MDR and energy efficiency results corresponding to the soft deadlines are consistent with those corresponding to the hard deadlines for varying contextual factors, such as message sizes, source-destination node pair distances, and the number of d-DSA nodes. Such plots are not shown here for brevity.

To summarize, the proposed band selection approach outperforms the homogeneous band access approaches for any message with hard or soft deadlines, in terms of both energy efficiency and MDR under all contextual factors such as message and geographical heterogeneity. This concludes that the proposed d-DSA architecture and dynamic band selection approach are promising solutions for designing energy-efficient communication systems for ubiquitous connectivity in rural areas.

5.6   Conclusions of This Chapter

In this chapter, we proposed an efficient routing scheme for the envisioned infrastructure d-DSA network architecture in rural communities, in which the locations of the communication devices are fixed. Specifically, we discussed how the proposed routing approach exploits distinct electro-magnetic characteristics of various spectrum bands, and intelligently matches any message requirement at each d-DSA node, to a suitable band type for achieving the desired QoS requirements, i.e., maximize energy-efficiency while ensuring pre-specified hard/soft delivery deadlines. Following this, we formulated the determination of hard deadline constrained energy-efficient (HcE) path as a linear optimization problem and proved that it is NP-Hard. Subsequently, we proposed a pseudo-polynomial dynamic programming algorithm to solve the HcE problem exactly and determine the optimal HcE path (and hence optimal band at each intermediate node) for any given message. We further proposed a greedy heuristic that provides a faster yet effective solution to the HcE problem. Additionally, we investigated our proposed (dynamic band selection) routing approach under scenarios where messages have soft deadlines. Compared to the homogeneous band access routing approaches, our proposed dynamic routing solution significantly improved the network energy efficiency while meeting various hard and soft delivery deadlines, irrespective of varying message and geographical heterogeneity.

Though our proposed approach is a good starting point and shows a great potential for achieving d-DSA network architectures for effective and efficient connectivity to rural communities, there are several future directions those need to be explored

and addressed. First, we would reformulate the centralized optimization problem of determining energy-efficient routes with hard/soft (or no) deadlines by considering (i) multiple concurrent messages with varying message generation/arrival rates, instead of a single message, (ii) limited channel availability within each spectrum band, (iii) infrastructure nodes with potentially MIMO capability (multiple antennas), (iv) limited memory and computational capability at each d-DSA node, and (v) interference from other secondary d-DSA nodes. Second, a centralized approach may not always be feasible in a rural setting, particularly considering the fact it may not always be feasible to have a dedicated common control channel that would accurately disseminate the network information in real-time. Hence, we would also investigate designing a distributed routing approach based on Reinforcement Learning, which bypasses the need of a dedicated common control channel, and enables each node to choose a suitable band and next-hop node, only based on the local network information.

Chapter 6 Routing with Dynamic yet Sufficiently Predictable d-DSA Architectures

In this chapter, we design efficient routing strategy, called *Diverse DSA aware Routing* (dDSAaR) for time-varying yet sufficiently predictable d-DSA network architectures, which are based on public transportation vehicles. Such an architecture is particularly suitable for providing connectivity to scenarios, where the fixed infrastructure is not able to provide the full coverage, a typical scenario in rural setting. In this chapter, we first model such sufficiently predictable d-DSA networks as *time-varying* graph in Section 6.1. Next in Section 6.2, we describe the details of the proposed dDSAaR protocol. The proposed protocol jointly exploits (i) the electro-magnetic characteristics of diverse set of spectrum bands, including licensed TV, LTE, CBRS bands, and unlicensed ISM band, and (ii) sufficiently predictable mobility of public transportation vehicles, in order to determine suitable message communication routes in the d-DSA network topology. More specifically, the protocol first gathers historical network information, such as public transportation mobility patterns and message sizes. It then uses a novel representation of the time-varying d-DSA network topology termed Space-Time-Band (STB) graph, that comprehensively includes spatial, temporal and band type information. Finally, the protocol computes the suitable communication route for each message, which includes the set of *suitable relay nodes* and the *optimal band type* at each relay node, such that the selected route enhances the network quality of service. Finally, we discuss the experimental evaluations in Section 6.4, and concluding remarks in Section 6.5.

6.1   Network Model

Since the location of nodes, their potential communication interactions over diverse bands and the channel availability in each spectrum band, and primary users' activities co-evolve over time, the d-DSA network can be considered as a *time-evolving network*. Unlike [93], such network can be effectively modeled as a sequence of graph snapshots, rather than a static graph. Each snapshot considers the nodes and their potential interactions over multiple bands at a certain time instant. Fig. 6.1 illustrates an example graph where nodes 1 and 2 can communicate over band 0 at time instant 0, whereas at time 1, they can communicate over both bands 0 and 1.

Consider a total time duration T, say 24 hours, to be divided into discrete and equal time slots, such as $\{0, 1, \ldots T\}$. At a given time slot t, let $G^t = \{V, S, E^t\}$ be a directed graph that represents the snapshot of d-DSA network, where V is the set of nodes, S is the set of bands, and $E^t \subseteq (V \times V \times S)$ is the set of directed communication links between node-pairs over any band at time slot t. We consider S = {TV, LTE, ISM, CBRS} where DSA is allowed (or in memoranda) by FCC, however, it can easily be extended to any other (un)licensed bands where DSA is allowed. Moreover, for ease of presentation, we assume that V is constant over time,
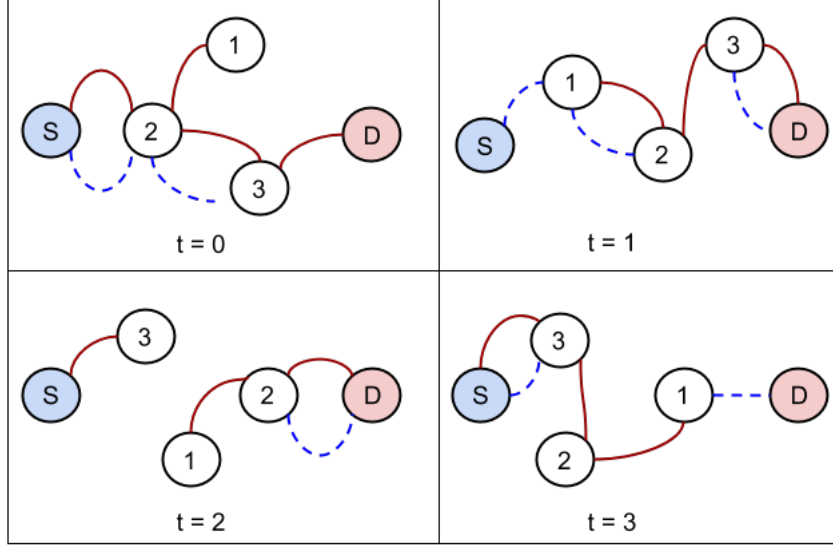
Figure 6.1: A time-evolving d-DSA network. Solid-black and dashed-brown links between any two nodes indicates the potential communication link over band types 0 (say TV band) and 1 (say LTE band), respectively.

whereas the set of potential links over different bands may change due to the varying node positions, primary user's activities, spectrum transmission range, and so on. Our approach can be suitably extended to consider scenarios where nodes join and leave the network. We model the time-evolving d-DSA network as a sequence of such graph snapshots $\{G^t | t = 1 \ldots T\}$.

Link existence. At time slot t, two nodes can communicate over a band type $s \in S$ only if their geographical distance is within the communication range γ^s. Given two nodes $v_i, v_j \in V$ at time slot t, we define the time varying *link function* $L_{ij}^{t,s}$ over band type s to be equal to 1, if v_i and v_j are within distance γ^s, and 0 otherwise. See Fig. 6.2 for illustration of link existence function in correspondence with the example graph shown in Fig. 7.1.

Network traffic. Although there could be messages with arbitrary sizes, we consider $\mathcal{M}$ discrete bins of size q, where each bin defines a *message type*. Consider a message $m = < id, u, d, c, t_m >$ with a unique identifier id, type c (i.e., size cq), generated by a source u at time t_m for a destination node (i.e., a hub) d. Now at an arrival time t, the *message transmission delay* [1], [2] incurred in transmitting the message m

---

[1] We do not consider channel access (or switching) delay as part of the message transmission delay $(\mathcal{T}_{ijc}^{t,s})$, as it is usually negligible (in the range of microseconds) compared to the actual data transmission.

[2] For simplicity, for a certain message m of type c, we consider that the message transmission delay $\mathcal{T}_{ijc}^{t,s}$ do not change for a given band s, for varying geographical locations, and times. This
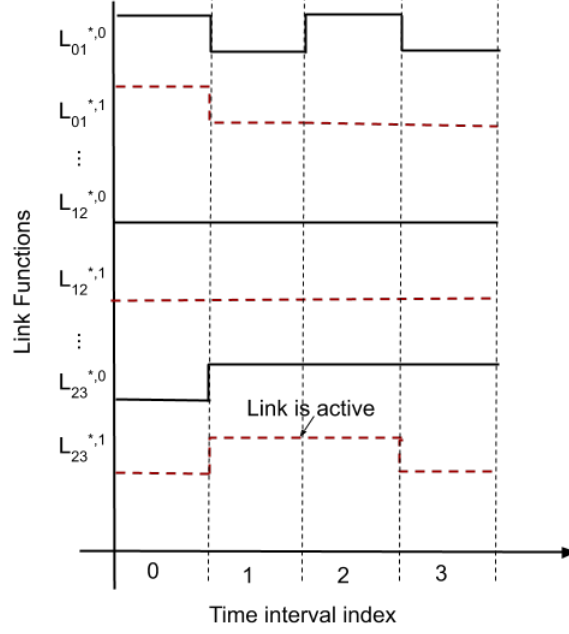
Figure 6.2: Time-varying link functions for all pair of nodes over band types 0 and 1 in the considered example d-DSA network graph in Fig. 6.1

from node v_i to v_j over band s, is given by

$$\mathcal{T}_{ijc}^{t,s} = \frac{cq}{\mathbb{R}_{ij}^{t,s}} = \frac{cq}{B_{ij}^{t,s} log_2(1 + \chi_{ij}^{t,s})} \qquad (6.1)$$

where $\mathbb{R}_{ij}^{t,s}$ is the effective bit rate of a channel in band s, and is calculated (using Shannon-Hartley theorem [74]) as $\mathbb{R}_{ij}^{t,s} = B_{ij}^{t,s} log_2\left(1 + \chi_{ij}^{t,s}\right)$, where $B_{ij}^{t,s}$ and $\chi_{ij}^{t,s}$ are respectively the channel bandwidth and the received signal power to noise ratio (SINR). Note that even for the same message type c (or size cq), the transmission delay $\mathcal{T}_{ijc}^{t,s}$ varies from one band to another, mainly due to the distinct channel bandwidth $B_{ij}^{t,s}$ offered by each band. For example, the TV and CBRS bands usually offer channel bandwidth of 6 and $40 - 60$ MHz, respectively. Refer to Fig 7.4 for details of typical bandwidths offered by various bands.

Message transmission. Consider that node v_i starts the transmission of message m at time t_a. The transmission is successful only if v_i and v_j are in the communication range γ^s for $\mathcal{T}_{ijc}^{t,s}$ time units. Conversely, m can be transferred from v_i to v_j over band s only if $L_{ij}^{t,s} = 1$, $\forall t \in \{t_a, (t_a + \mathcal{T}_{ijc}^{t,s})\}$.

In this work, we consider that *a message m needs to be delivered to its destination node with least network delay*, which is possibly the most common performance metric. (We restrict our discussion to network delay as a performance metric of interest.

---

assumption ensures that m takes the exact same $\mathcal{T}_{ijc}^{t,s}$ time units over band s between any node pair at any location and/or time. However, it is straightforward to adapt the formalism for varying $\mathcal{T}_{ijc}^{t,s}$, by incorporating path loss factor, noise level etc.
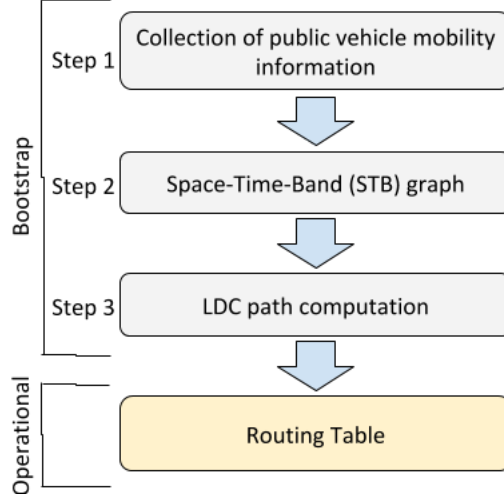
Figure 6.3: Overview of dDSAaR protocol

However, other metrics, such as energy consumption and number of spatial hops could be also incorporated.) Hence, the proposed dDSAaR protocol (discussed in the next section) primarily focuses on determining the *least delay cost* (LDC) communication path for each message in the network.

6.2 dDSAaR Routing Protocol

This section describes the proposed *diverse DSA aware routing* (dDSAaR) protocol which is at the basis of the d-DSA architecture. Specifically, the protocol works in two discrete rounds - the *bootstrap* and the *operational* rounds (See Fig. 6.3). A *round* length is defined by the round trip time of all vehicles (i.e., time duration between leaving and reaching the depot). Since, the round trip time for a certain vehicle may vary from another, we consider the least common multiplier of all round trip times in our experiments. In the bootstrap round, the protocol comprises three steps - (i) *Collection of historic mobility information of data mules*, (ii) *Construction of the space-time-band (STB) graph*, which provides a comprehensive view of the dynamic d-DSA network topology across space, time and band dimensions, and (iii) *LDC path computation*, where the LDC path is computed for each source-destination pair, message type $c \in \mathcal{M}$ and generation/arrival time $t \in [0, T]$. The resulting communication paths will represent the routing decision that will be employed for the next (i.e., operational) round. Specifically, such paths are shared (via hubs) in the form of *STB routing tables* with each d-DSA node in the network. Note that, while only the network manager [3] is active during the bootstrap (and runs all the three steps), all d-DSA nodes participate in the operational round.

---

[3]Recall the envisioned d-DSA architecture based on sufficiently predictable public transportation vehicle considers a prespecified connectivity hub as the network manager, which has access to the centralized geo-location whitespace database, and collects vehicle's mobility information over time. Refer to Chapter 3 for the details.

Table 6.1: Spectrum band profile

Band (MHz)	Frequency (MHz)	Bandwidth (MHz)
TV (54-216, 470-698)	600	3-6
LTE (700-900, 1700-2100)	900	20-30
ISM (2400-2500, 5700-5800)	2400	8-20
CBRS (3500-3700)	3500	40-60

Table 6.2: Overview of STB routing table at a node i

Message Type	Dest. Node	Time of Message Forwarding Lookup					
		0	...	t	...	t'	...
⋮	⋮	⋮	⋮	⋮	⋮	⋮	⋮
1	d_j			Store 2, Forward k, Band 1		Store 0, Forward l, Band 3	
⋮	⋮	⋮	⋮	⋮	⋮	⋮	⋮

Space-Time-Band (STB) Routing Table. As shown in Table 6.2, the STB routing table is a 2-D matrix, where the first column represents the message type, second column the destination node, and the rest represent the time layers (of the STB graph). For instance, an entry $< 2, k, 1 >$ denotes that a certain message (of type 1) to be transmitted to destination d_j at time t has to be stored (at current node i) for 2 time units before forwarding to node k over band 1. We refrain from discussing the selection of a common whitespace channel, out of all unoccupied channels, within a chosen band 1 between the node pair i and k (at time t) because such issues have been extensively studied in literature [20, 5]. (The list of whitespace channels in a certain band will be also shared by network manager along with STB routing table.)

Although, evident from DieselNet (See Figs. 6.4 and 6.5 showing bus routes for two consecutive rounds. Each color represents a transport vehicle.), the d-DSA network topology is sufficiently predictable, the network topology on the subsequent bootstrap and operational rounds may not be exactly the same, possibly due to events, e.g., traffic jams, delays and accidents since transport vehicles are involved. To address this, our protocol allows, during an operational round, a certain message to be stored at the current node until the next relay node for the current time is available. It is worth noting that such an approach will likely increase the network delay (also evident from experiments). Conversely, long term changes, such as new or different vehicle routes, are handled by a new bootstrap round, thus constructing an updated STB graph with the recent information. In normal scenarios (with no frequent long-term changes), one bootstrap will suffice subsequent multiple operational rounds.
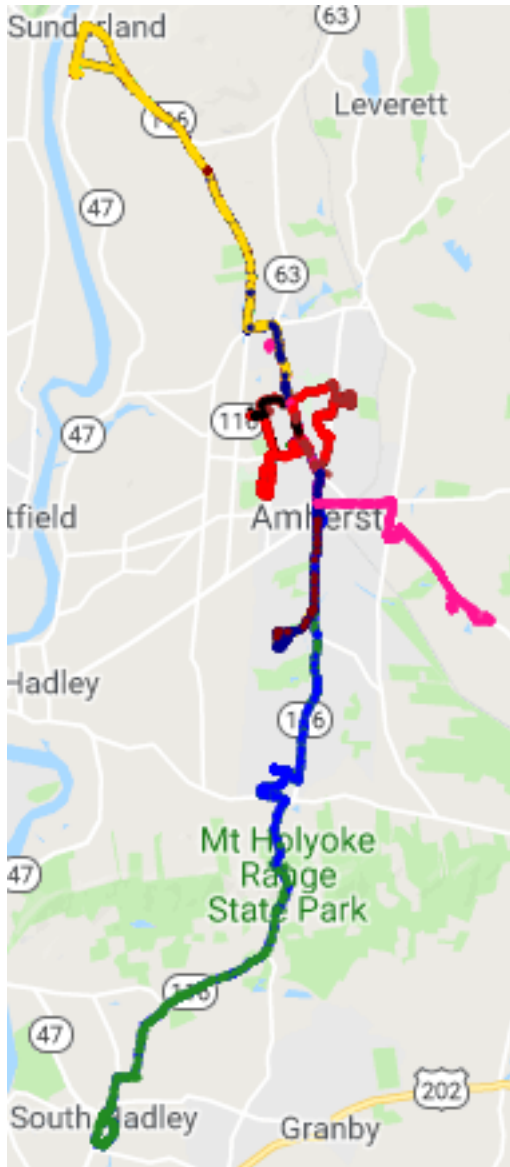
Figure 6.4: Bootstrap Round
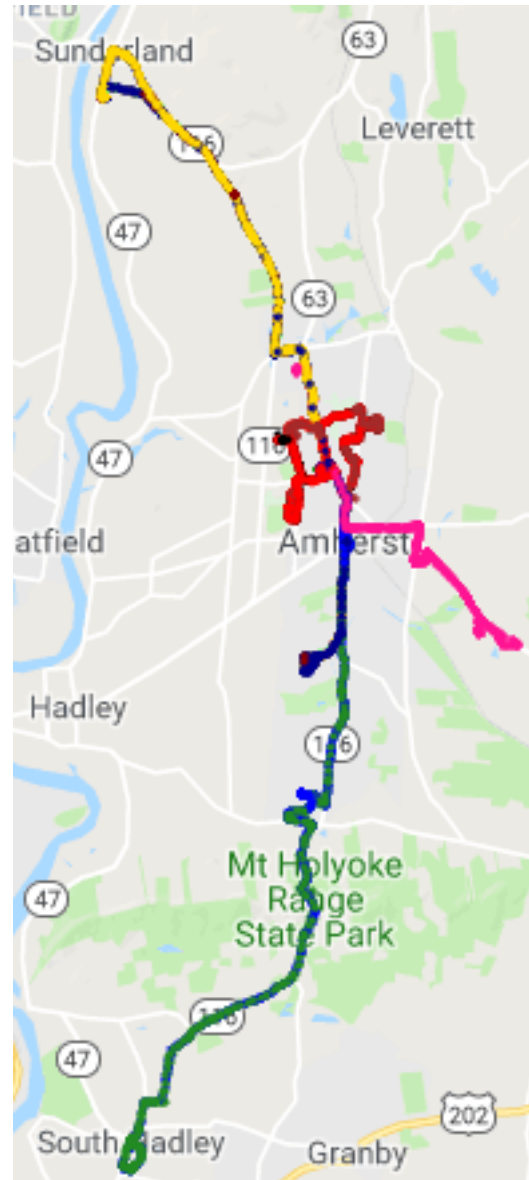
Figure 6.5: Operational Round

Figure 6.6: Bus route trajectories for two consecutive rounds – bootstrap round (morning [11 : 00 - 2 : 00] pm) and operational round (evening [2 : 00 - 5 : 00] pm) on Nov 6, 2007. Each color represents a bus traveling on its route.

Collection of Historical Network Information

The first step of the proposed protocol is to gather following historical network information, such as data mules (i.e., buses) mobility traces, Primary users' locations and activities, message traffic types, and message traffic requirements.

Data mules Mobility Information. The data mules, either public buses or service vehicles, follow predetermined schedules to reach, stay, and leave certain sensor blocks, as discussed in Chapter 3. For example, in case of DakNet, each bus makes 3 trips to a certain village on each day. Moreover, the bus waits approx. 9 mins at each stop. Given the fact that our work is based on the recurrent mobility patterns of data mules, their mobility information become a key part of the forwarding decision.

Message Traffic Information. The messages generated within a sensor block may have heterogeneous message sizes, which we categorize as different message types as discussed in Section 6.1. Given the distinct EM properties (esp. transmission range and channel bandwidth) of various bands, as discussed in Chapter 4, the message type is also an important factor for the forwarding decision.

   Hence according to our protocol, the network manager collects these information in the current bootstrap round, which are used to calculate the forwarding opportunities in the subsequent (one or more) operational rounds.

Space-Time-Band (STB) Graph

Given the historical mobility information of data mules (collected during bootstrap round) and the recent spectrum band information (obtained from the whitespace database), the network manager constructs the series (or sequence) of graph snapshots $\{G^t | t = 1 \dots T\}$, modeling the time-evolving d-DSA network. This series of graphs is used for the construction of the Space-Time-Band (STB) graph $\mathcal{G} = (\mathcal{V}, \mathcal{S}, \mathcal{E})$, which is a novel graph model comprehensively capturing the communication opportunities across space, time and multiple bands. The proposed STB graph is extended from the time expanded graph model proposed in the theory of network flows by Ford and Fulkerson [94]. Primarily, the STB graph $\mathcal{G}$ is a layered graph, where each layer corresponds to a discrete time interval of length τ defined as follows.

Definition 6.2.1 (Discrete time interval τ). Given the graph snapshots $\{G^t | t = 1 \dots T\}$ of the d-DSA network, the set of message types $\mathcal{M}$, and the set of bands S, the *discrete time interval* τ for the STB graph $\mathcal{G}$ is defined as the least *message transmission delay* $\mathcal{T}_{ijc}^{t,s}$ for any two nodes $v_i, v_j \in V$, at any time slot t, for the smallest message type (i.e., $c = 1$), over the band with the highest bit rate,

$$\tau = \min_{s \in S, \ i,j \in V} \mathcal{T}_{ij1}^{t,s} \tag{6.2}$$

   The time interval τ represents the time unit of the STB graph, therefore we also want the transmission delay $\mathcal{T}_{ijc}^{t,s}$ and the link function $L_{ij}^{t,s}$ to be expressed with the

same time resolution. Since these may not be exactly multiple of τ, we proceed as follows. The transmission delay is upper bounded to the next multiple of τ, and a message with such transmission delay can be transferred between v_i and v_j only if the link function equals 1 for the entire upper bounded transmission delay period, as detailed in the following.

Approximation of $\mathcal{T}_{ijc}^{t,s}$ and $L_{ij}^{t,s}$. We approximate the message transmission delay for every message type over any given band type as a multiple (z) of τ, where $z \in \{1, 2, \ldots Z\}$ and Z is maximum possible message transmission delay, i.e., $Z = \left(\max_{t \in T, s \in S, i, j \in V} \mathcal{T}_{ij|\mathcal{M}|}^{t,s} \right)$.

   Example 1. Consider the snapshot of d-DSA network at time slot $t = 1$ in Fig. 6.1 and two types of messages $c = 1$ with message size $q = 10$ Mb, and $c = 2$ with message size $2q = 20$ Mb. There are also two bands 0 and 1, which offer an effective bit rate of 6 and 20 Mbps between each node pair, respectively. Then, $\tau = \min \mathcal{T}_{ij1}^{t,s} = \frac{1q}{B_{ij1}^{1,2}} = \frac{1 \times 10}{20} = 0.5$ seconds. Since $\mathcal{T}_{ij2}^{1,0}$ is $\frac{2 \times 10}{6} = 3.33$, we upper bound it to the next multiple of τ, that is $\mathcal{T}_{ij2}^{1,0} = 3.5$, equivalent to 7τ. Regarding the link function ($L_{ij}^{t,0}$), consider forwarding a message of type 2 at time $t = 1$, from node i to j over band 0. Then, $L_{ij}^{t,0} = 1, \forall t \in [1, 1 + \mathcal{T}_{ij2}^{1,0}]$. Here since $\mathcal{T}_{ij2}^{1,0} = 3.33$, the time interval would be $[1, 4.33]$. However, we allow this transmission opportunity only if the link exists during the time interval $[1, 4.5]$, equivalent to the interval $[2\tau, 9\tau]$.

   Likewise, we approximate the link function for different pair of nodes over any given band type as a multiple l of τ. Again consider the above snapshot of d-DSA network at time slot $t = 1$. Here, $\tau = 0.5$ seconds. Consider forwarding any message of type 2 starting from time $t = 1$ seconds, from node i to j over band type 0, then the link function $L_{ij}^{t,0} = 1, \forall t \in [1, 1 + \mathcal{T}_{ij2}^{1,0}]$. Here since the transmission delay is $\mathcal{T}_{ij2}^{1,0} = 3.33$, the message transmission interval will be $[1, 4.33]$. We approximate this time interval by $[1, 4.5]$, equivalent to $[2\tau, 9\tau]$. Here $l = (9 - 2) = 7$.

   These approximations of message transmission delays and link functions allow us to capture all the message transmission and link transition information in the constructed STB graph $\mathcal{G}$ with a discrete and equal time interval of length τ. Note that, though we ignore non-zero time interval ($< \tau$) while approximating $\mathcal{T}_{ijc}^{t,s}$ and $L_{ij}^{t,s}$ to nearest multiples of τ, it does not negatively impact the actual message transmission. This is because τ is the least possible message transmission delay, and no messages can be transmitted in time interval $< \tau$.

Nodes and Structure. Given the series of snapshot $\{G^t | t = 1 \ldots T\}$, the STB graph $\mathcal{G}$ has a total of $(\hat{T} + 1)$ layers of nodes, where $\hat{T} = \frac{T}{\tau}$. At each layer t, we create $|S|$ copies of each node $v_i \in V$. Specifically, we add a node $v_i^{t,s}$ for each band $s \in S$. Thus, the node set $\mathcal{V}$ is:

$$\mathcal{V} = \left\{ v_i^{t,s} | i \in \{0, \ldots |V|\}, s \in S, \text{ and } t \in [0, \hat{T}] \right\}$$

   As a result, the total number of nodes is $|V| \times |S| \times (\hat{T} + 1)$. There are two types of communication links in the STB graph $\mathcal{G}$, as described in the following.

Temporal links. Intuitively, a temporal link represents the possibility of a node carrying the message between consecutive intervals of time, that is, the message is not forwarded at time $t\tau$. Formally, a temporal link $(v_i^{t,s}, v_i^{(t+1),s})$ connects two instances of a node v_i in band $s \in S$ across two consecutive layers corresponding to $t\tau$ and $(t+1)\tau$. An example of temporal link is shown in Fig. 6.7. The set of temporal links $(\mathcal{E}_o)$ in the STB graph $\mathcal{G}$ is as follows:

$$\mathcal{E}_o = \left\{ (v_i^{t,s}, v_i^{(t+1),s}) | i \in \mathcal{V}, s \in S, \text{ and } t \in [0, \hat{T}] \right\}$$
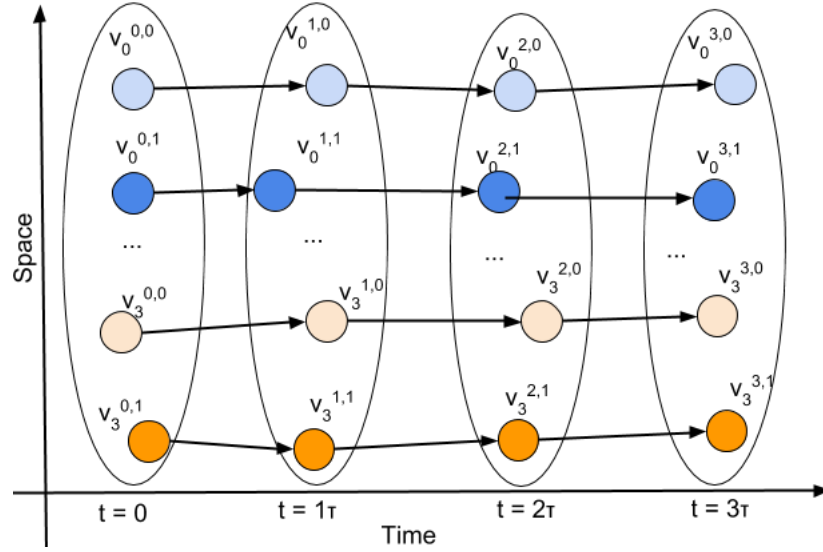
Figure 6.7: Example of temporal links of an STB graph $\mathcal{G}$. Each layer corresponds to a discrete time interval τ in the network lifetime. A temporal link connects the same node over a certain band type.

Spatial links. A spatial link represents a communication possibility from a node v_i to v_j, over a band s at time t. Formally, a spatial link is a tuple $(v_i^{t,s}, v_j^{t',s})$, where $t' = (t + \mathcal{T}_{ijc}^{t,s})$. Such link is added to the graph $\mathcal{G}$, if v_i and v_j are in communication range over band s during that time period, as specified by the link function. An example of Spatial Links in shown in Fig 6.8. For simplicity, we only show the spatial links that go from node $v_0^{0,(.)}$ (at layer 0 and band type, either 0 or 1) to $v_3^{t,(.)}$, (different layers and band types), and $0 < t \leq 3$,. Any spatial link connects different nodes over band type 0 (black line) and band type 1 (blue line) across different layers (corresponding to link delay cost). Moreover, a red dotted line shows that a node v_0 can switch from one band 0 to another type 1 within the same layer 0 (i.e., with no link delay cost).As a result, the set of all spatial links $\mathcal{E}_{\mathcal{T}}$, for a certain transmission delay $\mathcal{T}$, is calculated as:

$$\mathcal{E}_{\mathcal{T}} = \left\{ (v_i^{t,s}, v_j^{(t+\mathcal{T}),s}) | i, j \in V, s \in S, t \in [0, \hat{T}], \text{ and } L_{ij}^{t,s} = 1, \forall \{(t\tau, (t+\mathcal{T})\tau)\} \right\}$$

49

Note that at most $(\mathcal{T}_{max} \times |S| \times (|S| - 1))$ spatial links (corresponding to each spatial link delay over each band type) may exist in $\mathcal{G}$. Here, $\mathcal{T}_{max}$ is the maximum possible message transmission delay, computed as $\mathcal{T}_{max} = \left(\max_{s \in S, i,j \in V} \mathcal{T}_{ij|\mathcal{M}|}^{t,s} \right)$.

Example 2. Let v_0 and v_3 are in communication range over band types 0 and 1 for a time interval $[0,1]$, i.e., $L_{03}^{t,0} = L_{03}^{t,1} = 1$, $\forall t \in [0,1]$. Consider $\tau = 0.5$, and messages of (i) type 1, which takes τ time units over both bands 0 and 1, and (ii) type 2 that takes 2τ and τ time units over band 0 and 1, respectively. Then, following spatial links would exist in $\mathcal{G}$ – $(v_0^{0,0}, v_3^{1,0})$, $(v_0^{0,0}, v_3^{2,0})$ and $(v_0^{0,1}, v_3^{1,1})$ spatial links.
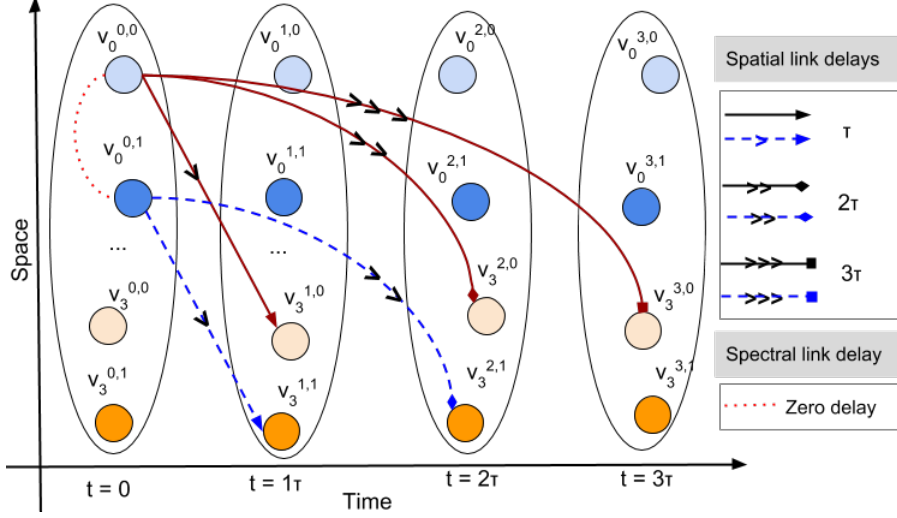
Figure 6.8: Spatial Links of the STB graph $\mathcal{G}$.

Overall, the complete set of communication links $\mathcal{E}$ is $\mathcal{E} = \mathcal{E}_o \cup \left(\cup_{\mathcal{T} \in \{1 \dots \mathcal{T}_{max}\}} E_{\mathcal{T}} \right)$. Note that we do not consider the switching of a certain node from one band to another as a separate link (See the dotted red line in Fig. 6.8). This is because, as previously discussed, the channel access delay is negligible and thereby, does not affect the LDC path computation (even if not integrated in the STB graph).

Link delay cost. We define the cost w_e of a link $e \in \mathcal{E}$ as its message transmission delay. In the case of temporal links, $w_e = \tau$, while w_e for spatial links is defined by the transmission delay (recall that is always a multiple of τ).

6.3   Least Delay Cost (LDC) Path Computation

In this section, we discuss the details of the third step of the proposed dDSAaR routing protocol, i.e., LDC path computation for each source-destination pair, corresponding to each message type in $\mathcal{M}$ and generation time. Before delving into the details of the proposed algorithm that determines the least delay path for each source-destination node pair, we formulate the LDC path determination as an optimization problem.

Problem Formulation

In this section, we formulate the problem of determining the least end-to-end delay cost (LDC) path route [4] for each message type $c \in \mathcal{M}$ and generation (or arrival) time $t \in [0, \hat{T}]$ as an optimization problem. The inputs to the problem are the STB graph, c, t, the source node u, and destination node v.

Variables. We introduce two variables $\delta^+(v_i^{t,s})$ and $\delta^-(v_i^{t,s})$ respectively to denote the set of incoming links and outgoing links at any node $v_i^{t,s}$ in STB graph. Then, we introduce a binary decision variable x_e which equals 1, if the message can be forwarded over a link $e \in \mathcal{E}$. Recall that a certain message (originating at any time layer $t\tau$) can only be forwarded over a link e if it meets one of the following conditions: (i) link e is a temporal link that connects successive layers $[t\tau, (t+1)\tau]$ in STB graph, (ii) link e is a spatial link over a certain band $s \in S$, and connects two layers $[t\tau, (t+w_e)\tau]$, where the link delay cost, $w_e = \mathcal{T}_{ijc}^{t,s}$.

Objective function. As shown in Eq. 6.3, the objective is to determine the least delay cost path for each source-destination node pair in the STB graph.

Constraints. Eq. 6.4 is a typical flow constraint to ensure the consistency of the routing scheme, i.e., there must exist a path from source u to the destination node v. It also ensures that once a message reaches to a node, then it must also depart from the same node.

Expression 7.12 denotes the binary decision variable.

$$\text{Minimize} \ \sum_{e \in \mathcal{E}} w_e x_e \tag{6.3}$$

$$\sum_{e \in \delta^-(v_i^{t,s})} x_e \quad - \quad \sum_{e \in \delta^+(v_i^{t,s})} x_e \quad = \quad \begin{cases} -1, \text{ if } v_i^{t,s} = u \\ 1, \text{ if } v_i^{t,s} = v \\ 0, \ otherwise \end{cases} \quad \forall i \tag{6.4}$$

$$x_e \in \{0, 1\}, \ \ \forall e \tag{6.5}$$

Note that the spectrum constraints, e.g., signal to noise (SNR) ratio, maximum allowable transmit power, unique access to a certain spectrum band at transmitter and receiver, and offered transmission coverage, are integrated in the spatial link in the STB graph. Also, although we consider the optimization problem for a given message, it will also work well for multiple messages. This is because a spatial link utilizing a certain band type comprises several channels, which can be concurrently accessed by multiple messages (should they choose the same band type in the same geographical location at the same time instance); unless in the unlikely rare event (as in rural areas considered in the work) that the number of such messages exceed the total number of available (unoccupied) channels in that band. Intuitively enough, a temporal link does not have any such issues with multiple messages, since a node usually have sufficient memory to store multiple messages.

---

[4]Though our focus in this chapter is to determine LDC paths (with least network delay), the proposed Space-Time-Band (STB) graphs are extensible to incorporate alternative performance optimizations, e.g., least number of spatial hops, least energy cost with hard or soft deadlines, etc.

Proposed LDC algorithm

In this subsection, we discuss the proposed LDC algorithm for determining the minimum delay path between each source-destination pair, given the STB graph, a message of type $c \in \mathcal{M}$ and the message arrival time $t \in [0, \hat{T}]$. Specifically, the algorithm determines the *next relay node* and selects the *band* for that node, starting at the source and ending at the destination. The path may include temporal edges, representing the choice of storing the message at the current node while waiting for better transmission opportunities in the future. Note that, we may apply the Floyd-Warshall algorithm to compute the shortest (least delay) paths between all pairs of nodes in a graph [78]. However, this algorithm will have a time complexity of $O(|\mathcal{V}|^3 |S|^3 \hat{T}^3)$, where $|\mathcal{V}|$ is the number of nodes, $|S|$ is the number of band types, and $(\hat{T}+1)$ is the number of layers in STB graph. Since in the STB graph, we have a copy of each node in the network for each band and time layer, and since the number of time layers is high due to the potential small value of τ, such straightforward approach is impractical.

To overcome this issue, we propose a faster algorithm that exploits the properties of the STB graph to reduce the search space and achieve a better complexity of $O(|V|^3 \hat{T})$.

Formal properties of LDC path over STB graph. The following theorems present two properties of the STB graph which are at the basis of our proposed LDC algorithm.

Theorem 6.3.1 (Band Invariant Property). *Let $p(u, v)$ denote the LDC path from a source u to a destination v in the STB graph. The optimal band between two consecutive nodes $v_i^{t,*}$, $v_j^{t',*}$, with $i \neq j$ and $t' \in (t, \hat{T}]$), in the path $p(u, v)$ is the band that offers least delay for which a transmission opportunity (a spatial link) exists, where (*) represents a certain band $s \in S$.*

Proof. (by contradiction) Let w_i be the transmission delay of the band s_i selected for spatial link between $v_i^{t,*}$ and $v_j^{t',*}$ in the LDC path $p(u, v)$. Consider, this is *not* the band with the least delay. This implies that there exists another band s_j with delay w_j, such that $w_j < w_i$, for which a spatial link exists between $v_i^{t,*}$ and $v_j^{t',*}$. We can now construct a path $p'(u, v)$ where we substitute s_i with s_j for the spatial link between $v_i^{t,*}$ and $v_j^{t',*}$. Since $w_j < w_i$, the weight of $p'(u, v)$ is *less* than that of $p(u, v)$. However, this is a contradiction since $p(u, v)$ is the LDC path between u and v. $\square$

The above theorem allows us to consider only one spatial link between two nodes in consecutive layers of the STB graph, corresponding to the optimal band with least delay, thus reducing the search space and ultimately the complexity. (It is straightforward to extend this approach to other metrics of interest, such as energy minimization.)

Theorem 6.3.2 (Delay Invariant Property). *Let $W(p(u, v), c, t)$ be the delay of the LDC path $p(u, v)$ between the source u and destination v for messages of type c at*

time layer t in the STB graph. The LDC path between the same node pair starting at $(t - \Delta t)$ *has the following delay:*

$$W(p(u,v), c, (t - \Delta t)) \leq W(p(u,v), c, t) + \Delta t$$

Proof. The LDC path starting at $(t - \Delta t)$ can be, in the worst case, the same path from node u to which we append additional temporal links from $(t - \Delta t)$ until time t, and then follow the same path to node v. In this case, the equality $W(p(u,v), c, t - \Delta t) = W(p(u,v), c, t) + \Delta t$ holds. Nevertheless, by starting earlier, there may exist better alternative paths, reducing the delay of the LDC path, and thereby proving the theorem. $\square$

This theorem suggests that sending a message over a transmission opportunity is always better than keeping the message. This idea is utilized in the initialization step of our algorithm.

Algorithm Description. Our proposed LDC algorithm is based on dynamic programming (DP) and comprises two steps: *Initialization* and *LDC Path determination*. The algorithm is executed for each message type $c \in \mathcal{M}$ to obtain the complete STB routing table. Let us now introduce the notion of *spatio-temporal (ST) intermediate node*.

Definition 6.3.1 (ST intermediate node). Consider a path $p = < v_1^{t_1,*}, v_2^{t_2,*}, \ldots, v_{l-1}^{t_{l-1},*}, v_l^{t_l,*} >$, an intermediate node is any node $v_i^{t_i,*}$ such that $v_i^{t_i,*} \in \{v_2^{t_2,*}, \ldots, v_{l-1}^{t_{l-1},*}\}$, i.e., except $v_1^{t_1,*}$ and $v_l^{t_l,*}$. Note that, the same node $v_i^{t,*}$ may appear multiple times at different time periods $t \in [0, \hat{T}]$, however are not considered as ST intermediate nodes.

Consider the LDC path $p_k(v_i^{t_i,*}, v_j^{t_j,*})$ from a node $v_i^{t_i,*}$ to another node $v_j^{t_j,*}$, with $t_i < t_j$, such that the ST intermediate nodes are in the subset $\{v_1^{t_1,*}, \ldots, v_k^{t_k,*}\} \subseteq \mathcal{V}$. In other words, $p_k(v_i^{t_i,*}, v_j^{t_j,*})$ is the LDC path that is calculated only using the first k nodes as ST intermediate nodes. We exploit DP to define a recursive relation that is used to efficiently calculate the LDC path delay $W(p_k(v_i^{t_i,*}, v_j^{t_j,*}), c, t_i)$ given $W(p_{k-1}(v_i^{t_i,*}, v_j^{t_j,*}), c, t_i)$, for a message type $c \in \mathcal{M}$ at arrival time $t_i \in [0, \hat{T}]$.
When k = 0, the path $p_0(v_i^{t_i,*}, v_j^{t_j,*})$ cannot contain any intermediate node. As a result, the path can be composed only by temporal links from $v_i^{t_i,*}$ to itself, i.e., $v_i^{t,*}$ at a later time $t \in (t_i, t_j)$, until a spatial link exists between $v_i^{t,*}$ and $v_j^{t_j,*}$. If multiple spatial links to $v_j^{t_j,*}$ exist from the same node $v_i^{t_i,*}$ at different times $t_i \in [0, t_j)$ over different bands, the link that results in the minimum overall delay is chosen:

$$W(p_0(v_i^{t_i,*}, v_j^{t_j,*}), c, t_i) = \min_{t_i \in [0, t_j)} \left(t_i + \min_{s \in S} \mathcal{T}_{ijc}^{t_i,s} \right)$$

This operation utilizes the spectrum invariant property (Theorem 6.3.1). If no spatial link exists, then

$$W(p_0(v_i^{t_i,*}, v_j^{t_j,*}), c, t_i) = \infty$$

When k > 0, there are two cases.

Case 1. If $p_k(v_i^{t_i,*}, v_j^{t_j,*})$ does not contain node $v_k^{t_k,*}$ as an intermediate node, then all of its intermediate nodes are in $\{v_1^{t_1,*}, \ldots v_{k-1}^{t_{k-1},*}\}$. Then, the delay of the LDC path $W(p_k(v_i^{t_i,*}, v_j^{t_j,*}), c, t_i)$ is the same as $W(p_{k-1}(v_i^{t_i}, v_j^{t_j,*}), c, t_i)$.

Case 2. If $p_k(v_i^{t_i,*}, v_j^{t_j,*})$ uses $v_k^{t_k,*}$ as an intermediate node, then $p_k(v_i^{t_i,*}, v_j^{t_j,*})$ can be broken into two sub-paths: one sub-path $p_{k-1}^1(v_i^{t_i,*}, v_k^{t_k,*})$ from $v_i^{t_i,*}$ to $v_k^{t_k,*}$, and $p_{k-1}^2(v_k^{t_k,*}, v_j^{t_j,*})$ goes from $v_k^{t_k,*}$ to $v_j^{t_j,*}$. Since these two paths can only contain the nodes in $\{v_1^{t_1,*}, \ldots v_{k-1}^{t_{k-1},*}\}$ as intermediate nodes, the delay of the LDC path $W(p_k(v_i^{t_i,*}, v_j^{t_j,*}), c, t_i)$ is the minimum between $W(p_{k-1}(v_i^{t_i,*}, v_j^{t_j,*}), c, t_i)$ and $W(p_{k-1}^1(v_i^{t_i,*}, v_k^{t_k,*}), c, t_i)$ $+ W(p_{k-1}^2(v_k^{t_k,*}, v_j^{t_j,*}), c, t_k)$. Notice that, the start time t_k for second sub-path $p_{k-1}^2(v_k^{t_k,*}, v_j^{t_j,*})$ would be given by $t_i + W(p_{k-1}^1(v_i^{t_i,*}, v_k^{t_k,*}), c, t_i)$, i.e., the summation of message arrival time and the delay for first sub-path $p_{k-1}^1(v_k^{t_k,*}, v_j^{t_j,*})$.

By applying the above recursive relation iteratively, until $k = |V|$ and $t = \hat{T}$, we can obtain the final solution as the LDC path for each source-destination pair for a given message type c generated at a certain time layer $t \in [0, \hat{T}]$.

(Step 1) Initialization. It computes the base case for all node-pairs and times. In this phase (as shown in Algorithm 3), for each message type c, we initialize the LDC delay path $W(p_0(v_i^{t,*}, v_j^{t+1,*}), c, t)$ to 1 (recall that the time unit for the STB graph is τ, as discussed in Section 6.2), for each temporal link between consecutive time layers t and $(t+1)$ (Lines 4 - 5). Moreover, for a spatial link (Lines 7 - 10), we compute the optimal band (i.e., with least link delay w), and then initialize $W(p_0(v_i^{t,*}, v_j^{t+w,*}), c, t)$ to w, provided that the following conditions are met: (i) the nodes $v_i^{t,*}$ and $v_j^{t+w,*}$ are in communication range for the entire duration of $[t, (t + w)]$, and (ii) the delivery of message of type c from $v_i^{t,*}$ to $v_j^{t+w,*}$ does not exceed the total time period, i.e., $\hat{T}$. This operation is based on the band invariant property (Theorem 6.3.1).

When there exists a worse LDC path from a node $v_i^{t,*}$ to $v_j^{t',*}$ at time layer t, compared to the path at next layer $(t+1)$, then we update the delay $W(p_0(v_i^{t,*}, v_j^{t+1,*}), c, t)$ to $W(p_0(v_i^{t+1,*}, v_j^{t',*}), c, t+1) + 1$ (lines 11-12). Here, $v_i^{t,*}$ uses a temporal link to reach to $v_i^{t+1,*}$, and then uses the path $p_0(v_i^{t+1,*}, v_j^{t',*})$ to get to the final node $v_j^{t',*}$. This operation significantly reduces the search space and also, does not affect the optimal LDC path, as shown in Theorem 6.3.2 (delay invariant property). Finally, we keep track of path and optimal bands in matrices P and S, respectively.

(Step 2) LDC Path Determination. After the first step, in Algorithm 4, we apply the recursive formula to compute $W(p_k(v_i^{t,*}, v_j^{t',*}), c, t)$ given $W(p_{k-1}(v_i^{t,*}, v_k^{t+w,*}), c, t)$ and $W(p_{k-1}(v_k^{t+w,*}, v_j^{t',*}), c, t + w)$, where w is equivalent to $W(p_{k-1}(v_i^{t,*}, v_k^{t+w,*}), c, t)$ (see lines 1-9).

Time complexity: The algorithms 3 and 4 have time complexity of $O(|\mathcal{V}|^2 \times |S| \times \hat{T})$ and $O(|\mathcal{V}|^3 \times \hat{T})$, respectively. Since the size of $|S|$ is negligible compared to that of $|\mathcal{V}|$, the time complexity of the proposed algorithm is $O(|V|^3 \times \hat{T})$.

Algorithm 3: Initialization

    Input: Discrete time interval τ, Link existence function, $L(i,j,s,t_1,t_2)$, where
        $i,j \in V$, $s \in S$, $t_1, t_2 \in \{0, \dots, \hat{T}\}$, message type c (message size qc)
    Output: LDC path $W(i,j,c,t)$ path, only based on temporal links and a
        single spatial link. Also, the path and band tracking matrices
        $P(i,j,c,t)$, and $S(i,j,c,t)$, respectively.

1 Initialize $W(i,j,c,t) = \infty$, $P(i,j,c,t) = S(i,j,c,t) = -1$, $\forall i,j,c,t$ **for**
   $t \leftarrow (\hat{T} - 1)$ **to** 0 **do**

2   **for** $i \leftarrow 0$ **to** V **do**

3   **for** $j \leftarrow 0$ **to** V **do**

4   **if** $i == j$ **then**

5 $W(i,j,c,t) = 1$, $P(i,j,c,t) = i$

6   **else**

7   **for** $s = 0$ to S **do**

8   delay cost, $w = \left\lceil \frac{qc}{\tau \times \mathbb{R}(i,j,s,t)} \right\rceil$ (in terms of τ)

9   **if** $(t + w) \leq \hat{T}$ and $W(i,j,c,t) > w$ and
                $L(i,j,s,t,(t+w)) \neq \infty$ **then**

10 $W(i,j,c,t) = w$, $P(i,j,c,t) = i$, $S(i,j,c,t) = s$

11   **if** $(t + 1) \leq \hat{T}$ and $W(i,j,c,t) > W(i,j,c,(t+1)) + 1$ **then**

12 $W(i,j,c,t) = W(i,j,c,(t+1)) + 1$ $P(i,j,c,t) = P(i,j,c,(t+1))$

6.4   Simulation Results

In this section, we evaluate the performance of d-DSA architecture utilizing dDSAaR protocol against the conventional non-DSA and DSA architectures that utilizes a standard DTN routing protocol (restricted to a single band).

Simulation Setting

We consider a simulation setting with 3 connectivity hubs and 8 sensor blocks, each equipped with a dropbox and 40-60 sensing nodes. For the data mules' mobility, we consider the vehicle mobility traces from a real vehicular testbed, DieselNet [95], that comprises 35 public transport vehicles operating in a 400 sq. kilometers surrounding the UMass Amherst campus. Among these buses, 20 are on the road everyday on an average. We only consider those buses having enough GPS traces ($\geq 60\%$ of time instances). This results into an average of 9 buses everyday. In the following, we show the experimental results for the first week of November, 2007 (i.e, November 1 - 7, 2007).

    We take the round length to be $T = 3$ hours, for it is the least common multiplier of all round trip times of all buses across different days for the considered week. Since the dDSAaR protocol requires a bootstrap round to construct the STB graph and

Algorithm 4: LDC Path determination

Input: $W(i, j, c, t)$, $P(i, j, c, t)$, and $S(i, j, c, t)$ where $i, j \in V$, $t \in \{0, \dots \hat{T}\}$, and c

Output: $W(i, j, c, t)$, considering all temporal and spatial links in the STB graph

1 **for** $k \leftarrow 0$ **to** V **do**
2   **for** $i \leftarrow 0$ **to** V **do**
3   **for** $j \leftarrow 0$ **to** V **do**
4   **for** $t \leftarrow 0$ **to** $\hat{T}$ **do**
5   Curr. path delay, $w_{curr} = W(i, j, c, t)$ $w_1 = W(i, k, c, t)$, $w_2 = \infty$
6   **if** $(t + w_1) < \hat{T}$ **then**
7                 $w_2 = W(k, j, c, (t + w_1))$
8   **if** $w_1 + w_2 < w_{curr}$ **then**
9                 $W(i, j, c, t) = w_1 + w_2$, $P(i, j, c, t) = P(k, j, c, (t + w_1))$
                 $S(i, j, c, t) = S(k, j, c, (t + w_1))$

compute LDC paths, we allocate 3 hour time window in the morning (11 am - 2 pm) as the bootstrap round. Then we consider another 3 hour time window in the afternoon (2 pm - 5 pm) as the operational round, where the performance of the d-DSA architecture and conventional non-DSA/DSA architectures are analyzed. (We re-run bootstrap round on each day as we observe that some buses change routes on different days.) Figs 6.4 and 6.5 depict the vehicle mobility routes for bootstrap and operation rounds for November 1, 2007, where each color denotes a unique bus across the subsequent rounds.

The sensor blocks and the connectivity hubs are randomly placed within the UMass Amherst campus and the surrounding county. All the sensing nodes and dropboxes are randomly placed within a radius of interval [0.5 - 1] km of a certain sensor block. The messages are generated in bursts at each sensing node. The inter-arrival time between bursts is drawn from an exponential distribution with mean of 5 minutes, and each burst contains [10 - 30] messages. The message size is chosen randomly as 1, 10, 50, 100, 250, 500, or 750 Mb.

We consider the allowable transmit power (by FCC) for all bands – 1 W for ISM band, 4 W for TV and LTE bands, and 10 W for CBRS band. Fig. 7.4 illustrates the complete details of the operating frequency and offered channel bandwidth in each band. The values of various controlling parameters are as follows: path loss factor = 2.5 (rural area), received power threshold = -85 dBm, signal to interference noise ration (SINR) = -120 dBm. These parameters are used to compute realistic values of the transmission range (using Frii's Transmission Equation [72]), and effective bit rate (using Shannon Hartley Theorem [74]), for each band. Finally, the energy consumed at a certain node is computed as the product of the transmit power and message transmission delay, $\mathcal{T}$ (similar to the energy consumption model presented

in Chapter 4).

Performance Metrics.

For the evaluation of the d-DSA architecture and the conventional non-DSA/DSA architecture, we consider the following performance metrics:

- *Message Delivery Ratio (MDR)* - the fraction of the total unique messages delivered to the connectivity hubs divided by the total messages generated in the sensor blocks;

- *Network Delay* - the average latency incurred in delivering the generated messages from the sensor blocks to the connectivity hubs;

- *Message Overhead* - the number of message copies with respect to the number of unique messages generated;

- *Energy Expenditure* - the average amount of energy dissipated at each d-DSA node to transfer the messages from the sensor blocks to the hubs.

Comparison Approaches.

While the proposed d-DSA architecture utilizes the dDSAaR protocol, unless otherwise stated, we consider *Epidemic routing* (ER) protocol [45] as the underlying routing protocol for conventional non-DSA/DSA architectures; because the ER protocol replicates and forwards messages to every encountering nodes, and thus offers the highest message delivery and least network delay. Besides, we also investigate other two standard protocols for non-DSA/DSA architectures, namely (i) *Hot potato routing* (HP) - a node forwards a message to the earliest encountering node., and (ii) *Spray and Wait routing* (SnW) [47] - A source node initially starts with L copies (Spray Phase). Next, each node (source or relay) with $L > 1$ copies forwards $\lceil \frac{L}{2} \rceil$ copies to another encountering node (with no copies) and keeps $\lfloor \frac{L}{2} \rfloor$ for itself. When a node is left with only one copy, it switches to the direct transmission mode. For our experiments, we consider $L = 25$ copies.

For extensive analysis, we also evaluate the d-DSA architecture utilizing extended spectrum-aware standard protocols, i.e., *Spectrum-aware ER* (S-ER), *Spectrum-aware HP* (S-HP), and *Spectrum-aware SnW* (S-SnW), to harness the availability of multiple bands and utilize the suitable (least delay) band to communicate with any neighbor node (within the rules of the protocol). For example, S-ER operates such that each node computes the list of neighbors (that are in the communication range over each band); and then for each neighbor, it computes the suitable band and forwards the message on that chosen band.

Experimental Results.

Now, we discuss the experimental results for the d-DSA architecture utilizing dDSAaR against the non-DSA/DSA architectures utilizing standard (single band) ER protocol and additionally, the d-DSA architecture utilizing spectrum-aware protocols (i.e.,

57

S-ER, S-SnW, and S-HP), in terms of all aforestated metrics. For the clarity of the plots, we do not show the results for standard HP and SnW protocols. However, HP and SnW show similar behavior with respect to ER (as that of S-HP and S-SnW against S-ER as discussed in the following). Besides, we show the results for the d-DSA architecture using dDSAaR in an *ideal* (highly predictable) scenario (where the mobility patterns across bootstrap and operational rounds are the same).

Message Delivery Ratio Analysis. Fig. 6.9 shows that the proposed d-DSA architecture utilizing the dDSAaR protocol achieves, on average, better MDR compared to that of conventional non-DSA/DSA architectures utilizing the standard ER protocol, for varying simulation times. This is because, unlike conventional architectures, the d-DSA architecture offers multiple communication links (formed over diverse bands) between each node pair, for the dDSAaR protocol to successfully deliver each message. Among the single band approaches, the LTE band performs the best as it offers both high communication range and bit rate. The ISM band, due to its very poor range, suffer the most.
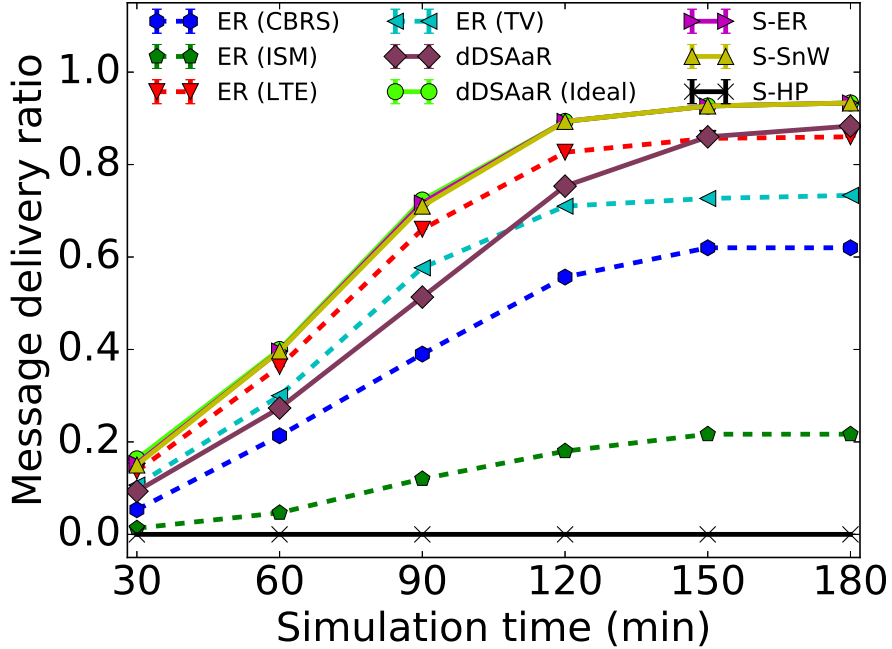
Figure 6.9: Message Delivery Ratio vs Simulation Time

The d-DSA architecture utilizing S-ER offers slightly better MDR than d-DSA architecture utilizing dDSAaR, further highlighting the benefits of the proposed d-DSA architecture (and usage of *diverse* DSA radio devices). However, S-ER incurs very high *message overhead* (see Fig. 6.10) because it replicates each message and forwards to each encountering 1-hop node on a chosen band. On contrary, the dDSAaR protocol incurs negligible overhead (just 1) for it utilizes the pre-computed routing table (during bootstrap round) to route each message in the network. The S-SnW

Table 6.3: Average percentage of band usage by each of the underlying routing protocol in the proposed d-DSA network architecture

Protocol	Spatial Links				Temporal Links
	TV	LTE	ISM	CBRS	
dDSAaR	8.03%	7.84%	0%	5.37%	78.75%
dDSAaR (Ideal)	8.21%	7.08%	0%	5.21%	79.5%
S-ER	43.57%	35.57%	1.14%	19.71%	N/A
S-SnW	49.7%	32.6%	0.8%	16.9%	N/A
S-HP	0%	0%	0%	0%	N/A

(with bounded yet high overhead) performs almost similar to S-ER whereas S-HP does the worst. Note that in ideal scenarios, the d-DSA architecture using dDSAaR protocol offers the best MDR and that also with overhead 1.
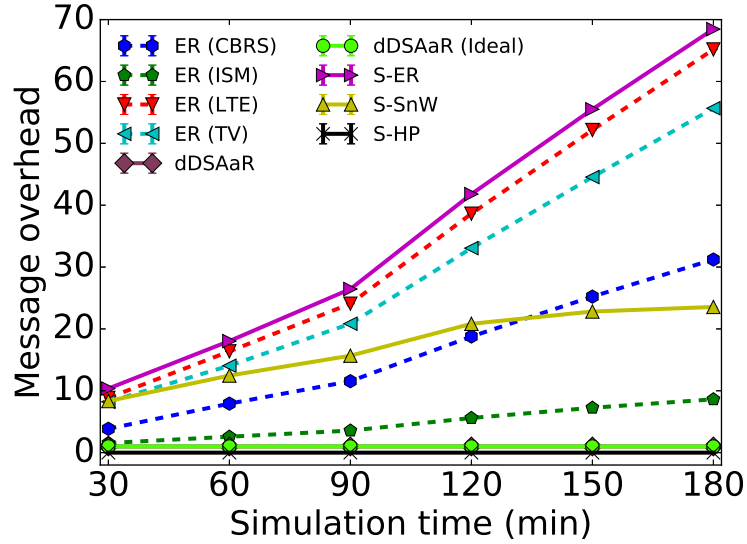
Figure 6.10: Message Overhead vs Simulation Time

Network Delay Analysis. As shown in Fig. 6.11, the d-DSA architecture utilizing dDSAaR consumes relatively higher network delay compared to other approaches, for varying simulation times. This is because unlike ER and SnW (and their spectrum-aware versions), dDSAaR utilizes precomputed LDC path to route messages, and stores the messages (i.e., temporal links) if needed, instead of flooding the network (See Table 6.3). Among individual band approaches, the TV band (with highest range) and ISM band (with lowest range) perform the best and worst, respectively.

Intuitively enough, given the ideal scenario, the proposed architecture yields the lowest network delay.
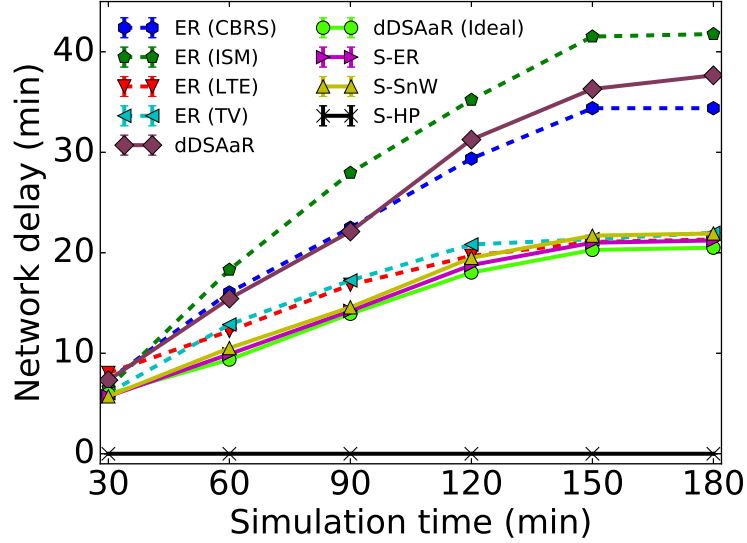
Figure 6.11: Network Delay vs Simulation Time

Energy Expenditure Analysis. Fig. 6.12 shows that the proposed d-DSA architecture employing dDSAaR incurs notably lower energy expenditure compared to other approaches, irrespective of the simulation times. The huge saving in energy can be attributed to negligible overhead (Fig. 6.10), and high utilization of temporal links which consume no energy (Table 6.3). Intuitively, the architecture with S-ER, experiences the worst energy expenditure due to very high overhead. Similarly, the TV band, characterized by poor bit rate, suffers from poor energy expenditure as it incurs very high transmission delay. ISM and S-HP consume less energy, however, their MDR is negligible.

**Varying node densities.** For varying node densities, we vary the number of data mules from one to nine, while the sensor blocks and hubs are kept unchanged. Figs. 6.13 - 6.16) show that the MDR, as expected, improves with increase in number of data mules. The network delay gradually decreases (until 3 mules) and remains more or less constant with increase in number of data mules. This can be attributed to the increased path route options due to the increased number of data mules in the network. The results for message overhead and energy expenditure are also consistent with previous results.

Analysis. Though the proposed d-DSA network architecture with dDSAaR protocol suffers from relatively higher network delay, our approach does really well in terms of all other metrics. In ideal (highly predictable) environments, our approach excels in all metrics, including network delay. Hence, the d-DSA architecture, along with dDSAaR, is a promising solution for improved rural connectivity.
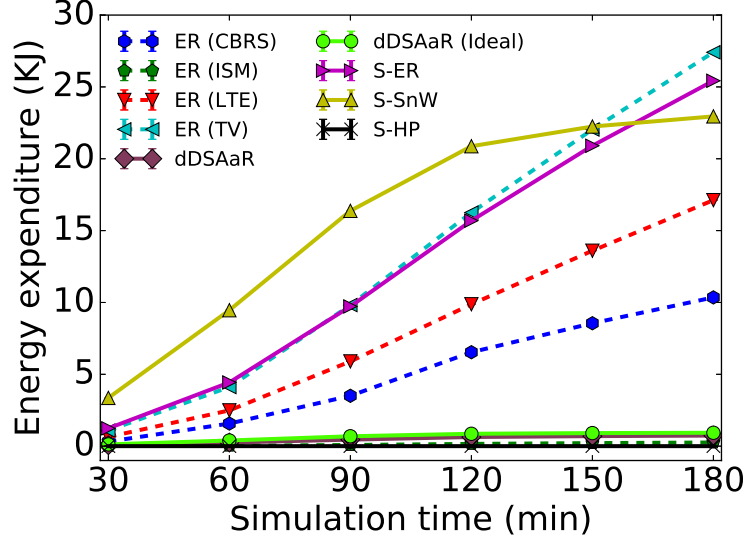
Figure 6.12: Energy Expenditure vs Simulation Time
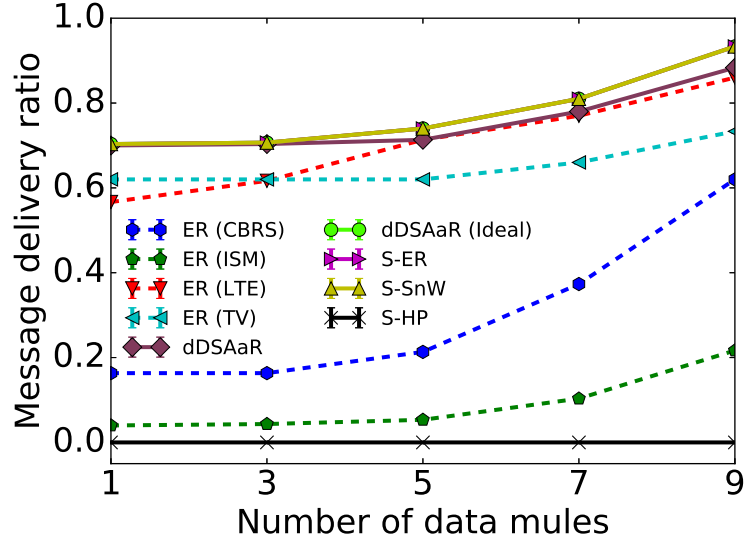
Figure 6.13: Energy Expenditure vs Number of Data Mules

6.5   Conclusion of This Chapter

In this chapter, we proposed a novel *diverse DSA aware Routing* (dDSAaR) protocol for time-varying d-DSA network architectures with sufficiently predictable mobiles nodes, as in the case of public transportation vehicles. This architecture is particularly suitable for providing connectivity to rural communities, where the fixed infrastructure is not able to provide full coverage, a typical scenario in rural setting. Specifically, the proposed dDSAaR protocol jointly exploits EM characteristics of
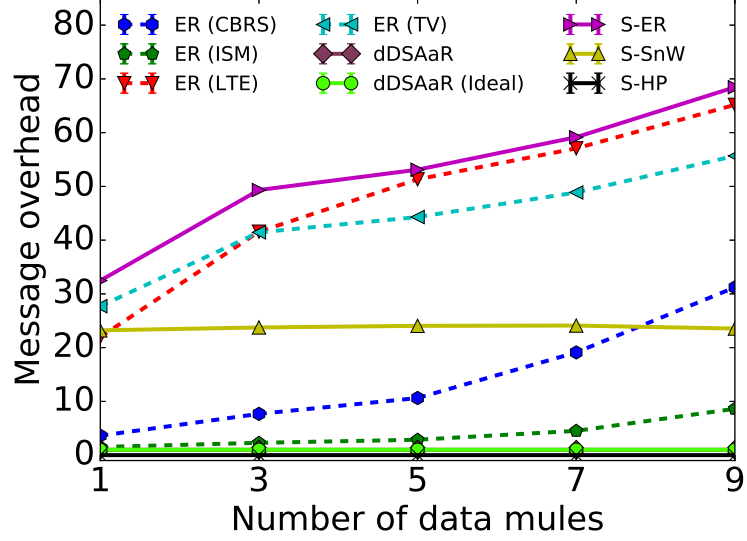
Figure 6.14: Message Overhead vs Number of Data Mules
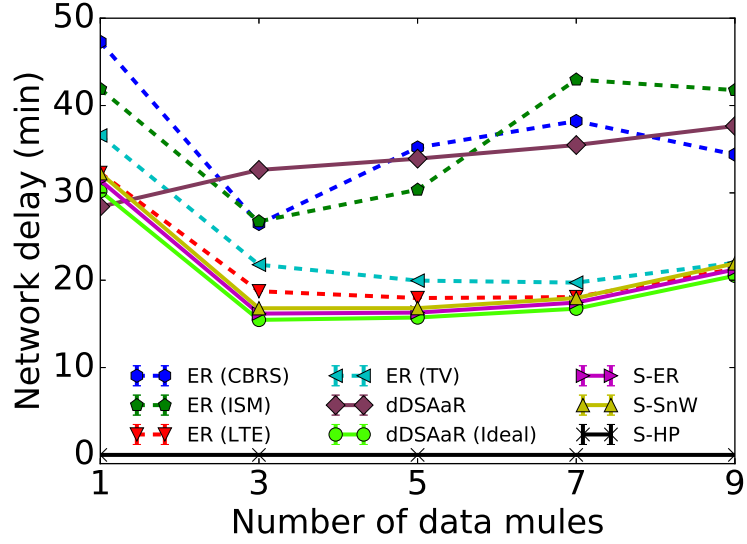
Figure 6.15: Network Delay vs Number of Data Mules

various spectrum bands and sufficiently predictable mobility of public transportation vehicles, and is based on the novel representation of time-varying d-DSA network topology, termed Space-Time-Band (STB) graph, that comprehensively captures the communication opportunities across the space, time, and multiple bands. Our experiments on the real UMass DieselNet dataset demonstrate that the proposed d-DSA architecture, utilizing dDSAaR routing, notably outperforms conventional single-band DSA architectures, utilizing standard routing protocols, and also d-DSA architecture using spectrum-aware versions in terms of several important metrics, such as, mes-
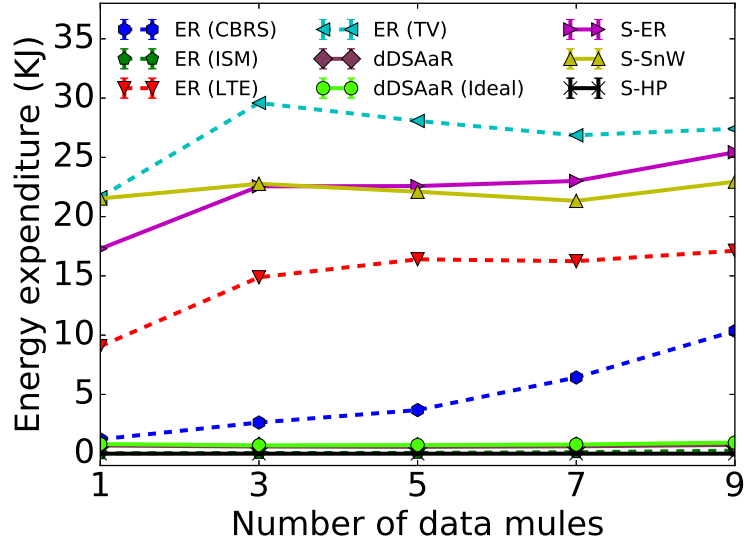
Figure 6.16: Energy Expenditure vs Number of Data Mules

sage delivery ratio, message overhead, energy expenditure, at the expense of a slight increase in network delay. Nevertheless, the delay improves with higher predictable mobility.

In the future, we plan to validate our routing approach with large-scale real and synthetic datasets. Furthermore, we will extend the STB graph by including an additional dimension, namely the possibility of nodes have multiple antennas (MIMO capability). Finally, the proposed routing protocol based on STB graph, is a centralized algorithm, which again may not be always feasible in rural setting. Hence, we would investigate designing efficient distributed routing strategies for such time-varying yet predictable d-DSA networks utilizing techniques, particularly reinforcement learning.

Chapter 7 Routing in Time-varying d-DSA Network Architectures with Unpredictable Mobility

In this chapter, we consider the challenging case of d-DSA network architectures for rural communities, in which the component nodes (equipped with d-DSA radio devices) may have unpredictable mobility (e.g., private cars). This results in a d-DSA aware delay tolerant network (d-DSA DTN) in which each node can utilize multiple communication opportunities over diverse spectrum bands, if available. We first model the d-DSA DTN network as a time-evolving graph in Section 7.1. We then highlight the shortcomings of routing schemes originally designed for standard (single-band) DTNs, while dealing with such d-DSA DTNs in Section 7.2. Following this, in Section 7.3 we formulate an integer linear programming (ILP) optimization problem that aims to determine a suitable path route for each message traffic in such a network, such that the end-to-end network delay is minimized. Since this would require complete knowledge of topology dynamics and future message traffic demands, it becomes an impractical solution for such d-DSA DTNs, which are both *dynamic* and *unpredictable.* Hence, in Section 7.4, we propose an efficient lightweight *d-DSA aware Geographical Routing* (dDSA-GR) protocol, which is based on georouting principle, and determines a path route, i.e., optimal *spectrum band* at each node, and *next hop relay node*, that minimizes end-to-end delay for each message in such d-DSA DTNs. Finally in Section 7.5, we compare the proposed dDSA-GR protocol against the standard (single-band) GR protocol, and other two benchmark DTN routing protocols, namely Epidemic and Spray and Wait, and also their extended d-DSA aware versions. Results on realistic traces based on the map of Lexington city, KY, USA show that the proposed dDSA-GR protocol achieves much better network delay, message delivery, energy efficiency, and negligible message overhead, compared to standard GR, ER, and SnW routing protocols, and their extended d-DSA versions.

7.1   Network Model

Since the location of d-DSA nodes, particularly urban vehicles, primary user's activities, communication opportunities over various spectrum bands, and the channel availability within each band may evolve over time, we model the d-DSA delay tolerant network (d-DSA DTN) as a time-evolving graph. Refer to the simple example d-DSA DTN graph illustrated in Fig. 6.1 (in Chapter 6), where nodes 1 and 2 can communicate over band 0 at time instant 0, whereas at time instant 1, they can communicate over both spectrum bands 0 and 1. Consider the total time duration T to be divided into discrete and equal time slots, such as, $\{0, 1, \ldots t \ldots T\}$, then at a given time slot t, let $G^t = (V^t, S^t, E^t)$ be a directed graph that represents the snapshot of the d-DSA DTN network at time slot t. Here V^t, S^t, and E^t respectively represent

the set of d-DSA nodes, (i.e., urban vehicles and gateways), set of spectrum bands, and set of direction communication links (or opportunities) between any node-pair over any spectrum band at time slot t. A link $e_{ij}^s \in E$ is the directed communication link from node i to j over band $s \in S$. Let t_{ij}^s denote the link delay incurred in transmitting a certain message packet over a communication link e_{ij}^s. Note that a link e_{ij} between nodes i and j over band s is only existent in graph G if it meets the following conditions – (i) nodes i and j are at a geographical distance d less than or equal to the communication range γ^s over band s, i.e., $d \leq \gamma^s$, and (ii) there exists a free channel in band s at both nodes i and j. For ease of presentation, we assume that V^t and S^t are constant over time, i.e., $V^t = V$, and $S^t = S$, $\forall t \in \{1, 2, \ldots, T\}$. However, our approach can be easily extended to consider d-DSA DTN scenarios where nodes join and leave the network.

7.2   Issues with Standard DTN routing protocols

In this section, we provide a brief overview of two standard routing strategies, namely Epidemic Routing [45] and Spray and Wait Routing [47], originally designed for the standard (single-band) DTNs. Following this, we highlight the shortcomings of such DTN routing strategies, while dealing with d-DSA DTNs, and thus motivating the need for designing new routing strategy for such d-DSA DTNs.

Standard DTN Routing Protocols: A brief overview

Epidemic Routing (ER)   [45] - The ER protocol is flooding-based routing protocol. In this protocol, a node replicates and forwards messages to all of its neighboring nodes (i.e., in communication range of each other). This forwarding operation is repeated at each encountering node, and thus, offers very high packet delivery and low network latency. However note that, this protocol is susceptible to huge message overhead, thus suffers from very high energy expenditure.

Spray and Wait Routing (SnW)   [47] - The SnW protocol is a controlled flooding-based routing protocol. In this protocol, the source node of a certain message initially starts with a prespecified L message copies. Then, any node i, either source or relay, that has $L > 1$ message copies, and encounters another node B (with no copies), it hands over $\lceil \frac{n}{2} \rceil$ copies to the encountering node j and keeps $\lfloor \frac{n}{2} \rfloor$ for itself. When node i is left with only one copy, it switches to direct transmission, and forwards the message only to the destination node. Here, the worst-case message overhead would be at most L.

Let us look at three examples of standard Delay Tolerant Networks (DTNs) and a d-DSA aware DTN as shown in Fig. 7.1. From the figure it is clear that in standard DTN, a certain node is restricted to utilize a pre-specified fixed band, and therefore can only communicate with any other node over the prespecified band. On contrary, in case of d-DSA DTN, a node can utilize various spectrum bands and can communicate with other node over any chosen band. Hence, considering that there exists S set of bands, then $|S|$ potential communication interactions (or links) may
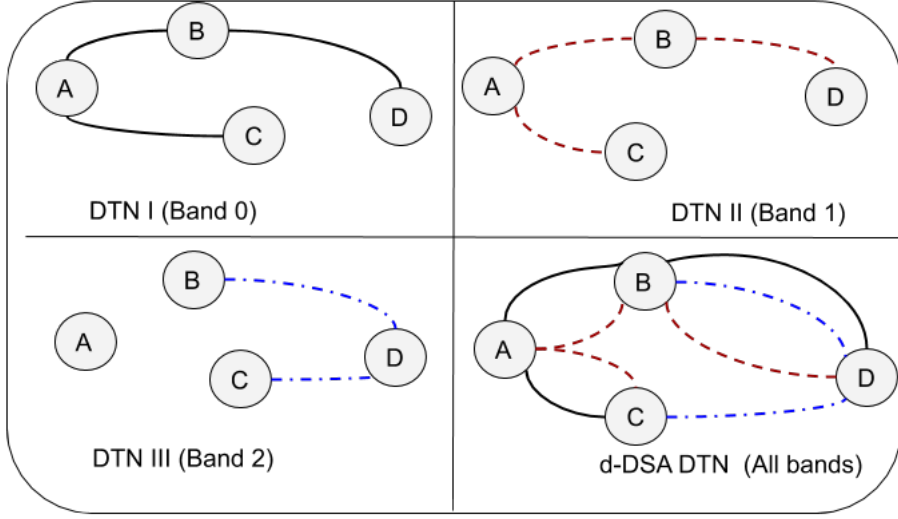
Figure 7.1: First three networks are examples of standard Delay Tolerant Networks (DTNs), where each node is restricted to communicate with any other node over a fixed band – be it band 0 (in DTN I), band 1 (in DTN II), and band 2 (in DTN III). Last network is an example of d-DSA DTN network where each node has utilize any of the considered three bands, i.e., Band 0, Band 1, and Band 2.

be possible between any node pair in the d-DSA DTN network, whereas only one link is possible in a standard DTN network.

Additionally from our discussion in Chapter 4, we know that EM characteristics, such as, transmission range and channel bandwidth, of various spectrum bands are distinct and unique to a certain band. For instance, TV band offers a very good coverage (usually tens of kms), however poor channel bandwidth (6 MHz), whereas ISM band offers a low channel bandwidth (usually 11 MHz), and transmission coverage (in range of few hundred meters). On contrary, CBRS band has a poor coverage, however, very high channel bandwidth (40-60 MHz). Finally, the LTE band has both high coverage (in range of few kms) and channel bandwidth (usually 20 MHz). A d-DSA node can harness these EM properties of various bands whereas a standard wireless device is restricted to a pre-specified fixed band.

Finally, let us note the following two important observations: (i) the cardinality of neighbors for a certain node (say i) in the d-DSA DTN greatly varies depending on the selected spectrum band. For example, if the chosen band is TV band (with high transmission coverage), then the node i will likely have a very high number of neighbors, whereas node i would have very few neighbors if the chosen band is CBRS band (due to its poor coverage), and (ii) the incurred delay in transmitting a certain message from a node i to another node j will vary significantly from one node another. For instance, the incurred delay in transmitting a certain message in TV band (with less channel bandwidth) will likely be much higher than that of CBRS band (with very high channel bandwidth).

Now, since the ER and SnW routing protocols were originally proposed for stan-

dard DTNs, they do not have the capability of exploiting the large set of communication links (due to various bands) offered by the d-DSA DTN networks. Moreover, these routing protocols lack the capability of dealing with distinct EM characteristics of various bands.

Hence in the following sections, we first formulate the routing problem in a d-DSA DTN topology, as an Integer Linear Programming (ILP) optimization problem. Though solving this optimization problem would provide an optimal routing strategy, it is impractical in such time-varying and unpredictable dDSA DTN scenarios. Thus, we propose a lightweight georouting principle based *d-DSA aware Geographical Routing* (dDSA-GR) protocol, that accounts for the availability of large set of communication opportunities over multiple spectrum bands, and determines a suitable path route for each message traffic, such that the desired QoS requirements are met as discussed in Section 7.4.

7.3 Problem Formulation

We consider a time-evolving d-DSA network topology where each node has the complete knowledge of future traffic demands, and dynamic topology evolution, i.e., all potential communication links at all time intervals $t \in [0, T]$ over all spectrum bands $s \in S$ (where each link e^s between a pair of nodes is formed over a common free channel in spectrum band s), and set of all available channels in a band s. The formulation is an adaptation of the dynamic version of the classical multi-commodity flow problem [96, 97].

Time Intervals. A simple approach to obtain the set of time intervals is to discretize time into very small, fixed-size intervals. However, this can lead to a very large number of time intervals and may not be practical. Instead, we consider the time intervals to be partitioned by a time duration equivalent to τ, which is the least message transmission delay (i.e., time consumed in transmitting the message with least message size over the spectrum band with least bandwidth.). Though this may also require further enhancement, here we assume that the time intervals have been determined. Let $\mathcal{I} = \{I_1, \ldots I_h \ldots I_T\}$ denote the set of time intervals. By construction, $I_h = [t_{h-1}, t_h)$ (and $t_{h-1} < t_h$). Therefore, the set $\mathcal{I}$ partitions the interval $[t_0, t_T)$.

We make the following important assumptions in the formulation: (i) both capacity and delay of an edge over any band s are constant over a time interval., and (ii) each edge in the network utilizes a unique free channel in a certain band s [1].

Traffic demand. Traffic demand is the set of all messages and is denoted by K. A message is a tuple (u, v, t, m) where (u, v) is the source-destination node pair, t is the generation/arrival time and m is the message size. For a message $k \in K$, the

---

[1]For simplicity, we do not consider channel coalescing, i.e., channel bonding (merging two or more contiguous channels together) nor channel aggregation (non-contiguous channels) in this formulation, however, it can be addressed with a bit higher complex formulation.

functions $s(k)$, $d(k)$, $w(k)$, and $m(k)$ are used to retrieve source node, destination node, start time, and message size, respectively.

Graph Construction. The definitions listed in Table 7.1 are based on the network architecture presented in Chapter 3.

Table 7.1: Graph Definitions

Notations	Definitions
$G(V, E, S)$	denote the set of nodes, edges and spectrum bands in the network graph G
E	$= \cup_{s \in S} E^s$, where E^s is the edge set over a certain band s
$e^s \in E^s$	where e^s is an edge over band s in the edge set E^s
$c^s : E^s \times R^+$	where $c_{e^s, t}$ is the capacity of edge e^s at time t
$d^s : E^s \times R^+$	where $d_{e^s, t}$ is the transmission delay of the edge e^s at time t
$n_{I_h}^s$	is the number of available orthogonal channels in a band s in the interval $I_h \in \mathcal{I}$
γ^s	is the transmission range of band s
pkt	is the packet size.
b_v	is the storage capacity of node v
nTx_v	is the number of transmitters at node v.
nRx_v	is the number of receivers at node v.
I_v^s	is the set of incoming edges over band s to node v
O_v^s	is the set of outgoing edges over band s from node v
$N_{v,t}^s$	is the set of neighbors of node v over band s at time t
K^v	$= \{k | k \in K \text{ and } d(k) = v\}$ i.e., the set of messages whose destination node is v

Variables. The variable definitions as listed in Table 7.2 capture the state and the transition in the proposed d-DSA network.

Table 7.2: Variable Definitions

Variables	Definitions
B_{v,t_h}^k	is the number of packets of message k occupying the buffer at node v at time $t_h \in T$
X_{e^s, I_h}^k	is the number of packets of message k transmitted over edge e^s during interval $I_h \in \mathcal{I}$
R_{e^s, I_h}^k	is the number of packets of message k received over edge e^s during interval $I_h \in \mathcal{I}$
y_{e^s, I_h}	is a binary variable that denotes whether an edge e^s (over band s) is selected for transmitting (or receiving) message(s) during interval $I_h \in \mathcal{I}$

The transmission variable X and reception variable R are used together to model the incurred propagation delay encountered in sending messages.

Objective function. The objective function is to minimize the worst-case end-to-end message transmission delay. The summation $\sum_{s\in S}\sum_{e^s\in I_v^s} X_{e^s,I_h}^k$ represents the number of packets belonging to message k that is incoming (on any spectrum band) into the node v in the time interval I_h. This is multiplied by the length of time that has incurred since the start of that message (i.e., $t_{h-1} - w(k)$) so as to obtain the total time delay incurred by that number of packets of message k that arrived in time interval I_h at node v. Finally, we minimize over all the time intervals (i.e., $I_h \in \mathcal{I}$) for all messages (i.e., $k \in K^v$) for all nodes.

$$\underset{v,k\in K^v, I_h\in\mathcal{I}_{\mathcal{E}}}{\text{Minimize}} \left((t_{h-1} - w(k)) . \sum_{s\in S}\sum_{e^s\in I_v^s} X_{e^s,I_h}^k \right) \tag{7.1}$$

$$\frac{X_{e^s,I_h}^k \times pkt}{m(k)} \le y_{e^s,I_h} \quad \forall e^s, I_h \tag{7.2}$$

$$\frac{R_{e^s,I_h}^k \times pkt}{m(k)} \le y_{e^s,I_h} \quad \forall e^s, I_h \tag{7.3}$$

$$\sum_{s\in S}\sum_{e^s\in I_v^s} y_{e^s,I_h} \le nRx_v \quad \forall I_h \tag{7.4}$$

$$\sum_{s\in S}\sum_{e^s\in O_v^s} y_{e^s,I_h} \le nTx_v \quad \forall I_h \tag{7.5}$$

$$\sum_{e^s\in O_v^s} y_{e^s,I_h} + \sum_{w\in N_{v,I_h}^s}\sum_{e^s\in O_w^s} y_{e^s,I_h} \le n^s \quad \forall I_h \tag{7.6}$$

$$\sum_{s\in S}\sum_{e^s\in I_v^s} R_{e^s,I_h}^k - \sum_{s'\in S}\sum_{e^{s'}\in O_v^s} X_{e^{s'},I_h}^k = \begin{cases} B_{v,t_h}^k - B_{v,t_{h-1}}^k + m(k), & if s(k) = v, w(k) = t_h \\ B_{v,t_h}^k - B_{t_{h-1}}^k, & otherwise \end{cases}$$

$$\tag{7.7}$$

$$\sum_{k\in K} N_{v,t_{h-1}}^k \times pkt \le b_v \quad \forall v, I_h \tag{7.8}$$

$$\sum_{k\in K} X_{e^s,I_h}^k \le c_{e^s,t_{h-1}} . |I_h| \quad \forall e^s, s, I_h \tag{7.9}$$

$$B_{v,t_0}^k = \begin{cases} m(k), & if\ v = s(k), t_0 = w(k) \\ 0, & otherwise \end{cases} \quad \forall k, v \tag{7.10}$$

$$B_{v,t_{\hat{T}}}^k = \begin{cases} m(k), & if\ v = d(k) \\ 0, & otherwise \end{cases} \quad \forall k, v \tag{7.11}$$

$$y_{e^s,I_h} \in \{0,1\}, X^k_{e^s,I_h} \in \left[0, \frac{m(k)}{pkt}\right] \tag{7.12}$$

<u>Constraints.</u> Equation 7.2 restricts the transmission of non-zero number of packets of message k over band s at interval I_h only if there exists an edge over band s at that time interval, whereas Equation 7.3 does the same for reception. Equations 7.4 and 7.5 respectively constrain the number of incoming and outgoing edges from/to node v by the number of receivers and transmitters (equipped with that node), at a certain time interval I_h. Equation 7.6 denotes that the number of transmissions (i.e., outgoing edges) in a certain band s at a certain node v and its vicinity (i.e., N^s_{v,I_h}) is limited by the prespecified number of channels in that band.

Equation 7.7 - 7.9 denote the conventional flow, node storage and edge capacity constraints. Eq. 7.7 depicts the flow constraint, which balances the change in the node storage occupancy against the network incoming and outgoing flow for each time interval. Equation 7.8 ensures that the storage of messages at a certain node does not exceed the pre-specified memory storage capacity limit. Equation 7.9 restricts the number of amount of messages sent over a certain link e^s (formed over a band s) to be limited by its capacity over that time interval.

Equations 7.10 and 7.11 are the initial and the final conditions of storage at a certain node v, at times t_0 and t_T, respectively. Equation 7.10 denotes that at start time t_0, only nodes that generate messages (at time t_0) have an occupied memory buffer. Equation 7.11 states that at the end time t_T, only nodes that are the destinations of the messages have an occupied memory buffer. Finally, Equation 7.12 provides the bounds of the decision variables used in the formulation.

The ILP formulation offers an upper bound of the achievable performance, but it would be impractical to solve such problem to determine optimal spectrum band and next hop node for such time-varying d-DSA networks. In fact, the problem not only has very high complexity and number of variables/constraints, but also assumes the knowledge in advance of the network dynamics, communication opportunities over various bands over time, message generation/arrival times etc. For these reasons, we propose a lightweight yet effective routing strategy as discussed in the next section.

7.4 d-DSA aware Geographical Routing Protocol

In order to address the shortcomings of standard (single-band) DTN routing strategies, and better exploit the multiple communication opportunities that may be available in the envisioned d-DSA network architectures (and d-DSA DTN networks), this section proposes a *d-DSA aware Geographical Routing* (dDSA-GR) protocol for such *dynamic* and *unpredictable* d-DSA DTN networks, and is mainly based on georouting principle (explained later in subsection 6). Of all the routes from a certain source node (i.e., a sensing node) to the destination (i.e., a gateway), we are particularly interested in a path route, i.e., *optimal spectrum band* at each node, and *optimal next-hop relay node*, that minimizes the *end-to-end network delay* of each information message traffic as the QoS metric. This QoS metric is important for the proposed d-DSA architecture; in order to support various rural applications in a timely manner.

Nevertheless, other QoS metrics, e.g., minimum hop count, energy efficiency etc. can be easily integrated in the proposed routing scheme. Here, we would like to point out that though the energy efficiency is not the key QoS metric of interest in this chapter, our dDSA-GR protocol would still excel in terms of energy efficiency (as evident from our evaluations in Section 7.5). This phenomenon can be mainly attributed to the relationship between the end-to-end delay and energy consumption, as explained in Chapter 4.

The proposed dDSA-GR protocol is a two-step protocol – (1) *Spectrum band selection* and (2) *Next hop node selection.*

Spectrum Band Selection

Unlike standard DTN routing protocols, an important step for the proposed routing strategy is to select a suitable spectrum band at each hop node in the path route between a certain source-destination node pair.

From our previous discussion on EM characteristics of various bands in Chapter 4, it is clear that keeping the transmit power, antenna gains, path loss, antenna height, and other factors constant, the lower frequency bands, such as, TV band, have higher transmission coverage whereas poor channel bandwidth (or effective bit rate). On the other hand, the higher frequency bands like CBRS band has poor transmission coverage, whereas offer very high channel bandwidth (and bit rate). Hence, there exists a clear trade-off on whether to choose a spectrum band with higher transmission coverage or higher channel bandwidth. Keeping these in mind, we propose a simple linear regression approach to select a suitable band s_i^* at a certain node i, which is as follows.

$$s_i^* = \max_{s \in S} w e^{-\frac{1}{\mathbb{R}^s}} + (1 - w)e^{-\frac{1}{\lambda^s}} \tag{7.13}$$

where $\hat{S}$ is the set of spectrum bands, $\mathbb{R}^s$ and λ^s represent the effective bit rate and transmission coverage corresponding to a certain channel c^s belonging to a spectrum band $s \in S$, respectively, and w is the weighing parameter, where $0 \leq w \leq 1$. If $w = 1$, the spectrum band which offers the highest channel bandwidth (and effective bit rate) is chosen first, loosely referred to as *Bandwidth-first* strategy. On contrary, if $w = 0$, then the band with better transmission coverage is chosen first, referred to as *Range-first* strategy. Finally if $0 < w < 1$, the intuition is choose a suitable spectrum band that excels at both transmission coverage and channel bandwidth, loosely referred as *Weighted* strategy. Evidently, the bandwidth-first strategy is useful for d-DSA network scenarios where the key objectives behind spectrum band selection is to minimize message transmission delays and incur minimum interference; suitable for dense and high load network scenarios. On contrary, the Range-first strategy would be intuitively be more suitable for sparse and low load d-DSA network scenarios, with fewer d-DSA nodes to communicate with, fewer primary users to interfere with, and fewer information messages to deliver.

Note that the chosen spectrum band s_i^* at a certain d-DSA node i must have at least one free (or non-interfered) channel, for (i) it ensures incumbent primary user

protection policy (and does not interfere with licensed primary users), and (ii) it enables seamless spectrum band sharing with other secondary d-DSA nodes in the d-DSA overlay network. Hence, a key requirement of proposed spectrum band selection is to select a suitable band that has at least one available channel, which is neither interfered by a primary user device nor a secondary d-DSA node. We discuss the details of the proposed algorithm for the spectrum band selection in the following.

Algorithm 5: Spectrum Band Selection

Input: A d-DSA node i, spectrum band set S
Output: Chosen spectrum band s^*, and neighbor list $N_i^{s^*}$

1 Initialize chosen spectrum band s^* as ISM band Neighbor list $N_i^{s^*} = $ find-neigh-nodes (s^*, γ^{s^*}) $\hat{S}$ = sort-spectrum-bands(w) is-first-band = $True$

2 **for** *current band,* $s \in \hat{S}$ **do**

3   N_i^s= find-neigh-nodes (s, γ^s)

4   **if** *is-first-band = True and is-common-channel-available(s, i, N_i^s) = True* **then**

5          $s^* = s$ $N_i^{s^*} = N_i^s$ is-first-band = $False$

6   **if** *is-common-channel-available(s, i, N_i^s) and $(|N_i^{s_{new}}| - |N_i^{s^*}|) > 0$ and* $B^s > B^{s^*}$ **then**

7          $s^* = s; N_i^{s^*} = N_i^s$

8 return s^*, $N_i^{s^*}$

Algorithm Overview. As shown in pseudocode 5, the proposed spectrum band selection algorithm first initializes the chosen spectrum band s^* as the ISM band at a certain d-DSA node i, for it is unlicensed and there are no policy restrictions on accessing a certain channel in ISM band. Then, as shown in line 1, the spectrum band set S is sorted based on non-increasing value of the unified metric (see Eq. 7.13). The value of weighing parameter w in the metric is taken as 1, 0, or any other value (for instance 0.5), depending upon the considered bandwidth-first, range-first or weighted strategy, respectively. As discussed previously, there is no bias on choosing one strategy over the other, and mainly depends upon the considered network scenarios. We discuss the impact of different values of w in the Evaluation section. Now, as shown in lines 4 - 5, it should be straightforward to choose the first spectrum band, say s, in the sorted spectrum band list $\hat{S}$ as the selected spectrum band s^*, provided that there exists non-zero free channel(s) at both node i and at atleast one node in the neighbor list N_i^s over first band s.

However, in order to further enhance the QoS metric, i.e., minimum end-to-end network delay, our algorithm attempts to select a new spectrum band, say $s \in \hat{S}$, as the optimal spectrum band s^* that offers the highest channel bandwidth, whereas also meets the following two constraints (i) there exists at least one available (non-interfered) channel in the newly selected spectrum band s, and (ii) the cardinality of neighbor list N_i^s over newly considered band s, is either better or equal to than the cardinality of neighbor list $N_i^{s^*}$ over the determined optimal spectrum band s^*.

See lines 2 - 7 for details. The key intuition behind this additional step is to improve the QoS metric by selecting a high bandwidth spectrum band that will likely incur lower message transmission delay (and thus improve QoS metric), and without compromising the neighbour list (or symbolically the transmission coverage).

Hop Relay Node Selection

This subsection discusses the proposed strategy for next hop node selection in the path route between any source-destination node pair in the d-DSA network. Note that the hop node selection is an important step and has been well investigated for standard (single-band) DTN routing protocols [45, 47]. Hence, for this step, our routing protocol utilizes existing hop node selection strategy from a well-known *georouting or position based routing principle* [98]. An overview of the georouting principle is as follows.

Georouting principle. Georouting is a routing principle that relies on the geographic position information of each node in the network. The underlying idea for georouting principle is as follows: Whenever a node i receives the message packet, it forwards it to one of its neighboring node lying towards the *direction* of destination node j. Hence, it is evident that the neighbor is selected using a forwarding rule that takes into account only the location of j and the network topology in the immediate (or one-hop) neighborhood of i. There are several variants of georouting, mainly based on the *forwarding rule* for selecting the next hop node, for instance, (i.a) *greedy forwarding* - Here, a node forwards the message to the neighbour that minimizes the distance to the destination. Alternatively, another notion for forwarding rule is (i.b) minimum projected distance on the source-destination-line as in *Most Forwarding within Radius (MRF)* and *Nearest with Forwarding Progress (NFP)* or (i.c) minimum angle between neighbor and destination as in *Compass Routing*. It is noteworthy that greedy strategy and MFR are loop free, i.e., a message packet can circulate among nodes in a certain constellation, whereas NFP and Compass Routing are not. Also notice that georouting can lead into a dead end, i.e., there is no neighbor closer to the destination, in case of traditional wireless networks. However, georouting fused with delay tolerant routing does not run into such a dead end issue, for the network topology changes and a suitable next hop node becomes available over non-infinite time period.

Proposed Next Hop Selection Approach. Our proposed routing protocol first selects a suitable spectrum band s^* at a certain d-DSA node i, and then determines the optimal next hop node h from the neighboring node list $N_i^{s^*}$ (over selected spectrum band s^*), which is based on a simple greedy variant of *georouting principle*. The key idea here is to forward message packets to nodes moving towards the destination node, i.e., whose geographical distance to the destination is decreasing with time, and moreover moving faster towards the destination. Specifically, a node i will forward a message packet destined for node j to a certain neighbor node h, out of all nodes in neighbor list $N_i^{s^*}$, if any of the following condition is met.

1. h is moving towards j, and i is either not moving or moving away from j.

2. i is moving away from j and h is not moving.

3. i, h are moving away from j, but h is closer to j.

4. Both i and h are moving towards j, but h is moving faster than i towards j

If none of these conditions is fulfilled, then node i continues to hold on to the packet. This forwarding rule is inspired from a DTN routing protocol, which is also based on georouting principle, referred to as MOVE protocol in the paper [98]. In this work, we refer to this georouting principle based DTN routing protocol as standard geographical routing (GR) protocol for ease of presentation. However, the standard GR protocol will also suffer from the issues highlighted in Section 7.2, and therefore can not be effectively applied to d-DSA DTNs.

Algorithm 6: Next Hop Node Selection Algorithm

Input: A d-DSA node i, Chosen spectrum band s^*, message packet m
Output: Chosen next hop node, h

1 Compute the *priority-node-list* based on the forwarding rules laid out in subsection 8

2 **for** *Node h in priority-node-list* **do**

3   **if** *m not in node h's buffer* **then**

4   Chosen channel c^{s^*} = get-common-channel(s^*,i,H)

5   **if** *chosen-channel not found* **then**

6   continue

7   **else**

8   Mark $h \rightarrow c^{s^*}$ as busy Mark $i \rightarrow c^{s^*}$ as busy Mark $j \rightarrow c^{s^*}$ as busy, where $j \in N_i^{s^*}$ break

9 return chosen hop h

Algorithm Overview. As shown in pseudo code 6, the proposed algorithm for next hop selection computes the priority-node-list based on the forwarding rules laid out in subsection 8 in decreasing priority order. Following this as shown in lines 2 - 8, the algorithm chooses the first node, say h in the priority-node-list as the optimal next hop node, provided that it meets the following conditions – (i) node h does not have the message packet m in its memory buffer, and (ii) there exists at least one free channel in chosen band s^* that is available at both nodes i and h. Note that, as shown in line 8, the chosen channel c^{s^*} in optimal band s^* is marked busy at nodes i, chosen hop node h, and all nodes in the neighbor list of transmitting node i, i.e., $N_i^{s^*}$. This ensures that there is no co-channel interference due to simultaneous transmission over the same channel in the same spectrum band, by two or more d-DSA nodes in each other's proximity.

74

Figure 7.2: Map for Lexington, KY, USA: Brown colored roadways are the primary roads in the Lexington city. Each vehicle is deployed over one of the randomly chosen primary road (We do not consider dotted line roads as we believe they are noise in the dataset).
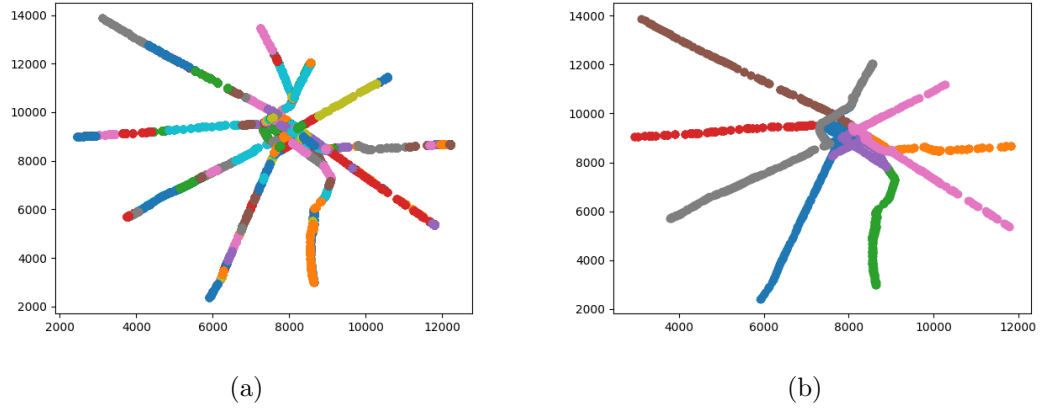

(a)

(b)

Figure 7.3: (a) Before processing the road network dataset, and (b) After processing the road network dataset

Once both the suitable spectrum band s^* and next hop node h are determined, the proposed routing protocol transmits the message packet over the chosen band s^* (on a non-interfered channel, neither by primary devices nor by other d-DSA devices in proximity) to the next hop node h.

7.5 Performance Evaluations

Experimental Setting

We have developed a discrete event-driven message packet based simulator [2] in Python for the large-scale experimental study. As shown in Fig. 7.2, we consider Lexington, KY, USA with an area of around 250 sq. km as a rural case scenario. The road networks [3], primarily the highways and roadways (highlighted in brown), with at least 30 GPS traces, in the Lexington city are considered for the experimental study, and are extracted from OpenStreetMap [99].

It is noteworthy to mention that given OpenStreetMap dataset is crowdsourced, the GPS traces for several highways and roadways are distributed over multiple linestrings in the extracted Lexington road network dataset. Specifically as evident from Fig. 7.2, there are approximately 10 roadways and highways, however there were as many as 183 linestrings in the extracted road network dataset. Hence, we intuit that a certain linestring in the dataset indicates a partial roadway segment rather than the entire roadway segment. Our intuition was confirmed by following observations: First, the euclidean distance between first and last coordinates in some linestrings in the dataset were as small as few hundred meters, which is very unlikely for a certain roadway or a highway in the city scenario. Furthermore, we noticed that the last coordinate in a certain linestring was also the first coordinate in another distinct linestring in the dataset. Finally, we plotted all 183 lines as depicted in Fig. 7.3(a), that also supports our intuition. Each color represents a certain linestring in the dataset.

Hence, we computed the final set of roadways and highways (from the list of partial road segments) in the Lexington city, by processing the dataset using the following simple rule: *Concatenate any two distinct linestrings together if the last coordinate in one linestring is the same as the first coordinate in another distinct linestring. Repeat the process until no two linestrings could be concatenated.* After processing the dataset, there were only 8 such roadways, which are shown in Fig.7.3(b), and are utilized for the experimental study.

All the experiments, unless otherwise stated, are performed with 15 sensor blocks, each equipped with 40-60 sensing nodes (such as sensors and smart devices), 5 gateways, and 30 urban vehicles. The computed 8 roadways and highways are the possible route trajectories for urban vehicles such as, public buses and taxis. The total time period is 6 hours.

Node Mobility Model. Here we discuss the node mobility model that we utilize to evaluate the proposed d-DSA architecture, and routing strategies, on the real map of Lexington city, KY, USA. The sensor blocks, primary users, and gateways are randomly placed in the area, and remain fixed throughout the simulation pe-

---

[2]The simulator code is made open source and is available at https://github.com/blu226/DSA-RoutingSimulations

[3] We do not consider dotted lines for our experimental study as we believe they are noise rather than actual roadways/highways.

Table 7.3: List of simulation parameters

Simulation parameters	Description
Underlying map information	Lexington city, KY, USA
Simulation area	250 sq. kms
Number of sensor blocks	15
Number of gateways	5
Number of urban vehicles	92
Average speed of urban vehicles	[150 - 400] meters/minute
Message generation mean time	$[10 - 20]$
Message burst size	[5 - 15]
Message packet size	5 Mb
Message packet TTL deadline	90 minutes
Number of primary users	200
Primary user ON/OFF mean time	$[1 - 4]$ minutes
Number of channels in each spectrum band	6
Node memory size	1000 Mb
Simulation time	360 minutes
Number of iterations	25

riod. We uniformly distribute the urban vehicles on each route and on each direction. More specifically, consider that there are 92 urban vehicles, and 8 routes (i.e., highway/roadway), then we deploy approx. $\frac{92}{2 \times 8} = 5.75$, i.e., 5 or 6 urban vehicles, on each direction (backward or forward) on each route.

The utilized mobility model attempts to replicate the mobility patterns of urban vehicles, such as, public buses, taxis etc., where each vehicle moves along a certain highway/roadway, and may visit several sensor blocks, like a bus depot, hospital or parking lot. Specifically, each vehicle travels back and forth on a pre-specified roadway with a random speed in the interval [150 - 400] meters/min. Moreover, to take into consideration that the urban transport vehicles would be spread out in a certain route and in each forward/backward direction, we initially deploy the vehicles at random GPS locations in a certain route, and the direction is again randomly selected.

Message Traffic Model. We consider a message traffic model with bursty generation of messages at each sensing node. The inter-arrival time between the bursts is taken from an exponential distribution with mean of 15 minutes, and the length of each message burst varies [5 - 15] messages. The message size of each message belongs to the set of discrete bins of message sizes: 1, 20, 50, 120 Mb. The packet size is taken as 5 Mb. Hence, the number of packets corresponding to a certain message, for instance 1 Mb, is given by $\lceil \frac{1}{5} \rceil = 1$, and for 120 Mb, is $\lceil \frac{120}{5} \rceil = 24$. The TTL value for each message packet is taken as 90 minutes [4].

---

[4]We take large values of TTL, as the proposed d-DSA network architecture is suitable for delay-tolerant rural communications

Table 7.4: Spectrum profile

Band Type (MHz)	Rep. freq. (MHz)	Bandwidth (MHz)	Rep. bandwidth (MHz)
TV Band (54-216, 470-698)	600	6 - 9	6
LTE Band (700-900, 1700-2100)	900	5-20	10
ISM Band (2400-2500, 5700-5800)	2400	3-50	20
CBRS Band (3500-3700)	3500	10-40	40

Buffer Management Model. For accessing the memory buffer by a certain node, we consider a priority queue (PQ) model, rather than a usually considered First-In-First-Out (FIFO) model [5]. According to the PQ model, the node's memory buffer is sorted in non-increasing order, based on following two parameters: (i) the destination node of a certain message packet is within the communication range of the chosen spectrum band, and (ii) message generation time. We utilize the existing approach of dropping the oldest message packet first (ODF) in case of buffer overflow.

Primary User Model. We deploy primary users randomly in the undertaken Lexington city area. The ON/OFF time for a primary user in a certain channel in a spectrum band is chosen randomly from the interval $[1 - 5]$ minutes.

EM characteristics Model. We consider the maximum allowable transmit power for all bands on a secondary basis, such as 1 W for ISM band, 4 W for TV and LTE bands, and 10 W for CBRS band. Recall that each band has a FCC mandated maximum allowable transmit power which can not be exceeded by any node operating on a DSA basis. The transmitter and receiver antenna gains are taken as 0 dBi. Please refer to Table 7.4 for details of considered frequency (Column 2) and channel bandwidth (Column 4) in each band. The values of other parameters are: path loss factor $= 2.7$ (suburban area), received power threshold $= -95$ dBm, Signal-to-Noise Ratio (SINR) $= -100$ dBm. These parameters are used to compute the transmission range (from Frii's Transmission Equation [72]) and effective bit rate (using Shannon Hartley Theorem [74]) for a certain channel in any given band.

Comparison approaches

We evaluate dDSA aware geographical routing (dDSA-GR) routing protocol specifically designed for the envisioned d-DSA network architecture against the basic ge-

---

[5]This is because we observe that the PQ model performs much better than FIFO model for buffer management, in both DTN and d-DSA aware DTN routing protocols.

ographical routing (GR) protocol and two other benchmark DTN routing protocols, i.e., Epidemic Routing (ER), and Spray and Wait Routing [6] (SnW). Furthermore for extensive analysis, we also evaluate our dDSA-GR protocol against the extended d-DSA aware Epidemic Routing (dDSA-ER) and d-DSA aware Spray and Wait (dDSA-SnW) protocols respectively, which also attempt to better exploit the multiple communication opportunities that may be available in the d-DSA architecture.

dDSA-ER Routing protocol. Similar to the proposed dDSA-GR routing protocol, the dDSA-ER protocol is also a two step protocol. The first step determines the suitable spectrum band, depending upon the unified metric shown in Eq. 7.13, similar to dDSA-GR protocol. In the second step, the dDSA-ER protocol works in the similar fashion to the basic ER protocol, and floods the message packets (depending upon the channel bandwidth in the chosen spectrum band) to each of the neighboring nodes. However, unlike standard ER, here a certain transmitter-receiver node communication can only occur if there exists a whitespace (non-interfered) common channel in the chosen spectrum band at both nodes.

dDSA-SnW Routing Protocol. The dDSA-SnW protocol is extended from the controlled flooding based standard SnW protocol, and works in two steps. The first step is to determine the suitable spectrum band. In the second step, the protocol forwards the message packets in the similar manner as that of SnW protocol. Again note that, similar to dDSA-ER protocol, the communication between a certain transmitter-receiver node pair can only occur if a non-interfered channel is available at both the communicating nodes in the chosen band.

Note that compared to dDSA-GR routing, the transmission energy consumed at the transmitter node remains the same in case of dDSA-ER and dDSA-SnW protocols, however, the reception energy consumed at the receiver nodes is multiplied by the cardinality of receiver nodes (to whom the packet is forwarded), corresponding to those protocols.

Simulation Experiments

In this section, we evaluate the performance of the proposed dDSA-GR routing protocol, against standard/non-DSA (single-band) GR, ER and SnW protocols, and also, the extended dDSA-ER and dDSA-SnW protocols, in terms of the following performance metrics –

- *Message Delivery Ratio* (MDR) - the fraction of total messages successfully delivered to the gateway (and therefore, the intended data center), to the total messages generated at all sensor blocks.,

- *Network Delay* - the average delay incurred in delivering all messages, for their sensor blocks to the gateway, and
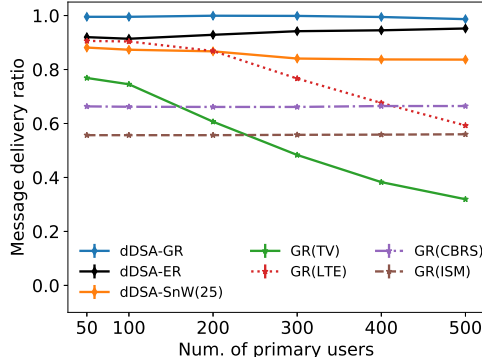
---

[6]There are several variants of Spray and Wait protocol however, we choose the binary Spray and Wait for the evaluation, as it is proven to be optimal SnW protocol under the unknown node mobility patterns, as in our case.
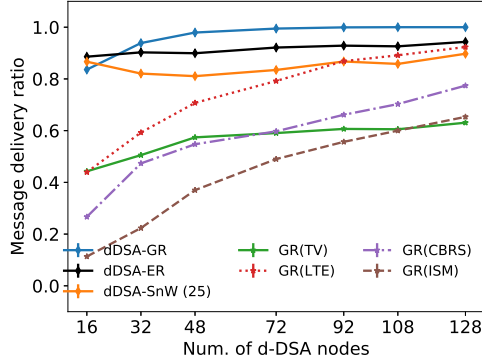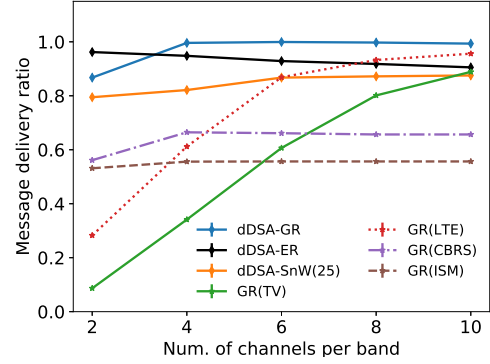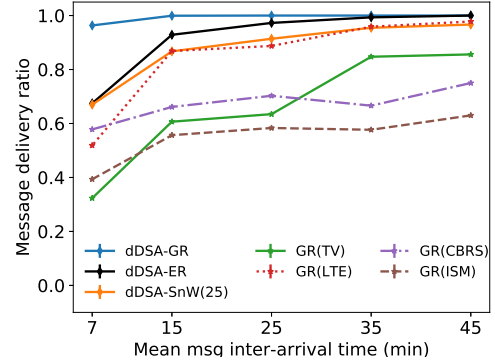
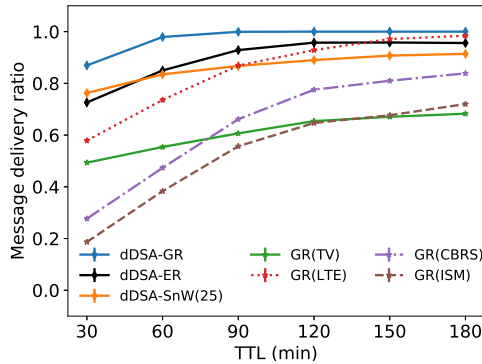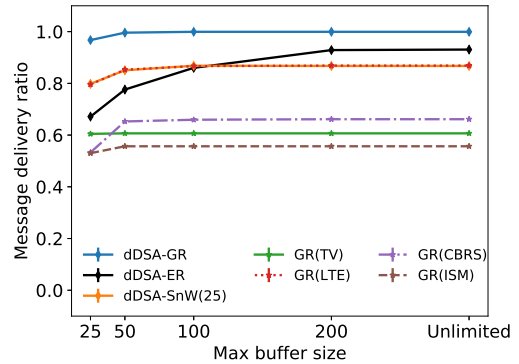Figure 7.4: Message delivery ratio analysis: (a) Number of d-DSA nodes, (b) Number of channels in each band, (c) Number of primary users, (d) Mean message inter-arrival times, (e) TTL deadlines, and (f) Maximum buffer sizes

- *Energy Expenditure* - the average amount of energy consumed to transfer the generated messages from all sensor blocks to the gateway.

For the clarity of plots, we do not show plots for standard ER and SnW routing protocols. However, the interested readers can refer to Appendix A for the comprehensive plots. Each of the performance metric is evaluated against the following parameters: varying (i) number of d-DSA nodes, (ii) number of channels per band, (iii) number of primary users, (iv) mean message inter-arrival times, (v) TTL deadlines, and (vi) maximum buffer sizes.

Message Delivery Ratio (MDR) Analysis. Figs. 7.4(a) - 7.4(f) show that the proposed dDSA-GR protocol significantly outperforms other two d-DSA aware protocols, i.e., dDSA-ER and dDSA-SnW, in terms of MDR, notwithstanding the considered parameters. This is because dDSA-GR is single-copy georouting principle based routing protocol, and incurs the least message overhead (see Fig. 7.5, for instance), and minimal message packet drops, due to buffer overflow and TTL expiry, for intuitively enough both buffer requirement and queuing delay would be minimum in case of dDSA-GR protocol compared to flooding-based dDSA-ER and dDSA-SnW protocols. Moreover, since the number of message transmissions is the least compared to other two d-DSA aware protocols, dDSA-GR would likely incur minimal channel interference in the chosen spectrum band, which would further enable dDSA-GR protocol to better exploit the spectrum resources, and deliver messages effectively (and thus highest MDR).
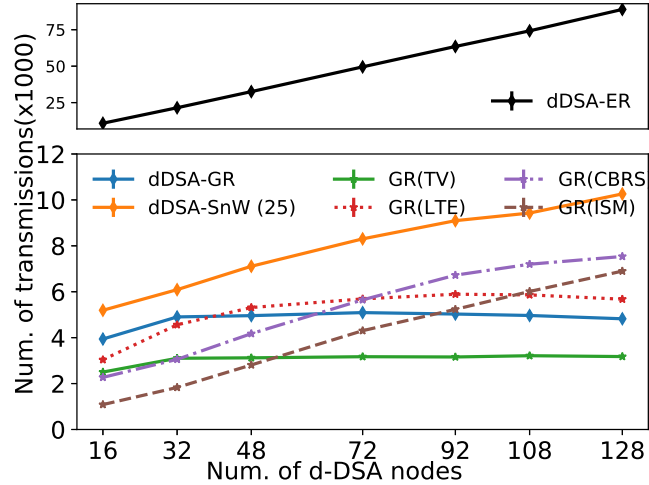
Figure 7.5: Number of packet transmissions vs number of d-DSA nodes

The proposed dDSA-GR protocol also greatly outperforms its standard (single-band) counterpart (i.e., GR protocol) in terms of MDR, under all considered parameters. This is particularly because, unlike standard GR restricted to a single-band, the dDSA-GR protocol is able to exploit the multiple communication opportunities provided by various spectrum bands in the undertaken d-DSA network scenario. Among

the standard GR approaches, the GR (LTE), i.e., GR protocol utilizing LTE band, performs the best in all d-DSA network scenarios, thanks to its high transmission range and high channel bandwidth (and effective bit rate).

Note that the MDR achieved by GR(TV) protocol does not improve much with increasing number of d-DSA nodes in the network. This is mainly because the GR(TV) protocol suffers severely from channel interference, incurred due to newly introduced d-DSA nodes in the network, besides the pre-existing primary users. Similar is the reason for improved MDR by GR(TV) with increasing number of channels, decreasing mean message inter-arrival times, and poor MDR with increasing number of primary users. The GR(CBRS) and GR(ISM) protocols improve gradually with increasing number of d-DSA nodes, thanks to the lower transmission coverage, and minimal channel interference due to both primary users and other secondary d-DSA nodes. Both these GR(CBRS) and GR(ISM) remain mostly unaffected by increasing number of channels per band, and primary users, for again they incur minimal channel interference, mainly due to the limited transmission range. It is straightforward to see that the MDR achieved by all standard and d-DSA aware protocols improve gradually with increasing mean message inter-arrival times, TTL deadlines and buffer sizes.

Network Delay Analysis. Figs. 7.6(a) - 7.6(f) show that the network delay achieved dDSA-GR protocol is much better compared to that of dDSA-ER and dDSA-SnW protocols, irrespective of considered network parameters. Again the reason is same as above, where dDSA-GR incurs minimal queuing delay at node's buffer, and better exploits multiple communication opportunities over diverse spectrum bands, that are more readily available for usage, for dDSA-GR incurs minimal channel interference (and thus higher chance of finding a common non-interfered channel in the chosen spectrum band). Note that dDSA-SnW incurs lower network delay for > 72 number of d-DSA nodes and > 4 channels per band, and similarly dDSA-ER for < 100 buffer size. However in these scenarios, these protocols suffer significantly in terms of MDR (see MDR plots in Figs. 7.4(a) - 7.4(f)), which is undesirable for effectively supporting various rural applications.

Compared to d-DSA aware GR protocol, the standard GR counterparts which are restricted to a single band, whether TV, LTE, CBRS or unlicensed ISM band, suffer greatly in terms of network delay, under all considered network parameters. Among standard GR protocols, GR (TV) incurs better network delay, followed by GR (LTE), GR (CBRS), and GR (ISM) protocols. This is mainly because GR(TV) requires very few hop nodes (See Fig. 7.8, for instance) in route to the destination node, thanks again to very high transmission range. However, recall GR(TV) offers very poor MDR, and is again not desirable protocol in order to support various rural applications. GR(CBRS) and GR(ISM) bands offer the worst network delay for they require several hops to get to the destination node. It is noteworthy to mention that that the network delay increases with increasing mean message inter-arrival times from 7 minutes to 25 minutes, and then decreases afterwards, for all evaluated protocols. This can be attributed to the poor message delivery for 7 and 15 minutes, due to very high message load, and after that the protocols are able to cope with

Figure 7.6: Network Delay Analysis: Varying (a) Number of d-DSA nodes, (b) Number of channels in each band, (c) Number of primary users, (d) Mean message inter-arrival times, (e) TTL deadlines, and (f) Maximum buffer sizes
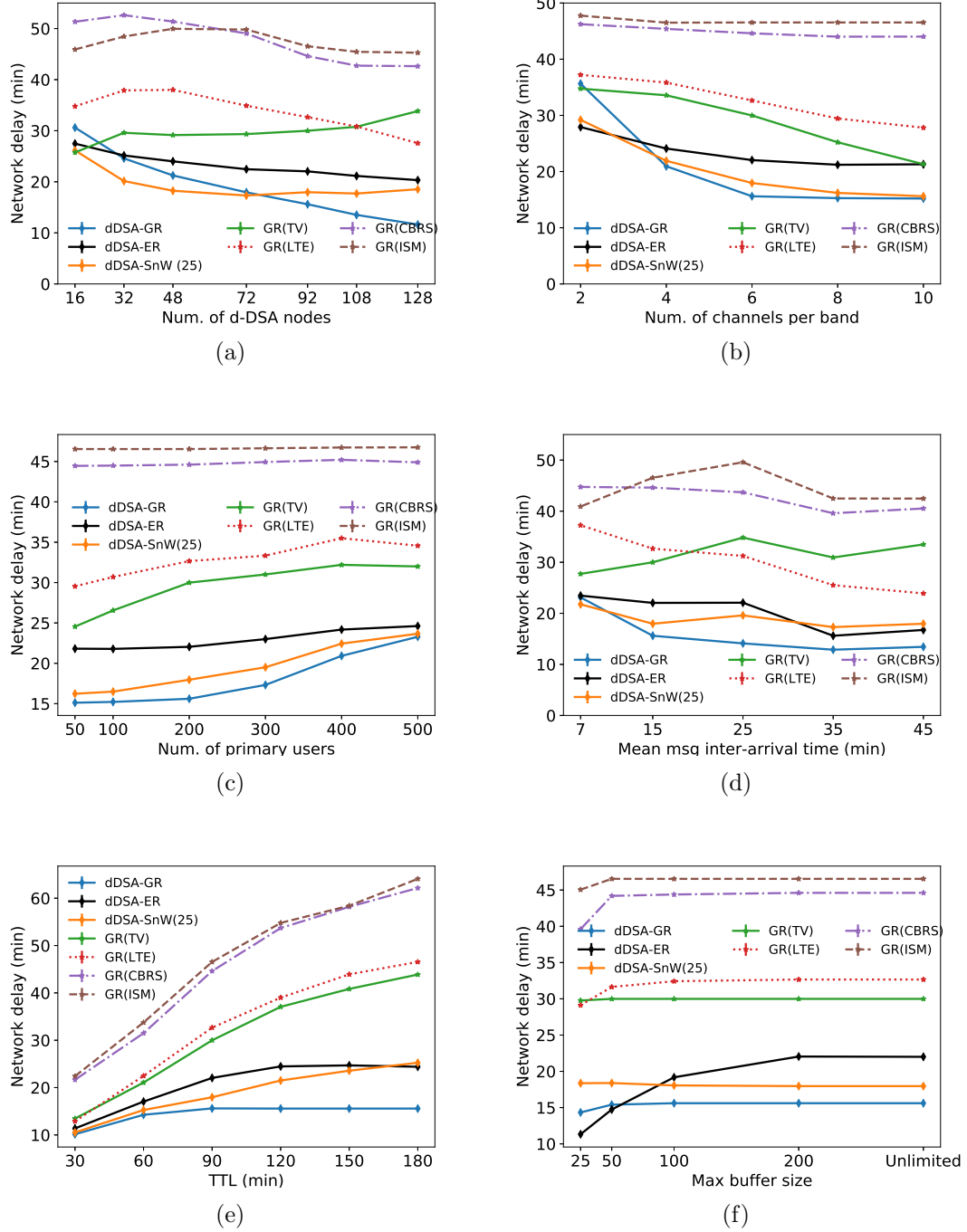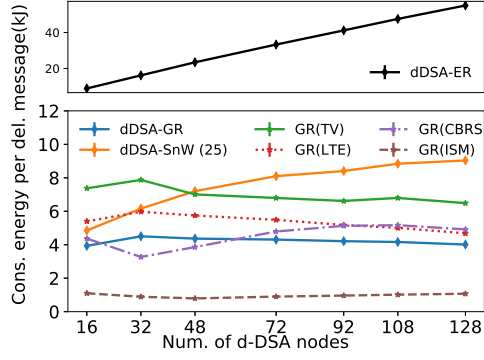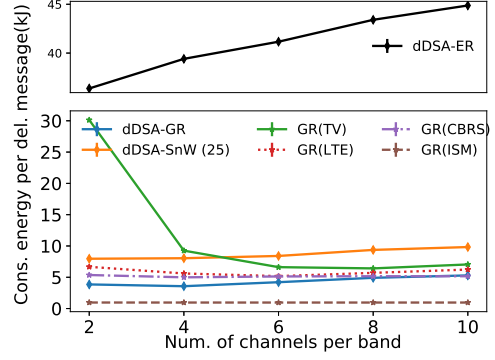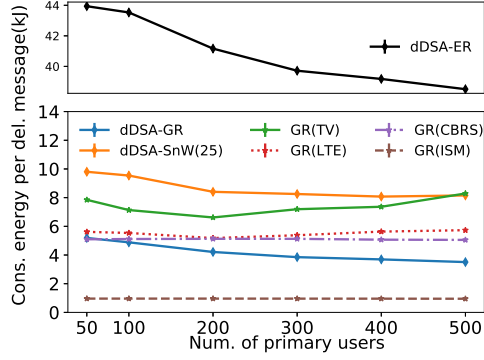
Figure 7.7: Energy Expenditure Analysis: Varying (a) Number of d-DSA nodes, (b) Number of channels in each band, (c) Number of primary users, (d) Mean message inter-arrival times, (e) TTL deadlines, and (f) Maximum buffer sizes
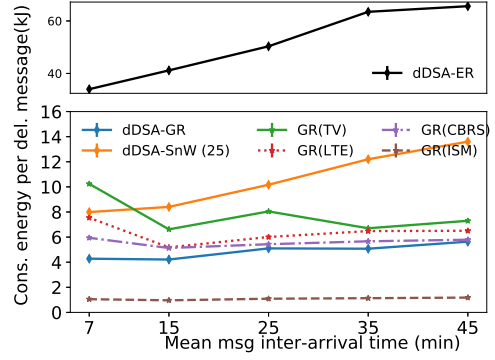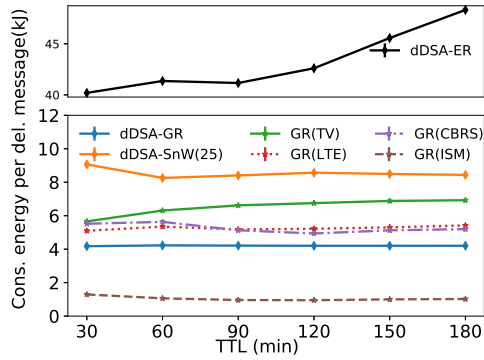
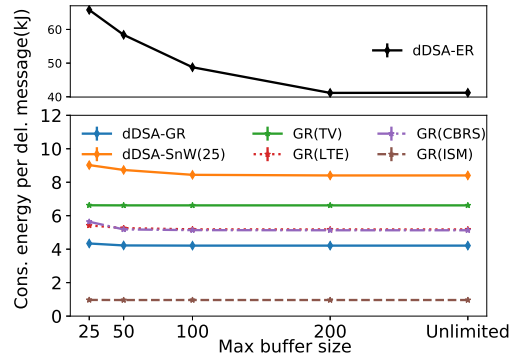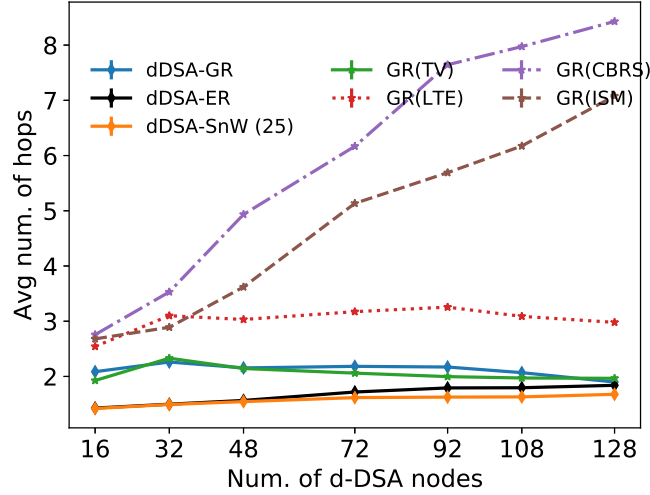Figure 7.8: Average number of hops vs number of d-DSA nodes

comparatively fewer messages, i.e., mean inter-arrival times ≥ 25 minutes.

Energy Expenditure Analysis. Figs. 7.7(a) - 7.7(f) depict that the energy consumed per delivered message by the proposed single-copy dDSA-GR protocol, and its standard GR counterparts are much lesser, compared to that of flooding based dDSA-ER protocol, under all considered parameters. The controlled flooding based dDSA-SnW (where, the maximum number of message copies is bounded, 25 in our experiments) incurs much better energy expenditure than that of dDSA-ER protocol. It is interesting to see that unlike standard GR protocols, all d-DSA aware protocols, i.e., dDSA-GR, dDSA-ER, and dDSA-SnW, improve with increasing number of primary users (Fig. 7.7(c)). This is because these protocols extensively utilize CBRS band (See Fig. 7.9 which shows bandusage for dDSA-GR protocol) in case of higher number of primary users, for it is least affected by interference from primary users. Now since CBRS band offer very high channel bandwidth and supports several concurrent message packets transmission, it significantly improves the message transmission time (See Eq. 4.3), and thus the consumed energy. Also notice that since MDR improves with increasing buffer size, the amount of energy consumed per delivered message also improves, particularly in case of dDSA-ER and dDSA-SnW protocols (Fig. 7.7(f)).

7.6 Conclusion of This Chapter

In this chapter, we evaluated the d-DSA network architecture that is based on dynamic and unpredictable mobile nodes, such as private cars, taxis etc., and is based on the innovative paradigm of diverse Dand-aware Dynamic Spectrum Access (in short, d-DSA). The proposed architecture equips urban transport vehicles (such as public bus) equipped with d-DSA radio devices, i.e., certain wireless devices equipped
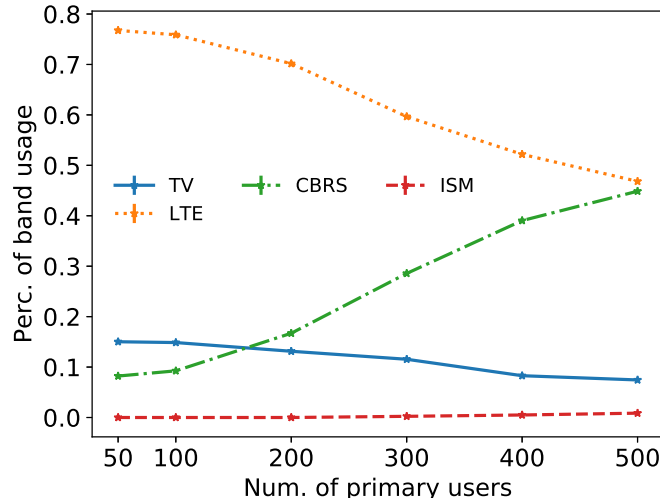
Figure 7.9: Percentage of band usage against varying number of primary users.

with software defined radios that are capable of accessing multiple spectrum bands, e.g., TV, LTE, and CBRS bands, on a secondary basis. We first highlight the short-comings of standard DTN routing schemes when applied to the newly formed d-DSA aware delay tolerant networks (dDSA DTN) (due to envisioned d-DSA architecture). Following this, we formulated an ILP optimization problem that aims to determine an optimal route for each message traffic, such that the end-to-end network delay is minimized. Since solving such an optimization problem assumes the global knowl-edge of topology dynamics and message traffic demands, it is impractical for d-DSA DTN networks, for such networks are highly unpredictable. Hence, we proposed ef-ficient d-DSA aware Geographical Routing (dDSA-GR) protocol, which is based on the georouting principle, and determines a suitable route, i.e., both optimal spectrum band and next hop node, that minimizes the network delay for each message traffic in such d-DSA DTN networks. Our large-scale experiments based on the map of Lexington, KY, USA show the proposed dDSA-GR protocol effectively exploits the multiple communication opportunities that may be available in such d-DSA DTN networks, and excels in terms of all performance metrics, including, network delay, message delivery ratio, energy expenditure, and overhead.

Chapter 8 Conclusions and Future Directions

This dissertation focused on designing a novel network architecture for providing ubiquitous connectivity in rural communities, which is based on the innovative paradigm of *Diverse Band-aware Dynamic Spectrum Access* (in short, d-DSA). According to this paradigm, static or mobile nodes in this d-DSA network architecture are equipped with software defined radios (SDRs) that are capable of accessing multiple spectrum bands, e.g., TV, CBRS, LTE, GSM, unlicensed ISM, and possibly futuristic mmWaves bands. In order to fully exploit the potential of d-DSA networking paradigm, while meeting the heterogeneous traffic demands that may be generated in rural communities, we design novel efficient routing strategies and optimization techniques for both static and time-varying (predictable and unpredictable) types of d-DSA network architectures. Our results based on realistic traces in a large variety of rural scenarios show that the proposed solutions, including d-DSA architecture, routing strategies and optimization techniques, are able to meet the heterogeneous traffic requirements of rural applications, and provide ubiquitous connectivity in rural communities.

We shall conclude the dissertation by discussing the future directions.

1. There are a few important issues that, if unaddressed, may seriously jeopardize the efficacy of both (i.e., static and dynamic) d-DSA architectures, namely (i) multiple concurrent messages with varying message generation/arrival rates, (ii) d-DSA nodes with potentially MIMO capability (or multiple antennas), (iii) limited memory and computational capability at each communication node, and (iv) interference from other secondary users. We will incorporate these and reformulate the centralized optimization problem (presented in Chapter 5) to minimize a desired quality of service metric, such as, energy efficiency, network delay etc. Following this, we will study and analyze the hardness of the problem, and solve it optimally utilizing various optimization techniques.

2. The centralized routing strategies proposed in this dissertation, are only feasible when a dedicated common control channel is available to share the control information, such as, list of available channels in a certain band, in the d-DSA network architectures. However, the availability of a dedicated common control channel may not always be possible in the rural context. Therefore, as a part of future work, we will design distributed routing strategies, which will be based on various techniques, particularly Multi-Objective Reinforcement Learning (MORL). Unlike traditional RL algorithms, the MORL algorithm introduced by Gabor [100] applies reinforcement learning to problems where there exist multiple objectives and the reward thus is a vector, instead of a scalar quantity. Hence, this becomes a promising model for designing distributed routing strategies for the envisioned d-DSA network architectures, for the routing strategies often need to satisfy multiple performance goals, for instance, end-to-end energy-efficiency under hard/soft deadline constraints.
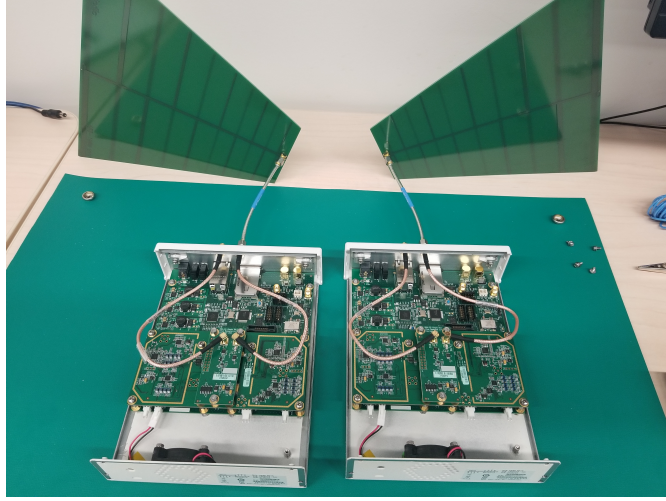
Figure 8.1: URSP platforms in our laboratory.

3. We will extend the unified graph model, Space-Time-Band (STB) graph, by including an additional dimension, namely the possibility of nodes have multiple antennas (MIMO capability) for the time-varying yet sufficiently predictable d-DSA network architectures. This model would be applicable for time-varying yet sufficiently predictable d-DSA network architectures where the component communication devices are equipped with multiple antennas. We would further extend and evaluate the efficacy of such d-DSA network architectures (and STB graph model) in case of urban communities, such as, smart cities, where the channel availability are much more constrained than in the rural scenario.

4. Finally, we will characterize the diverse DSA spectrum and interference, validate the design and modeling of proposed d-DSA architecture, and evaluate the routing strategies and optimization techniques through a small-scale Universal Software Radio Peripheral (USRP) platform based testbed as well as large-scale simulation experiments, based on both realistic and synthetic dataset traces.

   Small-scale Testbed. We plan to create the small-scale test-bed in our research laboratory at the University of Kentucky, that comprises six USRP N210 radio devices, each equipped with a WBX Daughterboard, and LP0410 Log Periodic PCB Antenna. USRP N210 hardware enables to design and implement flexible software radio systems. WBX Daughter board hardware is a full-duplex wide band transceiver and is ideal for applications requiring access to a number of different bands within its range from 50 MHz to 2.2 GHz. LP0410 antenna is a 400 MHz to 1 GHz Log Periodic PCB directional antenna and works with any daughter board that operates within 400 MHz to 1 GHz frequency range.

   Our laboratory already has two such devices (see Fig.8.1), and we intend to obtain four more devices. We use GNU Radio platform, a free software development framework that provides signal processing functions for implementing software defined radios, to implement the proposed routing schemes. Later, we

will deploy the testbed in various departmental buildings across UKY campus in Lexington to evaluate the static d-DSA architecture, outside the laboratory setting. Finally, we also envision to utilize the LexTran, a joint public transportation vehicle service by the city of Lexington and UKY, to evaluate the mobile d-DSA architecture.

Large-scale Experiments. We will implement the routing strategies and optimization techniques for both fixed and mobile d-DSA architectures in a realistic simulator to emulate the rural settings. Simulation scenarios will consider various parameters, such as message QoS requirements (e.g., energy expenditure, network latency, packet loss, or a combination thereof), heterogeneous data traffic, d-DSA topology density and distribution, number of primary users, spectrum usage patterns of PUs, channel count and availability in each spectrum band. For mobile d-DSA architecture, we will use real mobility traces (dataset) to model the mobility behavior of participating vehicles, such as public buses, taken from the repository CRAWDAD [101].

Bibliography

[1] P. Goswami, R. Mahapatra, and S. Divyasukananda, "Bridging the digital gap in rural india vivekdisha: A novel experience," in *IEEE National Conference on Communications (NCC)*, IEEE, 2013, pp. 1–5.

[2] H. E. Hudson, "Economic and social benefits of rural telecommunications: A report to the world bank," *Washington DC, USA*, 1995.

[3] Microsoft. (). `https://www.microsoft.com/empowering-countries/en-us/decent-work-and-economic-growth/tv-white-space/`.

[4] T. W. Bank. (). `https://data.worldbank.org/indicator/sp.rur.totl.zs?type=shaded&view=map`.

[5] S. Hasan, K. Heimerl, K. Harrison, K. Ali, S. Roberts, A. Sahai, and E. Brewer, "Gsm whitespaces: An opportunity for rural cellular service," in *Dynamic Spectrum Access Networks (DYSPAN), 2014 IEEE International Symposium on*, IEEE, 2014, pp. 271–282.

[6] S. Nandi, S. Thota, A. Nag, S. Divyasukhananda, P. Goswami, A. Aravindakshan, R. Rodriguez, and B. Mukherjee, "Computing for rural empowerment: Enabled by last-mile telecommunications," *IEEE Communications Magazine*, vol. 54, no. 6, pp. 102–109, 2016.

[7] K. Salemink, D. Strijker, and G. Bosworth, "Rural development in the digital age: A systematic literature review on unequal ict availability, adoption, and use in rural areas," *Journal of Rural Studies*, vol. 54, pp. 360–371, 2017.

[8] L. Townsend, A. Sathiaseelan, G. Fairhurst, and C. Wallace, "Enhanced broadband access as a solution to the social and economic problems of the rural digital divide," *Local Economy*, vol. 28, no. 6, pp. 580–595, 2013.

[9] Y. Ben-David, M. Vallentin, S. Fowler, and E. Brewer, "Jaldimac: Taking the distance further," in *Proceedings of the 4th ACM workshop on networked systems for developing regions*, ACM, 2010, p. 2.

[10] A. Pentland, R. Fletcher, and A. Hasson, "Daknet: Rethinking connectivity in developing nations," *Computer*, vol. 37, no. 1, pp. 78–83, 2004.

[11] M. C. Vuran, A. Salam, R. Wong, and S. Irmak, "Internet of underground things in precision agriculture: Architecture and technology aspects," *Adhoc Networks Journal (Elsevier)*, vol. 81, pp. 160–173, 2018.

[12] P. Loon, "`www.google.com/loon.`,"

[13] I. F. Inc., "`https://www.internet.org/projects`,"

[14] K. Heimerl and E. Brewer, "The village base station," in *Proceedings of the 4th ACM Workshop on Networked Systems for Developing Regions*, ACM, 2010, p. 14.

[15] H. Mehendale, A. Paranjpe, and S. Vempala, *Lifenet: a flexible ad hoc networking solution for transient environments*, 4. ACM, 2011, vol. 41.

[16] S. Saha, S. Nandi, P. S. Paul, V. K. Shah, A. Roy, and S. K. Das, "Designing delay constrained hybrid ad hoc network infrastructure for post-disaster communication," *Ad Hoc Networks*, vol. 25, pp. 406–429, 2015.

[17] LoRa, "`https://www.semtech.com/lora/what-is-lora`,"

[18] Sigfox, "`https://www.link-labs.com/blog/what-is-sigfox`,"

[19] P. Schmitt, D. Iland, M. Zheleva, and E. Belding, "Hybridcell: Cellular connectivity on the fringes with demand-driven local cells," in *IEEE Conference on Computer Communications*, 2016, pp. 1–9.

[20] I. F. Akyildiz, W.-Y. Lee, M. C. Vuran, and S. Mohanty, "Next generation/dynamic spectrum access/cognitive radio wireless networks: A survey," *Computer networks*, vol. 50, no. 13, pp. 2127–2159, 2006.

[21] M. Song, C. Xin, Y. Zhao, and X. Cheng, "Dynamic spectrum access: From cognitive radio to network radio," *IEEE Wireless Communications*, vol. 19, no. 1, 2012.

[22] [Online], "Fcc, second memorandum opinion and order, et docket no fcc 10-174, september 2010.,"

[23] M. Khalil, J. Qadir, O. Onireti, M. A. Imran, and S. Younis, "Feasibility, architecture and cost considerations of using tvws for rural internet access in 5g," in *Innovations in Clouds, Internet and Networks (ICIN), 2017 20th Conference on*, IEEE, 2017, pp. 23–30.

[24] P. Bahl, R. Chandra, T. Moscibroda, R. Murty, and M. Welsh, "White space networking with wi-fi like connectivity," *ACM SIGCOMM Computer Communication Review*, vol. 39, no. 4, pp. 27–38, 2009.

[25] R. H. Tehrani, S. Vahid, D. Triantafyllopoulou, H. Lee, and K. Moessner, "Licensed spectrum sharing schemes for mobile operators: A survey and outlook," *IEEE Communications Surveys & Tutorials*, vol. 18, no. 4, pp. 2591–2623, 2016.

[26] [Online], "Fcc report, 3.5ghz cbrs: Report and order and second further notice of proposed rulemaking, gn docket no. 12-354, april 2015.,"

[27] I. C. C. whitespace, "`http://www.ic.gc.ca/eic/site/smt-gst.nsf/eng/sf10928.html`," Last accessed on Jan, 2019.

[28] I. S. whitespace, "`https://www.imda.gov.sg/regulations-licensing-and-consultations/frameworks-and-policies/spectrum-management-and-coordination/spectrum-planning/tv-white-space`,"

[29] T. S. A. Whitespace, "`https://www.tenet.ac.za/tvws`,"

[30] O. Holland, S. Ping, A. Aijaz, J.-M. Chareau, P. Chawdhry, Y. Gao, Z. Qin, and H. Kokkinen, "To white space or not to white space: That is the trial within the ofcom tv white spaces pilot," in *Dynamic Spectrum Access Networks (DySPAN), 2015 IEEE International Symposium on*, IEEE, 2015, pp. 11–22.

[31] mtsfb. Malaysia whitespaceo, "`www.mtsfb.org.my/working‑group/tv‑white-space-ws-wg`,"

[32] T. K. Whitespace, "`www.techweez.com/2016/10/31/ca‑white‑spaces‑rules/`,"

[33] C. N. Whitespace, "`https://www.cran.na/images/docs/GGs/5480‑Gen\protect_N150.pdf`,"

[34] T. N. Whitespace, "`http://techweez.com/2014/01/15/microsoft‑whitespaces-broadband-namibia/`,"

[35] E. A. Whitespace, "`https://www.enacom.gob.ar/`,"

[36] A. Kumar, A. Karandikar, G. Naik, M. Khaturia, S. Saha, M. Arora, and J. Singh, "Toward enabling broadband for a billion plus population with tv white spaces," *IEEE Communications Magazine*, vol. 54, no. 7, pp. 28–34, 2016.

[37] Y.-C. Liang, A. T. Hoang, and H.-H. Chen, "Cognitive radio on tv bands: A new approach to provide wireless connectivity for rural areas," *IEEE Wireless Communications*, vol. 15, no. 3, 2008.

[38] P. Surampudi and S. Mohanty, "Lte-advanced in white space: A complementary technology," *Radisys White Paper*, 2011.

[39] [Online], "`http://www.rtl-sdr.com/rtl-sdr-wide-spectrum-analyzer/`,"

[40] M. M. Sohul, M. Yao, T. Yang, and J. H. Reed, "Spectrum access system for the citizen broadband radio service," *IEEE Communications Magazine*, vol. 53, no. 7, pp. 18–25, 2015.

[41] U. Herzog, A. Georgakopoulos, I.-P. Belikaidis, M. Fitch, K. Briggs, S. Diaz, Ó. Carrasco, K. Moessner, B. Miscopein, S. Mumtaz, *et al.*, "Quality of service provision and capacity expansion through extended-dsa for 5g," *Transactions on Emerging Telecommunications Technologies*, vol. 27, no. 9, pp. 1250–1261, 2016.

[42] I.-P. Belikaidis, A. Georgakopoulos, P. Demestichas, B. Miscopein, M. Filo, S. Vahid, B. Okyere, and M. Fitch, "Multi-rat dynamic spectrum access for 5g heterogeneous networks: The speed-5g approach," *IEEE Wireless Communications*, vol. 24, no. 5, pp. 14–22, 2017.

[43] V. K. Shah, S. Bhattacharjee, S. Silvestri, and S. K. Das, "Designing green communication systems for smart and connected communities via dynamic spectrum access," *ACM Transactions on Sensor Networks (TOSN)*, vol. 14, no. 3-4, p. 31, 2018.

[44] V. Shah, S. Bhattacharjee, S. Silvestri, and S. Das, "An effective dynamic spectrum access based network architecture for smart cities," *IEEE International Smart Cities Conference (ISC2)*, 2018.

[45] A. Vahdat and D. Becker, "Epidemic routing for partially connected ad hoc networks," *Technical Report CS-200006, Duke University*, 2000.

[46] K. Fall, "A delay-tolerant network architecture for challenged internets," in *Proceedings of the 2003 conference on Applications, technologies, architectures, and protocols for computer communications*, ACM, 2003, pp. 27–34.

[47] T. Spyropoulos, K. Psounis, and C. S. Raghavendra, "Spray and wait: An efficient routing scheme for intermittently connected mobile networks," in *ACM workshop on Delay-tolerant networking*, 2005, pp. 252–259.

[48] A. Seth, D. Kroeker, M. Zaharia, S. Guo, and S. Keshav, "Low-cost communication for rural internet kiosks using mechanical backhaul," in *Proceedings of the 12th annual international conference on Mobile computing and networking*, ACM, 2006, pp. 334–345.

[49] T. Hossmann, D. Schatzmann, P. Carta, and F. Legendre, "Twitter in disaster mode: Smart probing for opportunistic peers," in *Proceedings of the third ACM international workshop on Mobile Opportunistic Networks*, ACM, 2012, pp. 93–94.

[50] S. Saha, V. K. Shah, R. Verma, R. Mandal, and S. Nandi, "Is it worth taking a planned approach to design ad hoc infrastructure for post disaster communication?" In *Proceedings of the seventh ACM international workshop on Challenged networks*, ACM, 2012, pp. 87–90.

[51] K. Hazra, V. K. Shah, M. Bilal, S. Silvestri, S. K. Das, S. Nandi, and S. Saha, "A novel network architecture for resource-constrained post-disaster environments," 2019.

[52] P. Gardner-Stephen, "The serval project: Practical wireless ad-hoc mobile telecommunications," *Flinders University, Adelaide, South Australia, Tech. Rep*, 2011.

[53] R. B. Dilmaghani and R. R. Rao, "A wireless mesh infrastructure deployment with application for emergency scenarios," in *5th International ISCRAM Conference*, 2008.

[54] "Uavs," *Online]. Available: http://irevolution.net/category/dronesuavs/*, 2012.

[55] T. Yucek and H. Arslan, "A survey of spectrum sensing algorithms for cognitive radio applications," *IEEE communications surveys & tutorials*, vol. 11, no. 1, pp. 116–130, 2009.

[56] A. Ali and W. Hamouda, "Advances on spectrum sensing for cognitive radio networks: Theory and applications," *IEEE Communications Surveys & Tutorials*, vol. 19, no. 2, pp. 1277–1304, 2017.

[57] G.-M. Zhu, I. F. Akyildiz, and G.-S. Kuo, "Stod-rp: A spectrum-tree based on-demand routing protocol for multi-hop cognitive radio networks," in *Global Telecommunications Conference, 2008. IEEE GLOBECOM 2008. IEEE*, IEEE, 2008, pp. 1–5.

[58] K. R. Chowdhury and M. D. Felice, "Search: A routing protocol for mobile cognitive radio ad-hoc networks," *Computer Communications*, vol. 32, no. 18, pp. 1983–1997, 2009.

[59] Y. Liu, L. X. Cai, and X. S. Shen, "Spectrum-aware opportunistic routing in multi-hop cognitive radio networks," *IEEE Journal on Selected Areas in Communications*, vol. 30, no. 10, pp. 1958–1968, 2012.

[60] A. A. El-Sherif and A. Mohamed, "Joint routing and resource allocation for delay minimization in cognitive radio based mesh networks," *IEEE Transactions on Wireless communications*, vol. 13, no. 1, pp. 186–197, 2014.

[61] F. Tang and J. Li, "Joint rate adaptation, channel assignment and routing to maximize social welfare in multi-hop cognitive radio networks," *IEEE Transactions on Wireless Communications*, vol. 16, no. 4, pp. 2097–2110, 2017.

[62] M. Matinmikko, M. Mustonen, D. Roberson, J. Paavola, M. Hoyhtya, S. Yrjola, and J. Roning, "Overview and comparison of recent spectrum sharing approaches in regulation and research: From opportunistic unlicensed access towards licensed shared access," in *Dynamic Spectrum Access Networks (DYSPAN), 2014 IEEE International Symposium on*, IEEE, 2014, pp. 92–102.

[63] L. Zhang, M. Xiao, G. Wu, M. Alam, Y.-C. Liang, and S. Li, "A survey of advanced techniques for spectrum sharing in 5g networks," *IEEE Wireless Communications*, vol. 24, no. 5, pp. 44–51, 2017.

[64] I. F. Akyildiz, W.-Y. Lee, M. C. Vuran, and S. Mohanty, "A survey on spectrum management in cognitive radio networks," *IEEE Communications magazine*, vol. 46, no. 4, 2008.

[65] K. D. Singh, P. Rawat, and J.-M. Bonnin, "Cognitive radio for vehicular ad hoc networks (cr-vanets): Approaches and challenges," *EURASIP journal on wireless communications and networking*, vol. 2014, no. 1, p. 49, 2014.

[66] K. D. Singh, P. Rawat, and J.-M. Bonnin, "Cognitive radio for vehicular ad hoc networks (cr-vanets): Approaches and challenges," *EURASIP journal on wireless communications and networking*, vol. 2014, no. 1, p. 49, 2014.

[67] S. Bhattarai, J.-M. J. Park, B. Gao, K. Bian, and W. Lehr, "An overview of dynamic spectrum sharing: Ongoing initiatives, challenges, and a roadmap for future research," *IEEE Transactions on Cognitive Communications and Networking*, vol. 2, no. 2, pp. 110–128, 2016.

[68] S. Brahma and M. Chatterjee, "Spectrum sharing in secondary networks: A bargain theoretic approach," in *Wireless Communications and Networking Conference (WCNC), 2012 IEEE*, IEEE, 2012, pp. 1331–1336.

[69] S. Debroy, S. De, and M. Chatterjee, "Contention based multichannel mac protocol for distributed cognitive radio networks," *IEEE Transactions on Mobile Computing*, vol. 13, no. 12, pp. 2749–2762, 2014.

[70] D. Gurney, G. Buchwald, K. Ecklund, S. L. Kuffner, and J. Grosspietsch, "Geo-location database techniques for incumbent protection in the tv white space," in *IEEE Symposium on New Frontiers in Dynamic Spectrum Access Networks*, IEEE, 2008, pp. 1–9.

[71] S. Wang, Y. Wang, J. P. Coon, and A. Doufexi, "Energy-efficient spectrum sensing and access for cognitive radio networks," *IEEE Transactions on Vehicular Technology*, vol. 61, no. 2, pp. 906–912, 2012.

[72] Y. T. Lo and S. Lee, *Antenna Handbook: theory, applications, and design*. Springer Science & Business Media, 2013.

[73] M. Corinthios, *Signals, systems, transforms, and digital signal processing with MATLAB*. CRC Press, 2009.

[74] C. E. Shannon, "A mathematical theory of communication," *ACM SIGMOBILE Mobile Computing and Communications Review*, vol. 5, no. 1, pp. 3–55, 2001.

[75] K. R. Chowdhury and I. F. Akyildiz, "CRP: a routing protocol for cognitive radio ad hoc networks," *IEEE Journal on Selected Areas in Communications*, vol. 29, no. 4, pp. 794–804, 2011.

[76] T. Korkmaz and M. Krunz, "Multi-constrained optimal path selection," in *INFOCOM 2001. Twentieth Annual Joint Conference of the IEEE Computer and Communications Societies. Proceedings. IEEE*, IEEE, vol. 2, 2001, pp. 834–843.

[77] X. Yuan, "Heuristic algorithms for multiconstrained quality-of-service routing," *IEEE/ACM transactions on networking*, vol. 10, no. 2, pp. 244–256, 2002.

[78] T. H. Cormen, C. E. Leiserson, R. L. Rivest, and C. Stein, "Introduction to algorithms mit press," *Cambridge MA*, 1990.

[79] M. N. Anjum and H. Wang, "Dynamic scheduling and analysis of real time systems with multiprocessors," *Digital Communications and Networks*, vol. 2, no. 3, pp. 130–138, 2016.

[80] R. Zhou, Z. Li, C. Wu, and Z. Huang, "An efficient cloud market mechanism for computing jobs with soft deadlines," *IEEE/ACM Transactions on Networking*, vol. 25, no. 2, pp. 793–805, 2017.

[81] L. T. Phan, Z. Zhang, B. T. Loo, and I. Lee, "Real-time mapreduce scheduling," 2010.

[82] U. C. Devi and J. H. Anderson, *Soft real-time scheduling on multiprocessors*. University of North Carolina at Chapel Hill, 2006.

[83] H. Leontyev and J. H. Anderson, "A unified hard/soft real-time schedulability test for global edf multiprocessor scheduling," in *Real-Time Systems Symposium, 2008*, IEEE, 2008, pp. 375–384.

[84] Y. Khaluf and F. J. Rammig, "Task allocation strategy for time-constrained tasks in robot swarms.," in *ECAL*, 2013, pp. 737–744.

[85] P. Belotti, C. Kirches, S. Leyffer, J. Linderoth, J. Luedtke, and A. Mahajan, "Mixed-integer nonlinear optimization," *Acta Numerica*, vol. 22, pp. 1–131, 2013.

[86] Ettus, "https://www.ettus.com/product/details/UN210-KIT,"

[87] K. Johansson, A. Furuskar, P. Karlsson, and J. Zander, "Relation between base station characteristics and cost structure in cellular systems," in *Personal, Indoor and Mobile Radio Communications, 2004. PIMRC 2004. 15th IEEE International Symposium on*, IEEE, vol. 4, 2004, pp. 2627–2631.

[88] [Online], "https://www.microsoft.com/en-us/research/wp-content/uploads/2016/02/spectrum-microsoft\protect_tvwsimpact\protect_limpopo\protect_rural\protect_south\protect_africa.pdf,"

[89] H. Galperin and F. Bar, "The microtelco opportunity: Evidence from latin america," *Information Technologies & International Development*, vol. 3, no. 2, pp–73, 2006.

[90] K. Heimerl, S. Hasan, K. Ali, E. Brewer, and T. Parikh, "Local, sustainable, small-scale cellular networks," in *Proceedings of the Sixth International Conference on Information and Communication Technologies and Development: Full Papers-Volume 1*, ACM, 2013, pp. 2–12.

[91] L. Cheng, B. E. Henty, D. D. Stancil, F. Bai, and P. Mudalige, "Mobile vehicle-to-vehicle narrow-band channel measurement and characterization of the 5.9 ghz dedicated short range communication (dsrc) frequency band," *IEEE Journal on Selected Areas in Communications*, vol. 25, no. 8, 2007.

[92] X. Wu, S. Subramanian, R. Guha, R. G. White, J. Li, K. W. Lu, A. Bucceri, and T. Zhang, "Vehicular communications using dsrc: Challenges, enhancements, and evolution," *IEEE Journal on Selected Areas in Communications*, vol. 31, no. 9, pp. 399–408, 2013.

[93] V. K. Shah, S. Bhattacharjee, S. Silvestri, and S. K. Das, "Designing sustainable smart connected communities using dynamic spectrum access via band selection," in *Proceedings of the 4th ACM International Conference on Systems for Energy-Efficient Built Environments*, ACM, 2017, p. 12.

[94] L. R. Ford Jr and D. R. Fulkerson, *Flows in networks*. Princeton university press, 2015.

[95] J Burgess., J Zahorjan, R. Mahajan, B. N. Levine, A. Balasubramanian, A. Venkataramani, Y. Zhou, C. B., N Banerjee, M. Corner, and D. Towsley, *CRAWDAD dataset umass/diesel (v. 2008-09-14)*.

[96] M. A. Fonoberova and D. D. Lozovanu, "The minimum cost multicommodity flow problem in dynamic networks and an algorithm for its solving," *Computer Science*, vol. 13, no. 1, p. 37, 2005.

[97] B. Hoppe and É. Tardos, "The quickest transshipment problem," *Mathematics of Operations Research*, vol. 25, no. 1, pp. 36–62, 2000.

[98] J. LeBrun, C.-N. Chuah, D. Ghosal, and M. Zhang, "Knowledge-based opportunistic forwarding in vehicular wireless ad hoc networks," in *2005 IEEE 61st Vehicular Technology Conference*, IEEE, vol. 4, 2005, pp. 2289–2293.

[99] M. Haklay and P. Weber, "Openstreetmap: User-generated street maps," *IEEE Pervasive Computing*, vol. 7, no. 4, pp. 12–18, 2008.

[100] Z. Gábor, Z. Kalmár, and C. Szepesvári, "Multi-criteria reinforcement learning.," in *ICML*, vol. 98, 1998, pp. 197–205.

[101] D. Kotz and T. Henderson, "Crawdad: A community resource for archiving wireless data at dartmouth," *IEEE Pervasive Computing*, vol. 4, no. 4, pp. 12–14, 2005.

Vijay K. Shah
vijay.shah@uky.edu

Education

2015–2019   PhD in Computer Science
University of Kentucky (UKY), Lexington, USA
Advisors: Dr. Simone Silvestri and Dr. Sajal K. Das
CGPA: 4/4

2009–2013   B. Tech in Computer Science and Engineering
National Institute of Technology (NIT), Durgapur, India
CGPA: 8.85/10

Professional Experience

2017–Present   Graduate Research Assistant
Computer Science Department, University of Kentucky, Lexington

2016–2017   Graduate Research Assistant
Computer Science Department, Missouri &T, Rolla

2015–2016   Graduate Teaching Assistant
Department of Computer Science, Missouri &T, Rolla

2013–2015   Computer Scientist
Belzabar Software Design Pvt. Ltd, New Delhi, India

Summer 2012   Summer Intern
Belzabar Software Design Pvt. Ltd, New Delhi, India

Research Interests

Wireless Networked Systems, Dynamic Spectrum Sharing, Network Optimization, and Reinforcement Learning

Selected Awards and Scholarships

- Recipient of Outstanding Computer Science Graduate (PhD) Student for year 2019, by the College of Engineering at University of Kentucky, USA. Was nominated for the Outstanding CS Graduate (PhD) Student Award for year 2018.

- Recipient of six ACM/IEEE/NSF Student Travel Grant Awards, including, IEEE SECON'19, ACM SIGCOMM COMSNETS'19, Supercomputing Conference'17 and '18, ACM BuildSys'17, ACM WiSec'17, and IEEE PerCom'16

- Recipient of two University/Department Student Travel Grant Awards, namely, UKY computer science department travel grant award 2018, and Missouri S&T's council of graduate studies (CGS) travel grant award 2017

- One of the two recipients of the best poster awards at both 1st and 2nd Annual Commonwealth Computational Summit (CCS^2), i.e., CCS^2 2017 and CCS^2 2018, organized by the University of Kentucky.

- Second place at CS Student (Ph.D. Category) Research Poster Competition (CSSRPC 2017), organized by Computer Science Department at Missouri S&T, Rolla, USA.

- Third place at Missouri S&T's "Hackathon for Humanity 2015" Competition. Developed Hobby.coop, a web platform for peer-to-peer tool and equipment rental. Jointly shared with Doug Mcgeehen and Bryce Mehring.

- One of the eight selected candidates for Graduate Student Leadership Development Program (GSLDP 2015) awarded by President's Academic Leadership Institute of the University of Missouri System.

- Second place at National level Programming contest "Decathlon" at the Annual Techno-Management Festival (Aarohan) organized by National Institute of Technology, Durgapur, India.

- Second place at National level Robotics event "RoboStunts" at the 2010 Annual Techno-Management Festival (Techniche) organized by Indian Institute of Technology Guwahati, India.

- Awarded Nepal Aid Fund Scholarship 2009-13 sponsored by the Government of India, for admission to undergraduate engineering programs in top-notch institutions in India, like NITs and IIITs. (Top $\approx 0.01\%$)

- Awarded Mahatma Gandhi Scholarship 2006-07 sponsored by Indian Embassy at Kathmandu, Nepal for pursuing Higher Secondary Education (10 +2 Science).

Refereed Publications

Refereed Conference Publications

Remark: INFOCOM, BuildSys, and CNS are top leading conferences on computer communications, built environments, and network security. COMSNETS and BICT are amongst the premier conferences on communication and biological networks.

1. <u>V. K. Shah</u>, S. Silvestri, B. Luciano and S. K. Das, "X-CHANT: A Diverse DSA based Network Architecture for Next-generation Challenged Networks", in IEEE Conference on Computer Communications (INFOCOM), 2019.

2. K. Hazra*, <u>V. K. Shah</u>*(Co-first authorship), M. Bilal, S. Silvestri, S. K. Das, S. Nandi, and S. Saha, "A Novel Network Architecture for Resource-Constrained Post-Disaster Environments", in ACM/IEEE Conference on Communication Systems and Networks (COMSNETS), 2019.

3. <u>V. K. Shah</u>*, S. Roy*(Co-first authorship), S. Silvestri, and S. K. Das, "Towards Energy-efficient and Robust Disaster Response Networks", in ACM ICDCN Workshop on Emergency Response Technologies and Services (EmeRTeS), 2019.

4. <u>V. K. Shah</u>, S. Silvestri, S. Bhattacharjee, and S. K. Das, "An Effective Dynamic Spectrum Access based Network Architecture for Smart Cities", in IEEE Smart Cities Conference (ISC2), 2018.

5. <u>V. K. Shah</u>, S. Bhattacharjee, S. Silvestri, and S. K. Das, "Designing Sustainable Smart Connected Communities using Dynamic Spectrum Access via Band Selection", in ACM Conference on Systems for Energy-Efficient Built Environments (BuildSys), 2017.

6. <u>V. K. Shah</u>, S. Roy, S. Silvestri, and S. K. Das, "CTR: A Cluster based Topological Routing for Disaster Response Network", in IEEE Conference on Communications (ICC), 2017.

7. S. Bhattacharjee, N. Ghosh, <u>V. K. Shah</u>, and S. K. Das, "QnQ: A Reputation Model to Secure Mobile Crowdsourcing Applications from Incentive Losses", in IEEE Conference on Communications and Network Security (CNS), 2017. AR: 29.9% (= 41/137)

8. S. Bhattacharjee, N. Ghosh, <u>V. K. Shah</u>, and S. K. Das, "W2Q: A Dual Weighted QoI Scoring Mechanism in Social Sensing using Community Confidence", in IEEE PerCom Workshop on Information Quality and Quality of Service for Pervasive Computing (IQ2S), 2017.

9. S. Roy, <u>V. K. Shah</u>, and S. K. Das, "Characterization of E. coli Gene Regulatory Network and its Topological Enhancement by Edge Rewiring", in EAI Conference on Bio-inspired Information and Comm. Technologies (BICT), 2015.

10. S. Saha, <u>V. K. Shah</u>, R. Verma, R. Mandal, and S. Nandi, "Is It Worth Taking A Planned Approach To Design Ad Hoc Infrastructure For Post Disaster Communication?", in ACM MobiCom Workshop on Challenged Networks, 2012.

11. S. Patra, S. Saha, <u>V. K. Shah</u>, S. Sengupta, K. G. Singh, and S. Nandi, "A Qualitative Survey on Multicast Routing in Delay Tolerant Networks", in Springer Recent Trends in Wireless and Mobile Networks (WiMO), 2011.

Refereed Journal Publications

Remark: TMBMC, TMC, and TOSN are leading top journals on biological networks, mobile computing, and sensor networks.

12. S. Roy, <u>V. K. Shah</u>, and S. K. Das, "Design of Robust and Efficient Topology using Enhanced Gene Regulatory Networks", to appear in IEEE Transactions on Molecular, Biological and Multi-Scale Communications (TMBMC), 2019.

13. S. Bhattacharjee, N. Ghosh, <u>V. K. Shah</u>, and S. K. Das, "QnQ: Quality and Quantity based Unified Approach for Secure and Trustworthy Mobile Crowdsensing", to appear in IEEE Transactions on Mobile Computing (TMC), 2019.

14. <u>V. K. Shah</u>, S. Bhattacharjee, S. Silvestri, and S. K. Das "Designing Green Communication Systems for Smart & Connected Communities via Dynamic Spectrum Access", in ACM Tran. on Sensor Networks (TOSN), Vol.14, Issue 3-4, 2018.

15. S. Saha, S. Nandi, P. S. Paul, <u>V. K. Shah</u>, A. Roy, and S. K. Das, "Designing delay constrained hybrid ad hoc network infrastructure for post-disaster communication", in Elsevier Ad Hoc Networks, 2015.

Publications Under Submission

16. V. K. Shah, B. Luciano, S. Bhattacharjee, S. Silvestri, and S. K. Das, "A Diverse Band-aware DSA Network Architecture for Delay-Tolerant Smart City Applications", IEEE Transactions on Network Service and Management (TNSM), 2019.

17. V. K. Shah*, S. Roy*(*Co-first authorship*), S. Silvestri and S. K. Das, "Bio-DRN: Robust and Energy-efficient Bio-inspired Disaster Response Networks", in IEEE Conference on Mobile Ad-Hoc and Smart Systems (MASS), 2019.

Research Experience

- *Diverse band-aware DSA Networking*- Envision a novel wireless networking paradigm of Diverse Band-aware Dynamic Spectrum Access (in short, d-DSA), that enables a certain wireless device equipped with software-defined radios to dynamically access any spectrum band, e.g., TV, LTE, GSM, CBRS, and unlicensed ISM bands, on the condition of non-interference with the primary licensees. This research addresses the unique technical and deployment challenges of the d-DSA paradigm, including spectrum characterization, routing strategies, and network optimization, with a primary focus on providing rural broadband connectivity.

- *Post-Disaster Communications* - Build a functional end-to-end Disaster Response System (DRS) prototype, that promptly deploys a secure, reliable and energy-efficient temporary communication network in the post-disaster environments (e.g., hurricane), for efficient rescue and relief operations. Specifically, we develop novel network architecture, efficient routing

protocols, topology design mechanisms, and resource allocation strategies for the envisioned holistic DRS prototype.

- *Biological Networks* - Study and analyze the graph theoretic properties of biological networks of living organisms like E. Coli and Yeast, and utilize them to design robust communication topologies for wireless networks, such as, wireless sensor networks.

- *Participatory Sensing (PS)* - Develop novel risk tolerance and reputation aware trust models for PS applications to address reliability, and trustworthiness of user's data and services; by using behavioral theoretic approaches and decision theory.

Teaching and Advising Experience

- *Teaching Assistant* - CS 1510, Data Structures, Missouri S&T, Fall 2015, Fall 2016; and CS 1971, Introduction to C++, Missouri S&T, Spring 2015

- *Guest Lecturer* - CS 686, Complex Networks, University of Kentucky, Lexington Fall 2018; and CS 1510, Data Structures, Missouri S&T, Rolla Fall 2016

- *Undergraduate Student Advising* - 5 undergraduates, namely, (i) Brian Luciano, Senior@University of Kentucky, Lexington, (ii) Rishab Singhal, Indian Institute of Technology, Guwahati, India (now@JP Morgans), (iii) Tej Patel, Junior@University of Kentucky, Lexington, (iv) Eric Chheang, Junior@University of Kentucky, Lexington, and (v) Parker Jones, Senior@University of Missouri, Columbia

Skillset

- *Programming Languages*: Python, C/C++, Java, and Android development

- Network hardwares: Raspberry Pi B+, GNU Radio Companion (GRC), Universal Software Radio Peripheral (USRP) platforms like N210 devices, WBX Daughterboard

- *Network Simulators* - Opportunistic Network Simulator (ONE), OMNET++, and Contiki

- *Web Technologies*: AngularJS, Apache Web Server, Bootstrap, HTML5, JavaScript/jQuery, CSS3, and CGI-Perl

- *Miscellaneous*: GIS tools - OpenJump and GeoJSON, Databases - MySQL, PostgreSQL, and Oracle, Version control systems - SVN and GIT, Java web framework - Apache Struts and Spring, and Shell scripts

Other Academic Activities

- Technical Program Committee (TPC) member - ACM/IEEE Internet of Things Design and Implementation (IoTDI) Posters/Demos, 2018 and IARIA conferences like ACCSE, INNOV, and EMERGING 2018.

- Conference and *Journal Reviewer - IEEE ICNC 2017-19, ACM MSWiM 2018, IEEE ICC 2017-18, IEEE WoWMoM 2017-19, IEEE GLOBECOM 2017-18, IEEE LCN 2017-18, IEEE SMARTCOMP 2017-19, IEEE Med-Hoc-Net 2018, IEEE MASS 2017, Wireless Days 2018, IEEE PerCom 2016, Network of Future 2017, IEEE WCNC 2019, ACM IoTDI 2018, *Ad-hoc Networks 2016, *Hindawi 2018, *PLOS ONE 2019